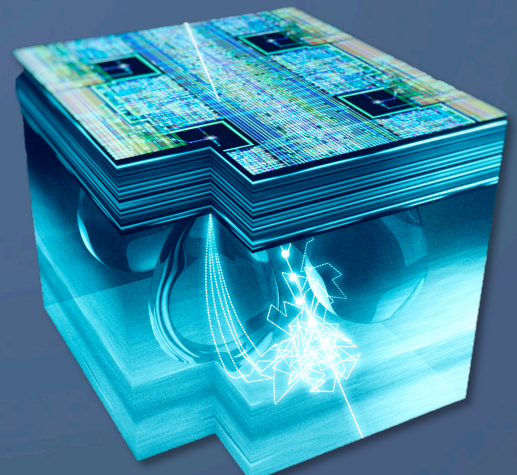




CMOS Active Pixel Sensors A Novel Detection Technology for Particle Physics

Luciano Musa – CERN



Physics Colloquium, Physikalisches Institut, Ruprecht-Karls-Universität Heidelberg, 27 April 2018

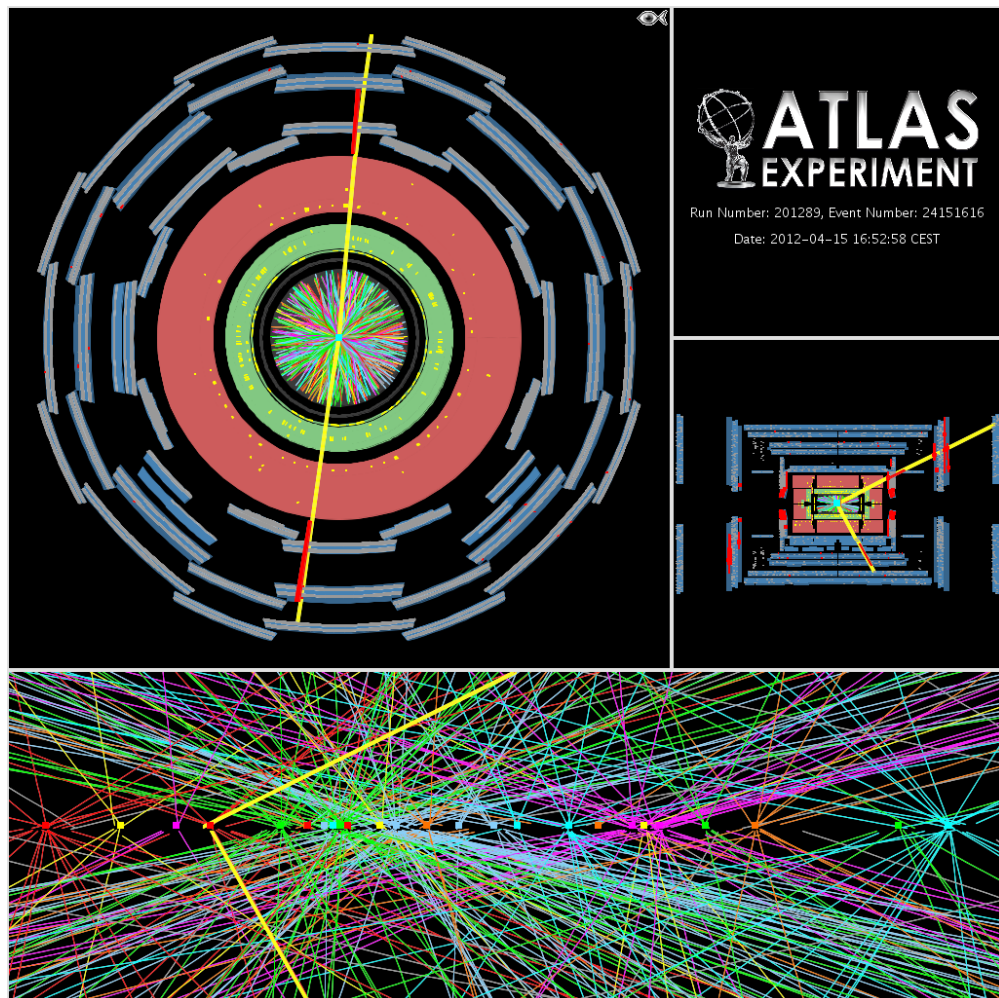
Outline

- Silicon detectors in HEP – a brief historical excursus
- First applications of CMOS APS in HEP (STAR, ALICE)
- CMOS APS Fully Depleted
- Novel developments and future applications in HEP
- Applications to medical imaging

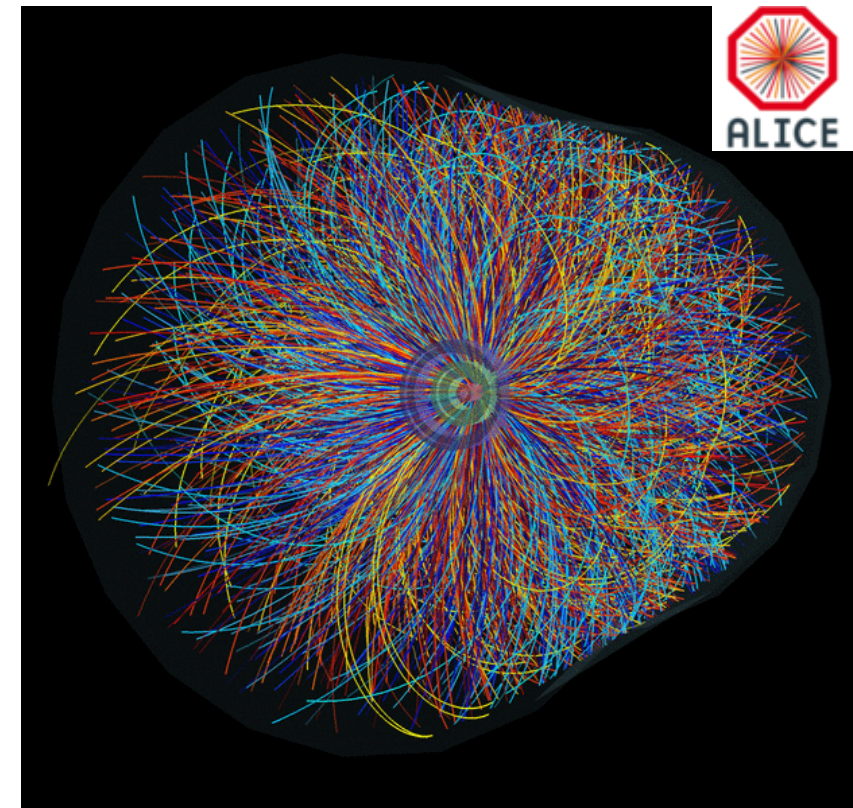
Silicon detectors in HEP

Brief historical excursus

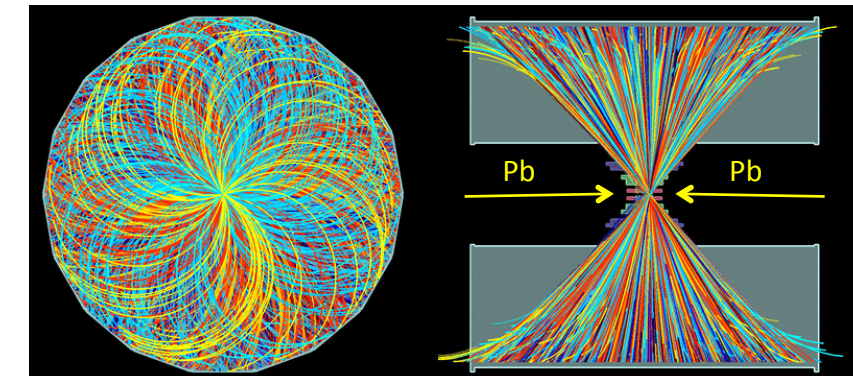
Silicon Trackers – Key to solve complex events close to IP



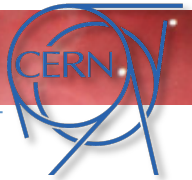
LHC pp collisions: a candidate Z boson event in the dimuon decay with 25 reconstructed vertices (ATLAS, April 2012)



LHC Pb-Pb collision (ALICE, Sep 2011)



Silicon detectors at the heart of all LHC experiments

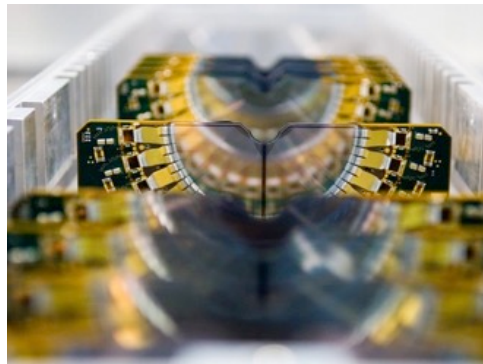


Complex systems operated in a challenging high track density environment

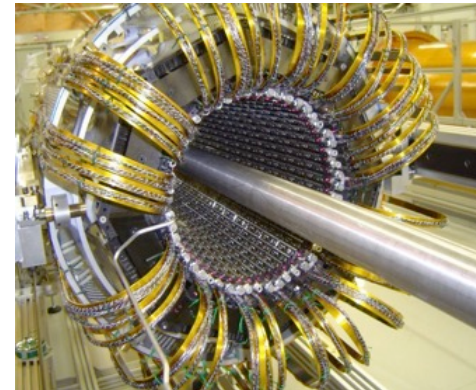
Innermost regions usually equipped with pixel detectors



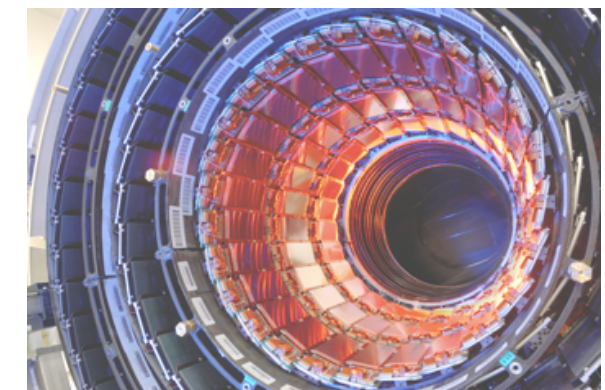
ALICE **Pixel** Detector



LHCb VELO



ATLAS **Pixel** Detector



CMS Strip Tracker IB



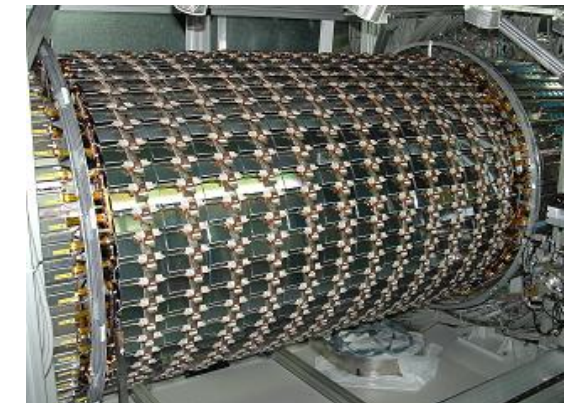
CMS **Pixel** Detector



ALICE Drift Detector

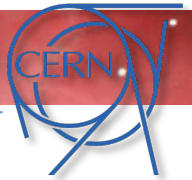


ALICE Strip Detector

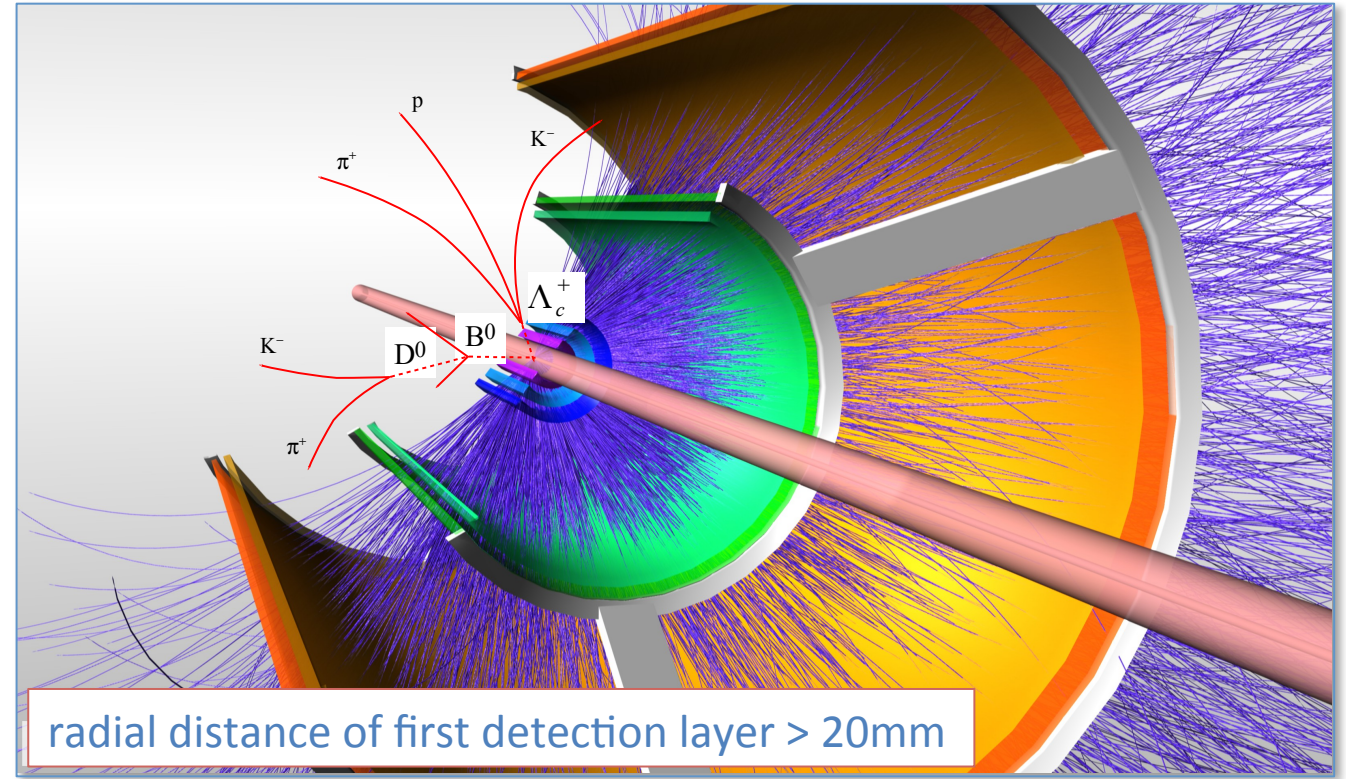
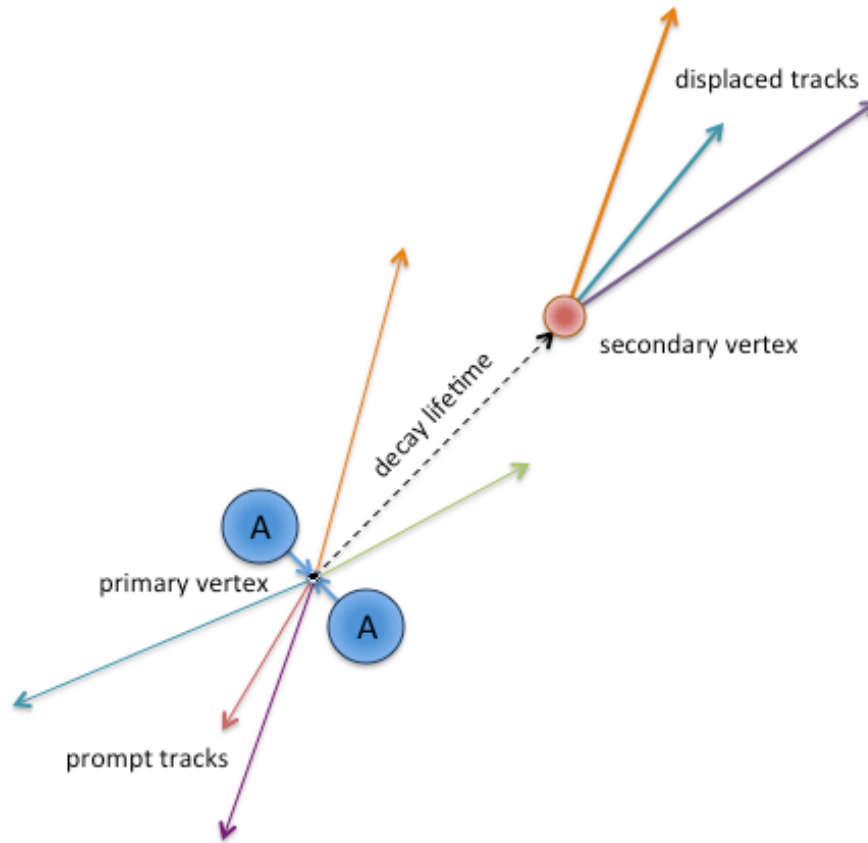


ATLAS SCT Barrel

Measurement of the decay topology of short-lived particles

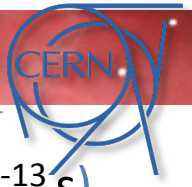


The first detection layers, the closest to the IP, are crucial for the measurement of the interaction vertex (primary vertex) and the decay vertex of short-lived particles (secondary vertex)



typical (proper) decay length of charm and beauty hadrons: $\approx 100\mu\text{m}$ and $\approx 500\mu\text{m}$ respectively

The rise of silicon detectors in HEP



Towards end of 1970's: intensive R&D on devices which could measure short-lived particles ($10^{-12} - 10^{-13}$ s)

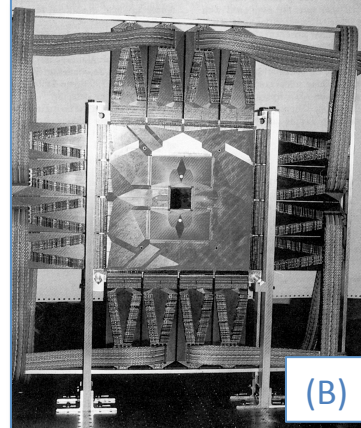
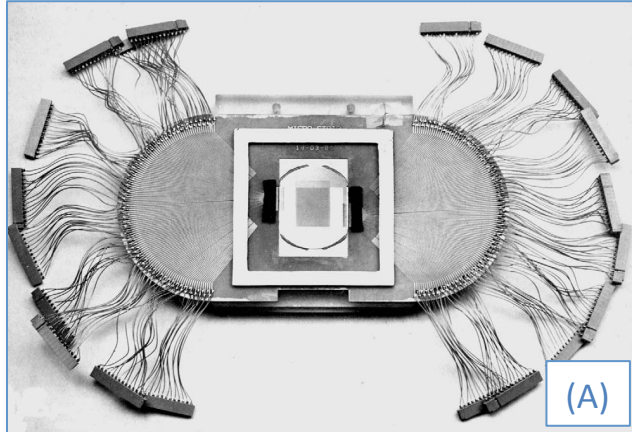
R&D at CERN⁽¹⁾ and Pisa⁽²⁾ demonstrated that strip detectors (100-200 μm pitch):

- exhibit high detection efficiency (>99%), good spatial resolution (~20 μm) and good stability
- allow precise vertex reconstruction

However the technology for the fabrication of these devices was very tricky, thus limiting their availability

1980 – fabrication of silicon detectors using standard IC planar process (PIN diode → μ strip detector)

J. Kemmer, et al., “Development of 10-micrometer resolution silicon counters for charm signature observation with the ACCMOR spectrometer”, Proceedings of Silicon Detectors for High Energy Physics, Nucl. Instr. and Meth. 169 (1980) 499.

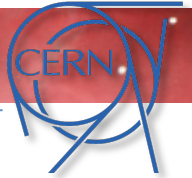


First use of silicon strips detectors by NA11(CERN SPS) and E706 (FNAL)

(A) NA11 (1981): 6 planes ($24 \times 36\text{mm}^2$): resistivity 2-3 $\text{k}\Omega\text{cm}$, thickness 280 μm , pitch 20 μm

(B) E706 (1982): 4 planes ($3 \times 3 \text{ cm}^2$) + 2 planes ($5 \times 5 \text{ cm}^2$)

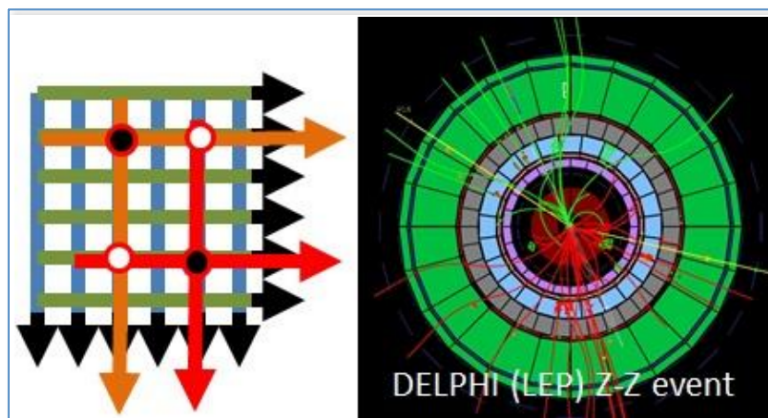
The rise of silicon detectors in HEP



The next step forward came with the advent of the VLSI technology that allowed coupling ASIC amplifier chips directly to the detectors

1990s - LEP, first silicon vertex detectors were installed in **DELPHI** and **ALEPH** experiments, then **OPAL** and **L3**

1989 - first DELPHI vertex detector, consisting of two layers of single-sided strip detectors



Projective geometry → ambiguity at high multiplicities (high occupancy)

This started to become apparent already at DELPHI:

- High number of ambiguities → reconstruction efficiency suffered a lot, especially in the forward direction

Not usable close to IP in hadron colliders (LHC) or HI experiments at SPS

Another problem at (very) high particle load → degradation of the sensor by the high radiation dose

This implies starting with a signal-to-noise ratio, which can only be obtained with detector with small capacitance

The Inception of Silicon Pixel Detectors



“The silicon micropattern detector: a dream?”

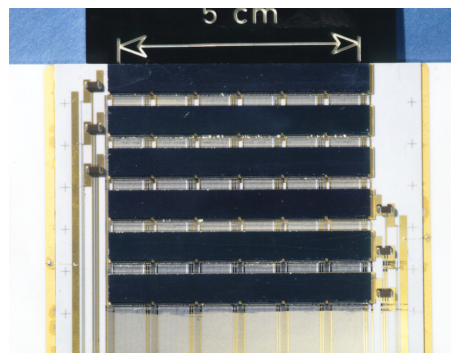
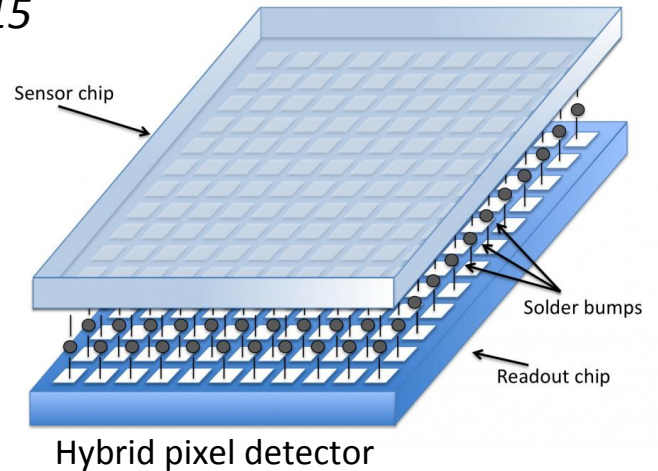
E.H.M Heijne, P. Jarron, A. Olsen and N. Redaelli, *Nucl. Instrum. Meth. A* 273 (1988) 615

“Development of silicon micropattern detectors”

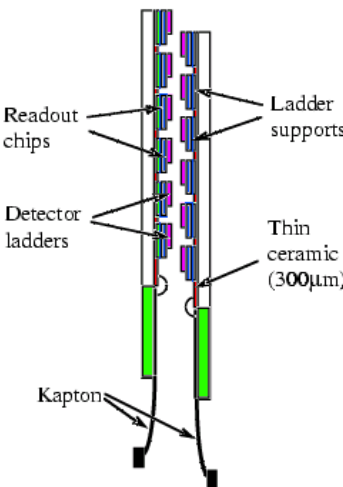
CERN RD19 collaboration, *Nucl. Instrum. Meth. A* 348 (1994) 399

1995 – First Hybrid Pixel detector installed in WA97 (CERN, Omega facility)

1996/97 – First Collider Hybrid Pixel Detector installed in DELPHI (CERN, LEP)

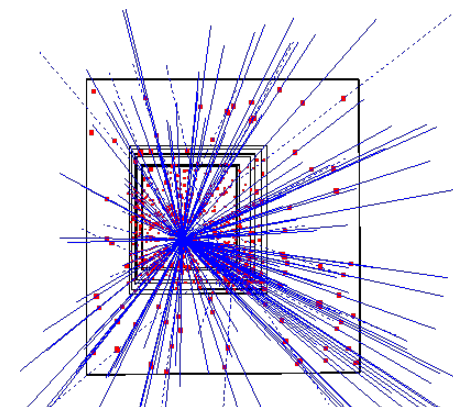


E. Heijne, E. Chesi



- $5 \times 5 \text{ cm}^2$ area
- 7 detector planes
- $\sim 0.5 \text{ M}$ pixels
- Pixel size $75 \times 500 \mu\text{m}^2$
- 1 kHz trigger rate
- Omega2 chip

CERN – WA97 Experiment (1995)



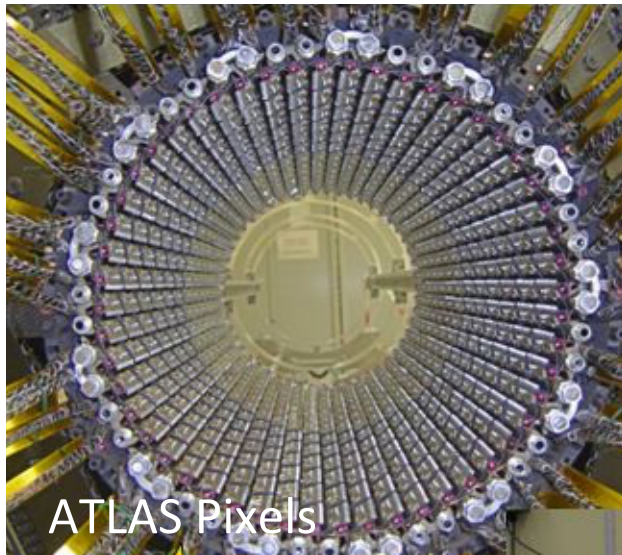
No-field, Pb-Pb, 153 reconstructed tracks

Work carried out by RD19 for WA97 and NA57/CERN

Pixel Detectors at the LHC experiments



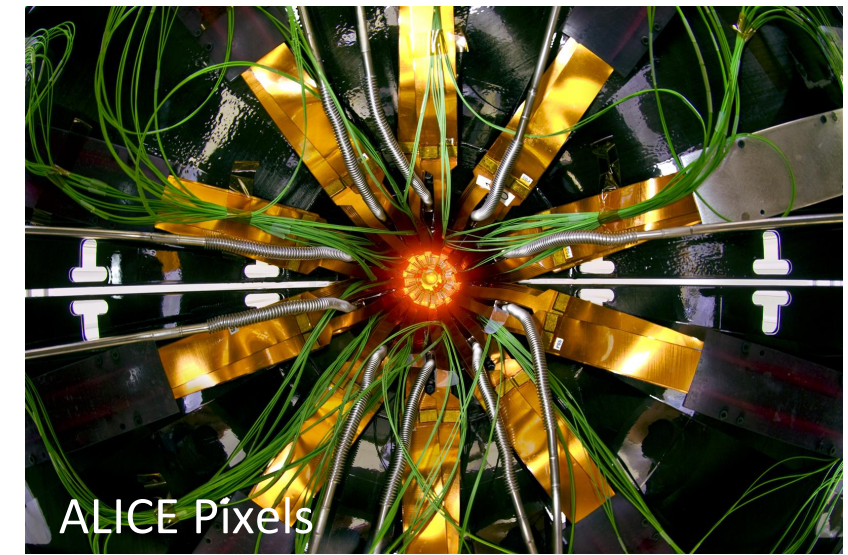
10 years after the first use in WA97... silicon pixel detectors at the heart of the LHC experiments



ATLAS Pixels



CMS Pixels



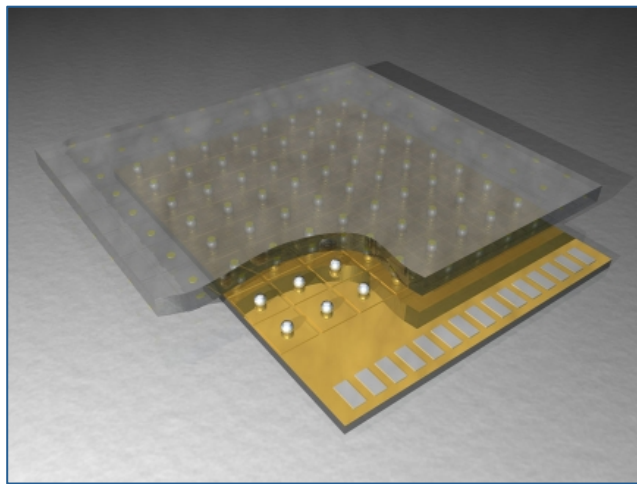
ALICE Pixels

Parameters	ALICE	ATLAS	CMS
Nr. layers	2	3	3
Radial coverage [mm]	39 - 76	50 - 120	44 – 102
Nr of pixels	9.8 M	80 M	66 M
Surface [m^2]	0.21	1.7	1
Cell size ($r\phi \times z$) [μm^2]	50 x 425	50 x 400	100 x 150
Silicon thickness (sens. + ASIC) - x/X_0 [%]	0.21 + 0.16	0.27 + 0.19	0.30 + 0.19

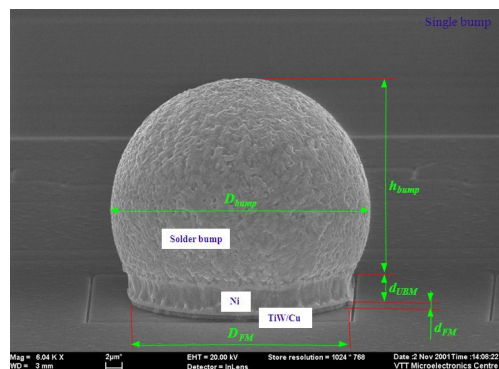
Beyond Hybrid Pixel Detectors ...



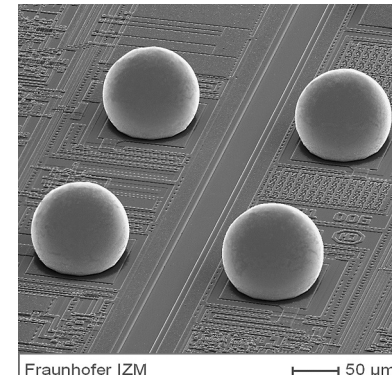
- Limited number of sensors producers (~10 world-wide)
- no industrial scale production → **high cost**



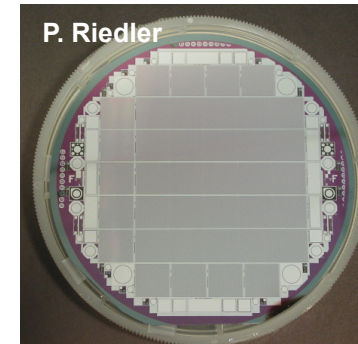
Azom.com



VTT Microelectronics Centre



Fraunhofer IZM



- Complex and **costly** interconnection between sensors and ASIC
- Interconnection technology (micro-bump bonding) limits:
 - **pitch** (currently ~ $30\mu\text{m}$)
 - input capacitance → **power**

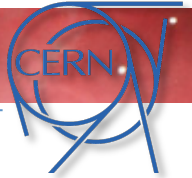
Lower production cost

Higher integration (pitch, x/X_0)

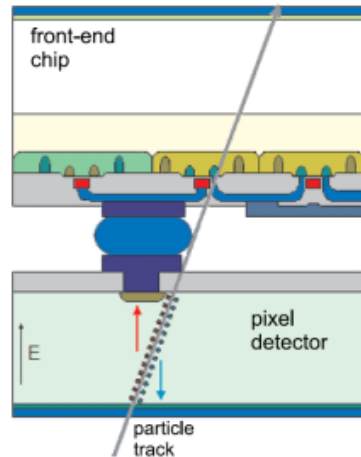
Lower power (x/X_0 , cost)

→ CMOS Pixel Sensors

Beyond Hybrid Pixel Detectors ...

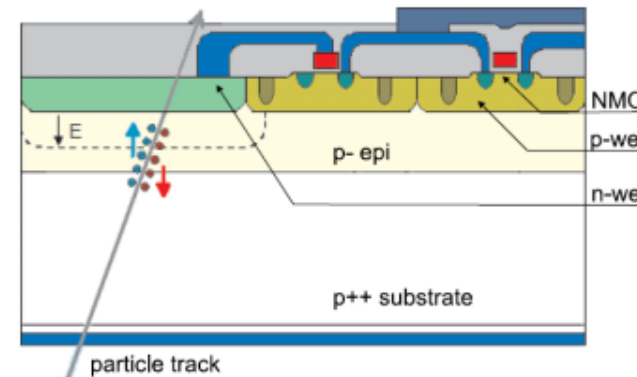


Hybrid Pixel Detector



N. Wermes (Univ. of Bonn)

Monolithic Pixel Detector



N. Wermes (Univ. of Bonn)

Since the very beginning of pixel development (CERN RD 19):

dream to integrate sensor and readout electronics in one chip

Motivation to reduce: cost, power, material budget, assembly and integration complexity

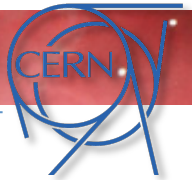
Several major obstacles to overcome:

- CMOS generally not available on high resistivity silicon (needed as bulk material for the sensor) ✓
- Full CMOS circuitry not possible within the pixel area (only one type of transistor → slow readout) ✓

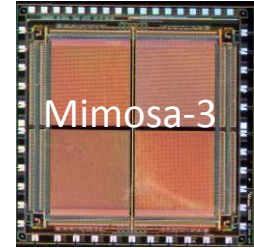
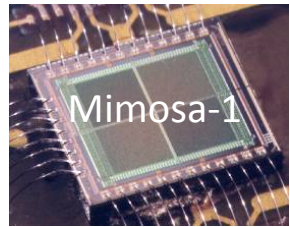
Exist in many different flavours: **CMOS**, HV CMOS, DEPFET, SOI

The following will cover only CMOS Active Pixel Sensors (CMOS MAPS) = **CMOS Active Pixel Sensors (CPS)**

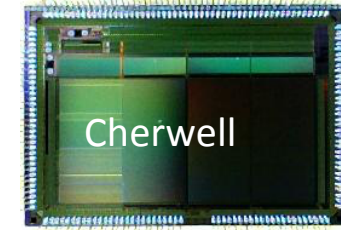
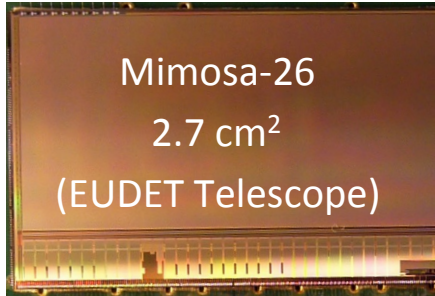
Beyond Hybrid Pixel Detectors - Monolithic Pixel Detectors



Owing to the industrial development of CMOS imaging sensors and the intensive R&D work (IPHC, RAL, CERN)



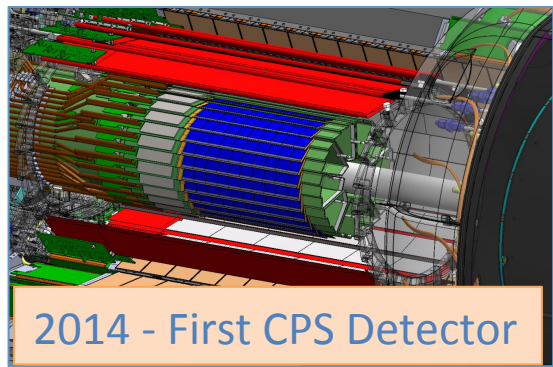
...



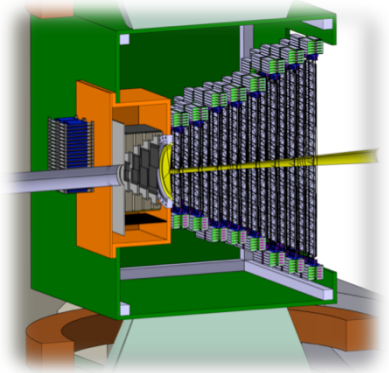
1999

2016

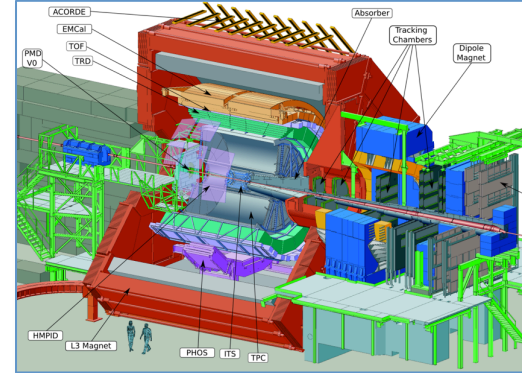
... several HI experiments have selected CMOS pixel sensors for their inner trackers



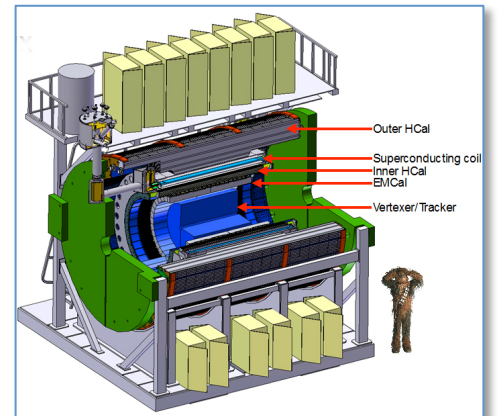
STAR HFT
 0.16 m^2 – 356 M pixels



CBM MVD
 0.08 m^2 – 146 M pixel



ALICE ITS Upgrade (and MFT)
 10 m^2 – 12 G pixel



sPHENIX
 0.2 m^2 – 251 M pixel

First application to Vertex Detectors

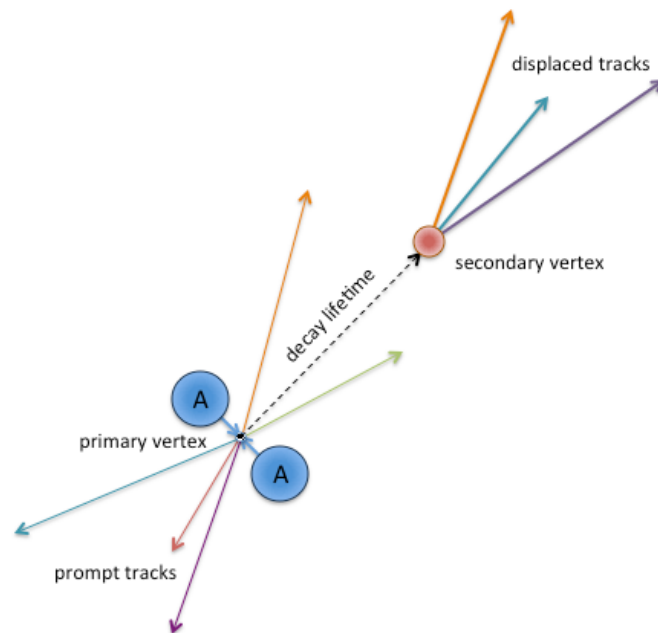
Measurement of short-lived particles

Secondary Vertex Determination

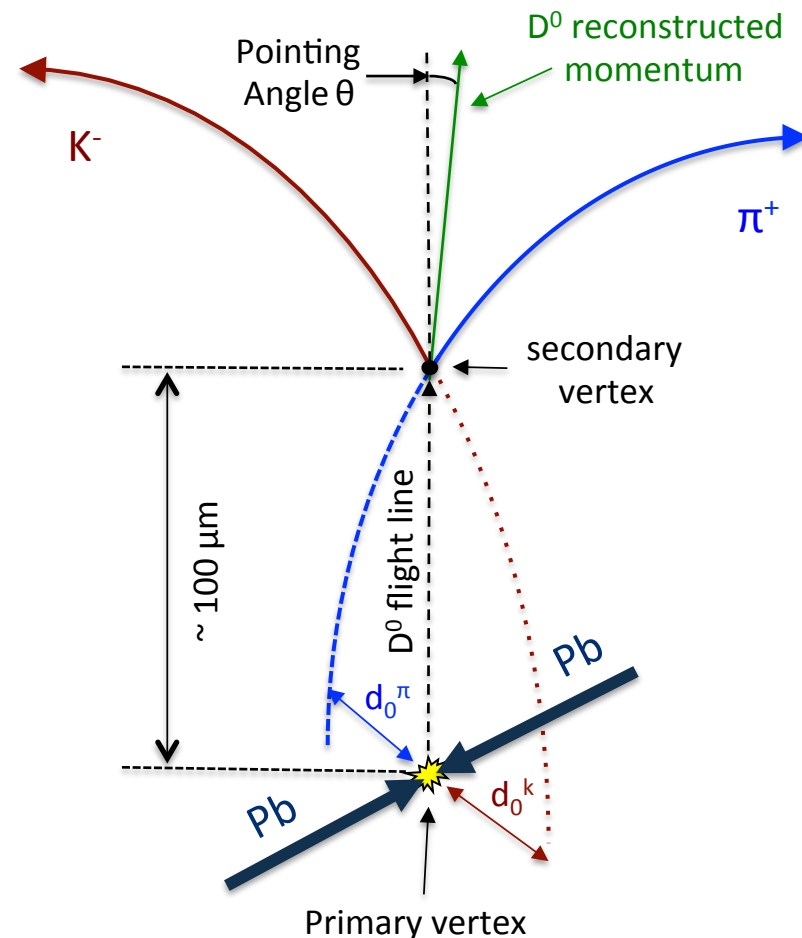


Open charm

Particle	Decay Channel	$c\tau$ (μm)
D^0	$K^- \pi^+$ (3.8%)	123
D^+	$K^- \pi^+ \pi^+$ (9.5%)	312
D_s^+	$K^+ K^- \pi^+$ (5.2%)	150
Λ_c^+	$p K^- \pi^+$ (5.0%)	60

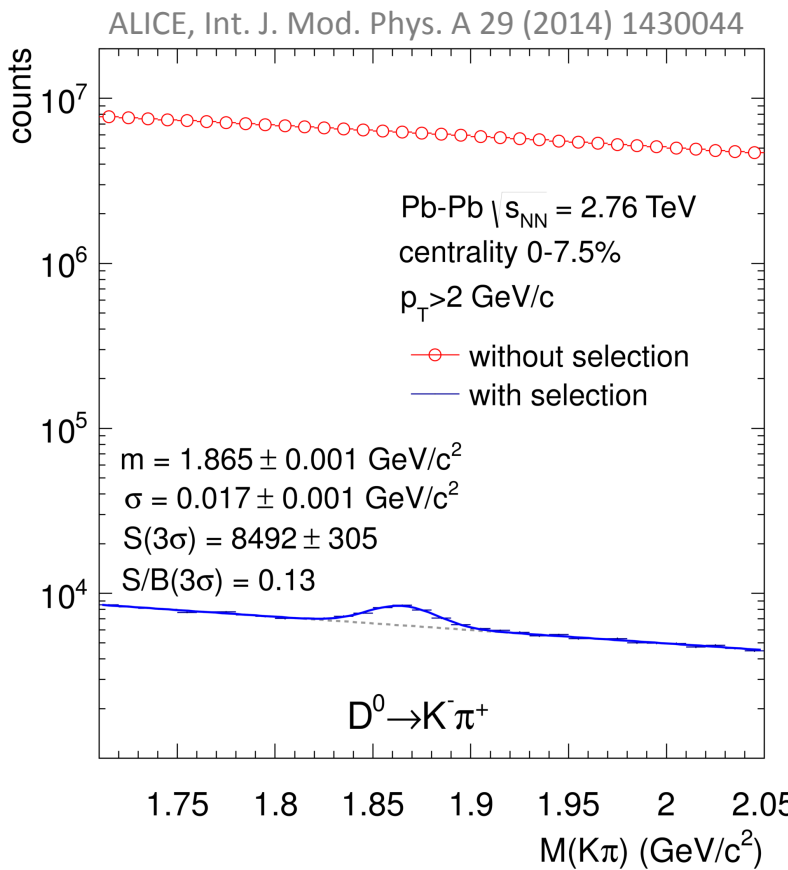


Example: D^0 meson



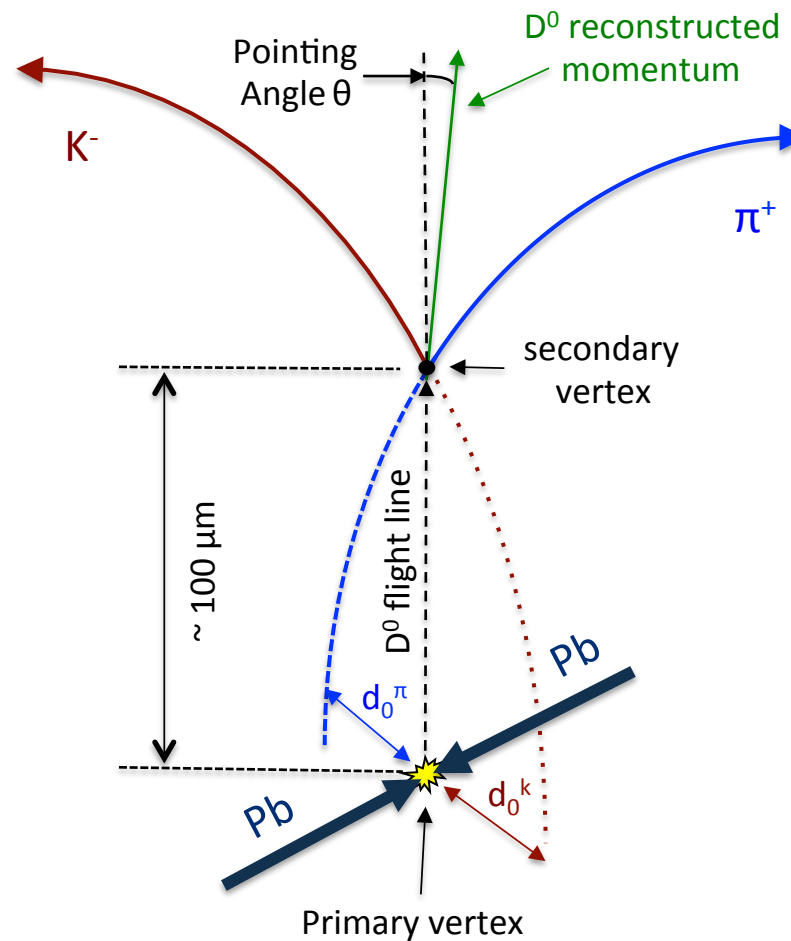
Analysis based on invariant mass, PID and decay topology

Secondary Vertex Determination



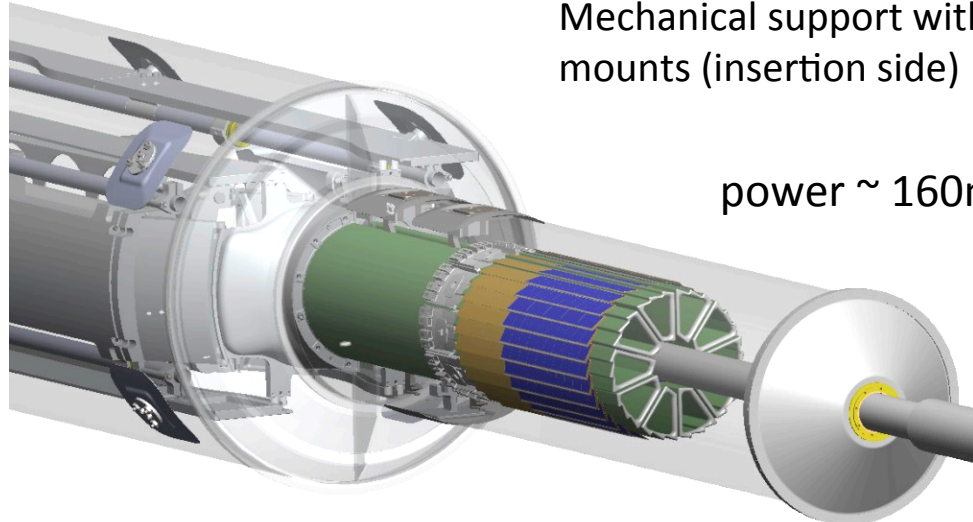
Invariant mass distribution of $K^-\pi^+$ pairs before and after applying selection criteria on the relation between the secondary (D^0 decay) and primary vertices

Example: D^0 meson



Analysis based on invariant mass, PID and decay topology

STAR Pixel Detector – First application of CMOS APS to HEP

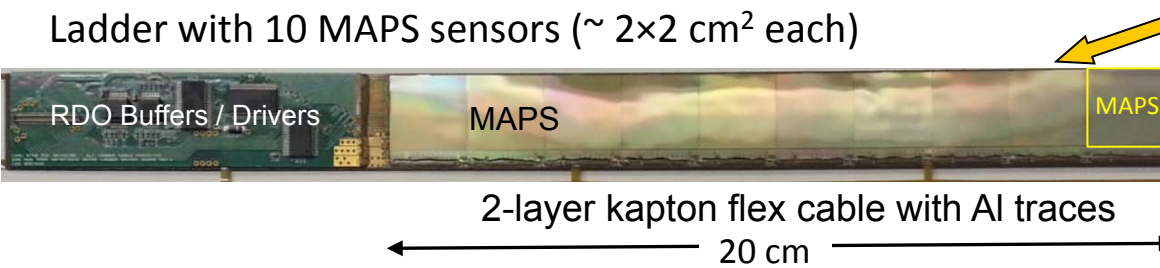


Mechanical support with kinematic mounts (insertion side)

power $\sim 160\text{mW/cm}^2$

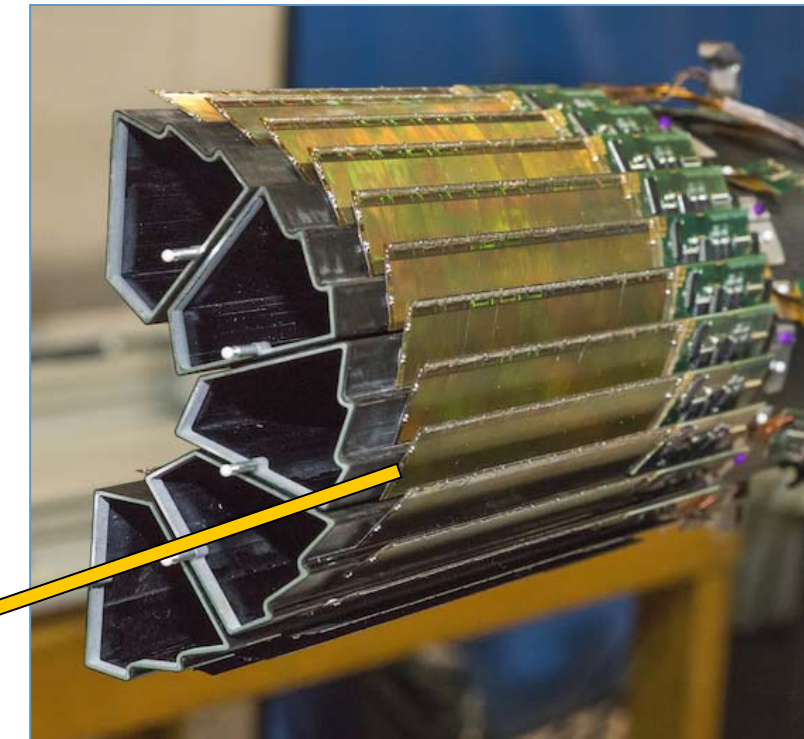
- 2 layers
- 10 sectors total (in 2 halves)
- 4 ladders/sector

Rolling Shutter
 $\sim 180\mu\text{s}$ integr. time



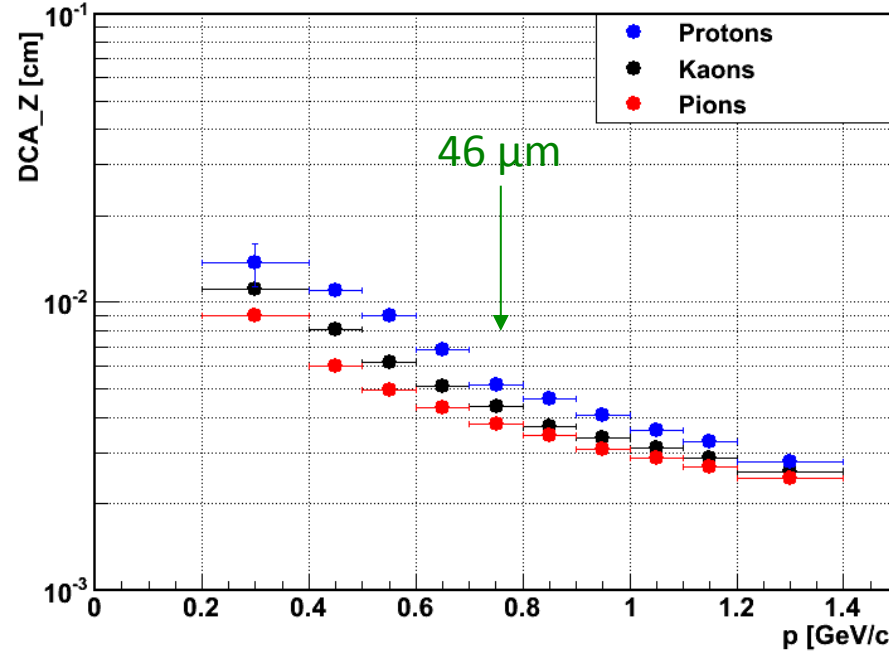
Key dates

- 3-sector prototype May 2013
- Full detector Jan 2014



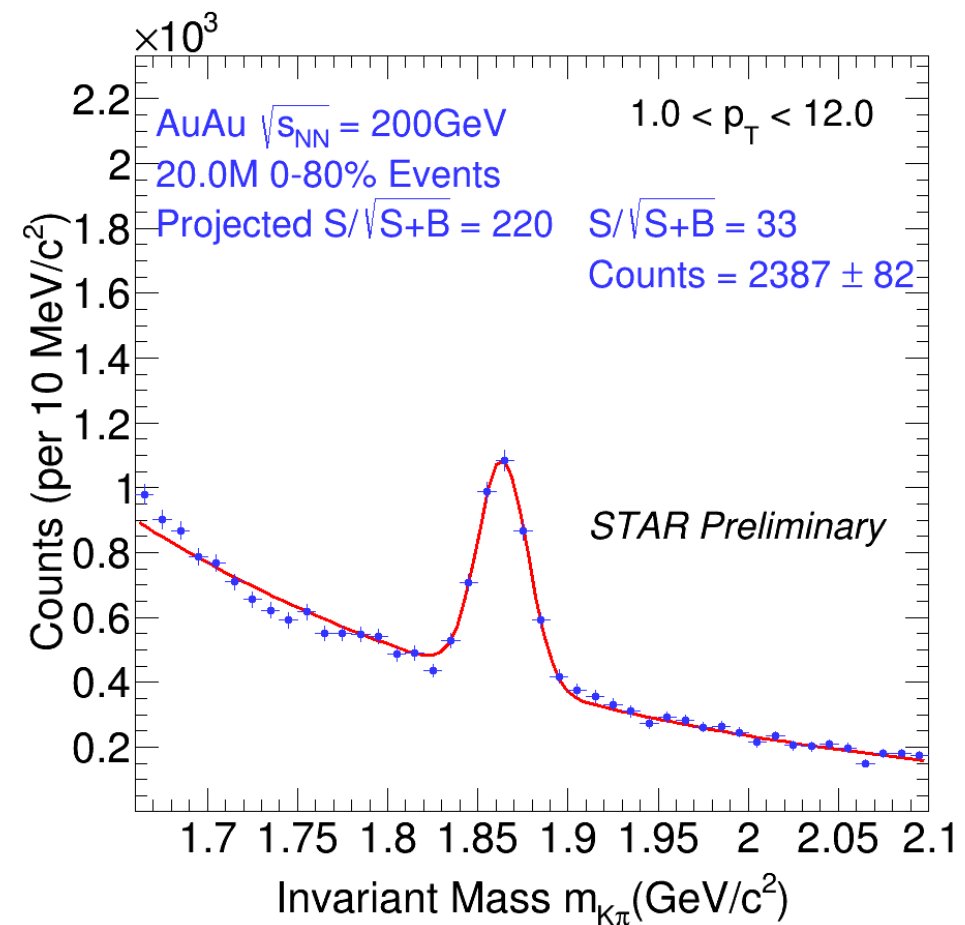
carbon fiber sector tubes
($\sim 200\text{ }\mu\text{m}$ thick)

STAR Pixel Detector – Performance



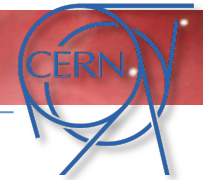
DCA pointing resolution

- ▶ 46 μm for 750 MeV/c Kaons
- ▶ ~ 30 μm for $p > 1 \text{ GeV}/c$



$D^0 \rightarrow K \pi$ production in $\sqrt{s_{NN}} = 200 \text{ GeV}$ Au+Au collisions

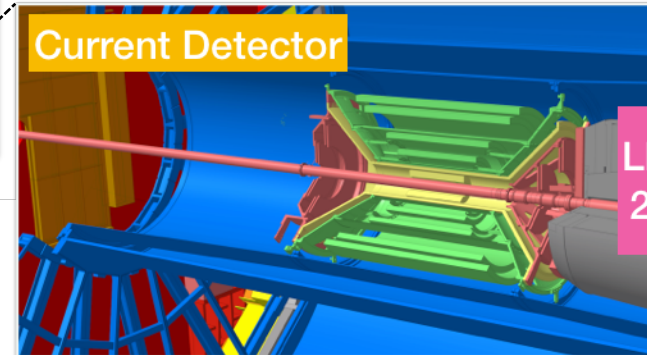
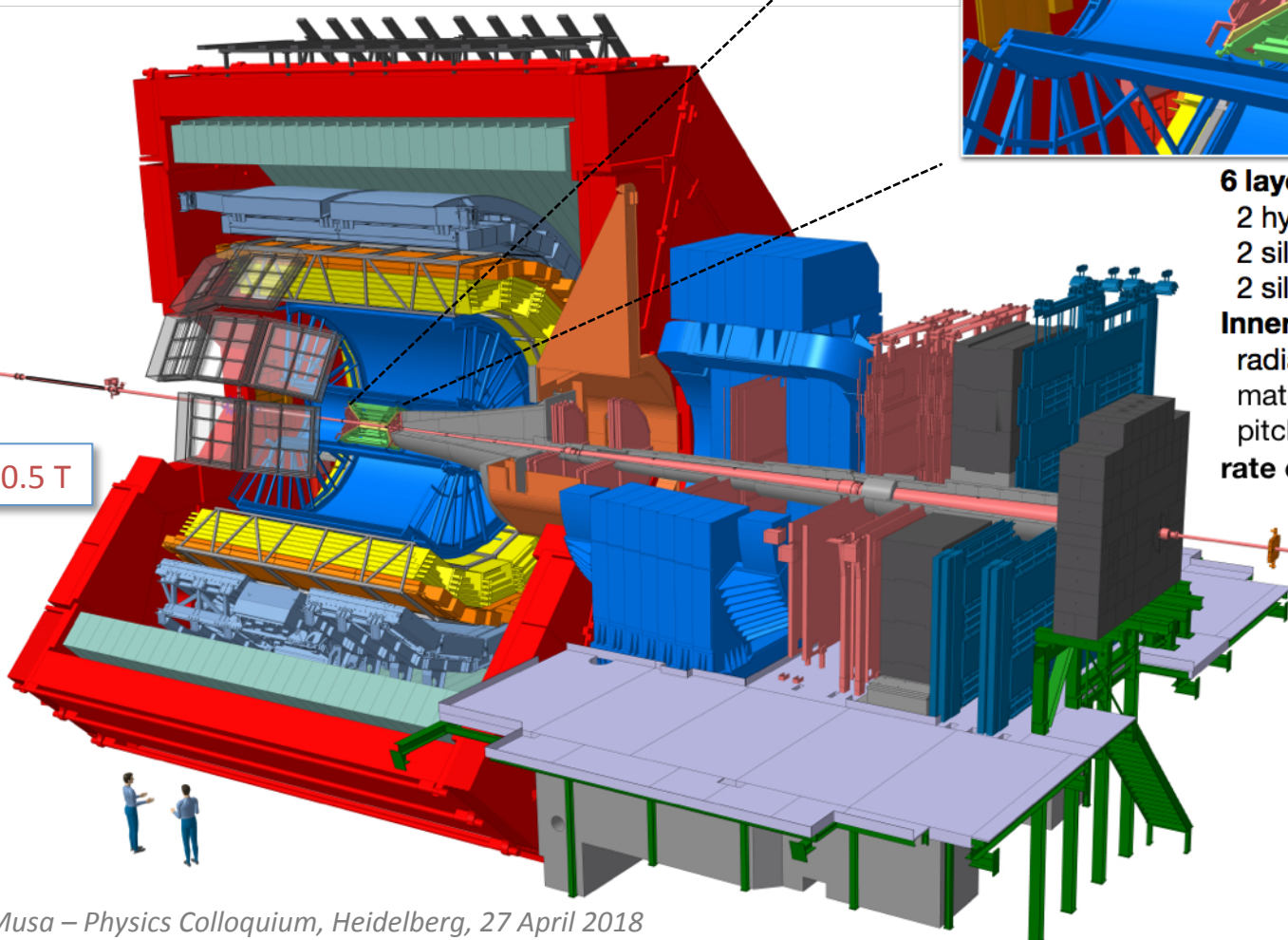
New Inner Tracking System based on CMOS sensors for ALICE



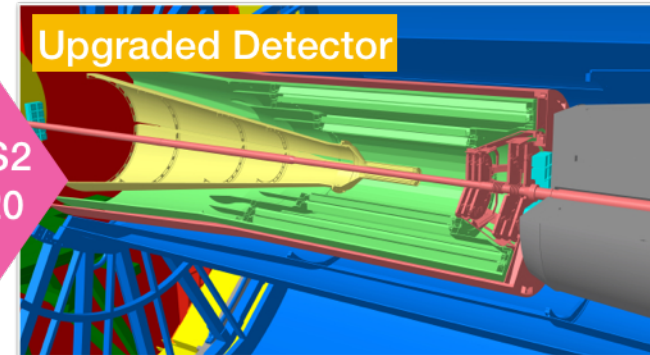
New Inner Tracking System (ITS)

- CMOS Pixels
- improved resolution, less material, faster readout

Novel MAPS technology



LHC LS2
2019/20



6 layers:

- 2 hybrid silicon pixel
- 2 silicon drift
- 2 silicon strip

Inner-most layer:

- radial distance: 39 mm
- material: $X/X_0 = 1.14\%$
- pitch: $50 \times 425 \mu\text{m}^2$

rate capability: 1 kHz

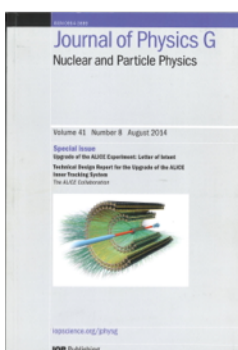
7 layers:

- all Monolithic Active Pixel Sensors

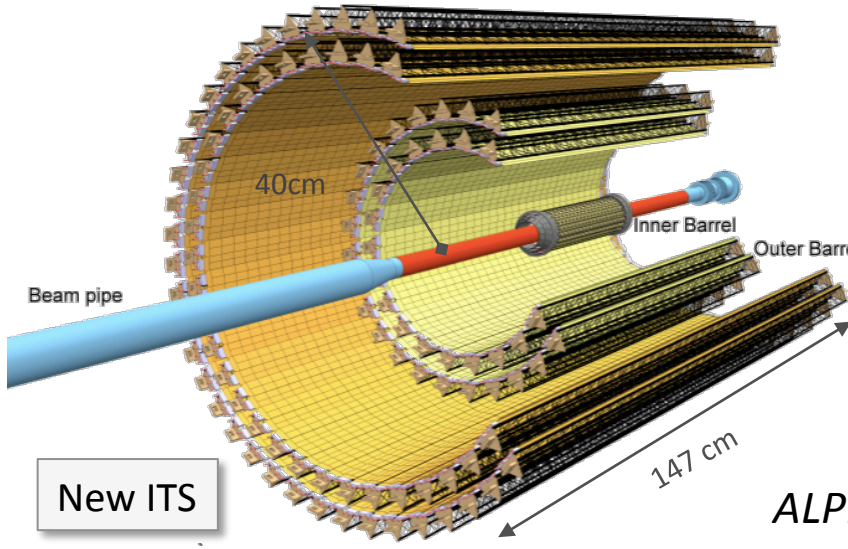
Inner-most layer:

- radial distance: 23 mm
- material: $X/X_0 = 0.3\%$
- pitch: $O(30 \times 30 \mu\text{m}^2)$

rate capability: 100 kHz (Pb-Pb)



A new ITS: closer to IP, thinner, higher position resolution



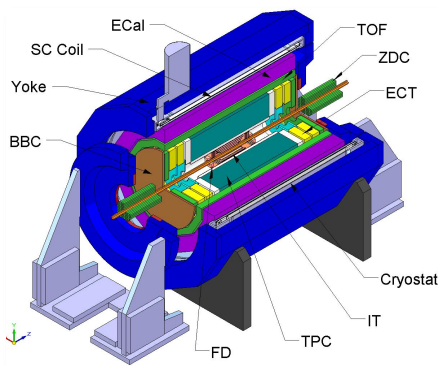
$1.5 \leq \eta \leq 1.5$

- Closer to IP: 39mm \rightarrow 22mm
- Thinner: $\sim 1.14\% \rightarrow \sim 0.3\%$ (for inner layers)
- Smaller pixels: $50\mu\text{m} \times 425\mu\text{m} \rightarrow 27\mu\text{m} \times 29\mu\text{m}$
- Increase granularity ($\times 10^3$): 20 chan/cm³ \rightarrow 2k pixel/cm³
- 10 m² active silicon area: **12.5 G-pixels, $\sigma \approx 5\mu\text{m}$**

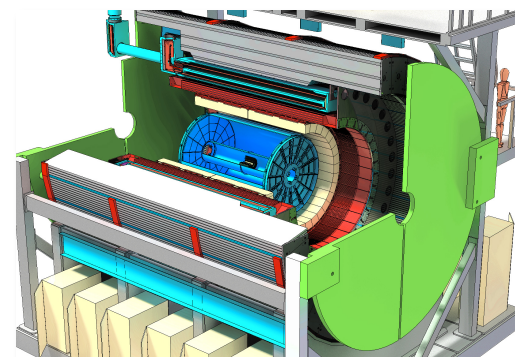
ALPIDE (ALICE Pixel Detector) - Developed for the ALICE upgrade (ITS and MFT)

will be used (or it is proposed) for several other HEP detectors and non HEP applications

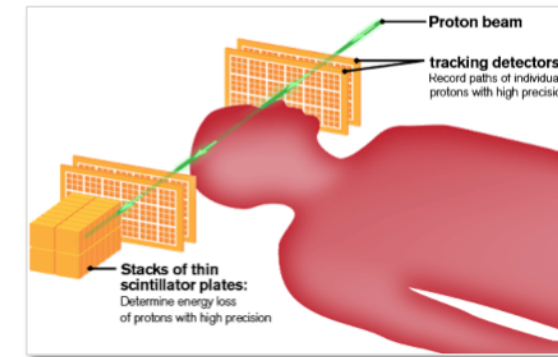
NICA MPD (@JINR)



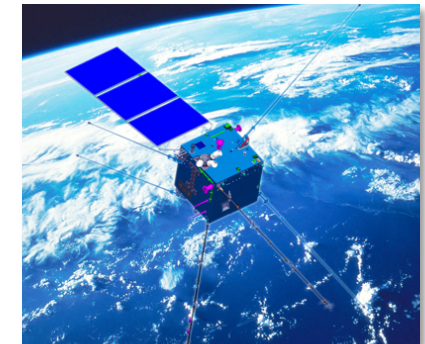
sPHENIX (BNL)



proton CT (tracking)

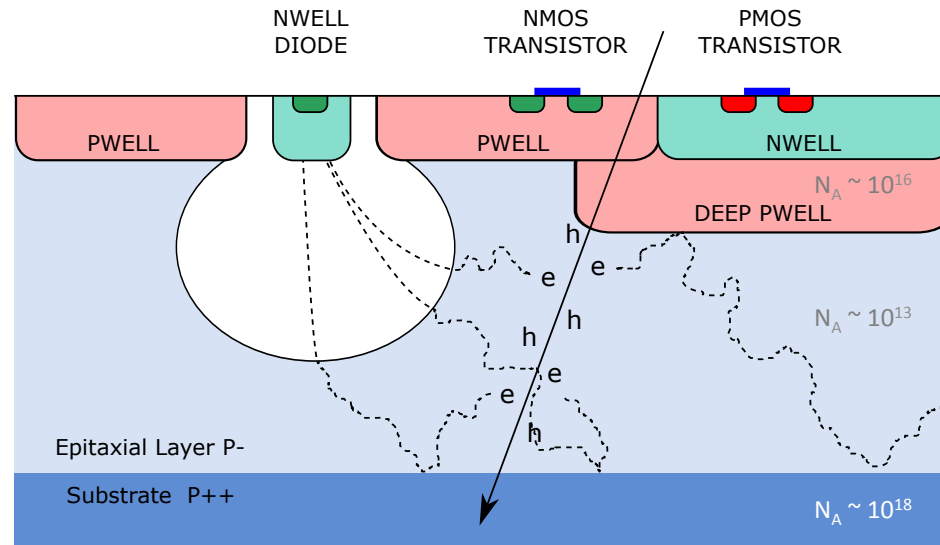


CSES – HEPD2



...

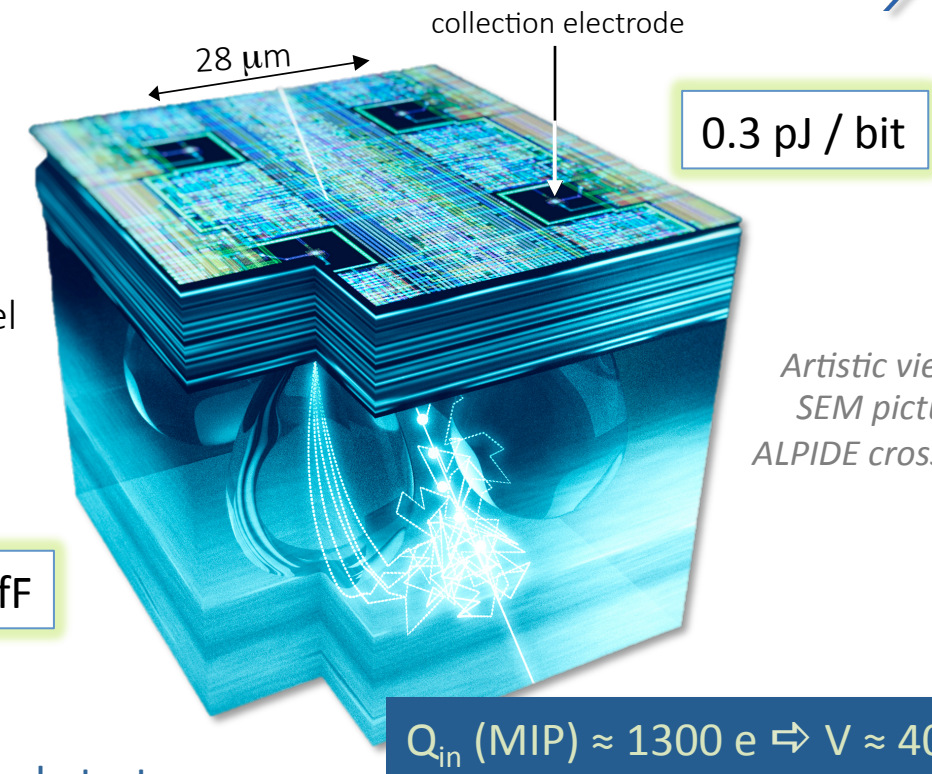
CMOS Pixel Sensor using $0.18\mu\text{m}$ CMOS Imaging Process



pixel capacitance $\approx 5 \text{ fF}$ (@ $V_{bb} = -3 \text{ V}$)

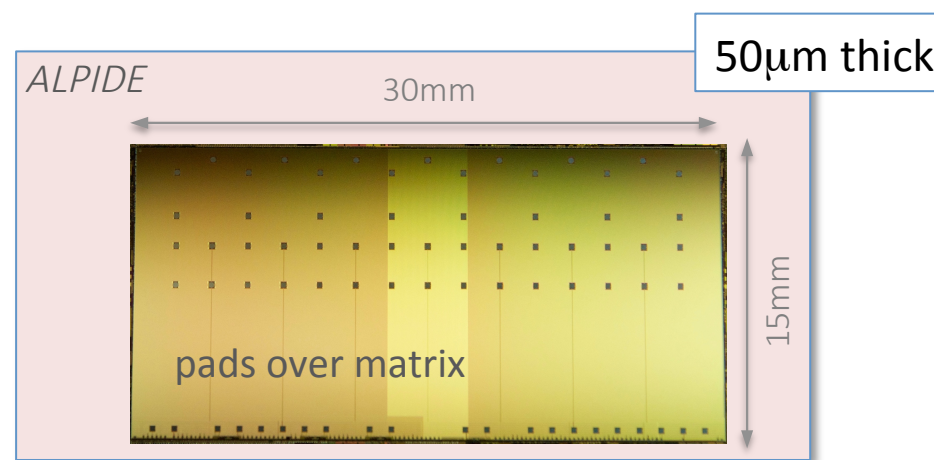
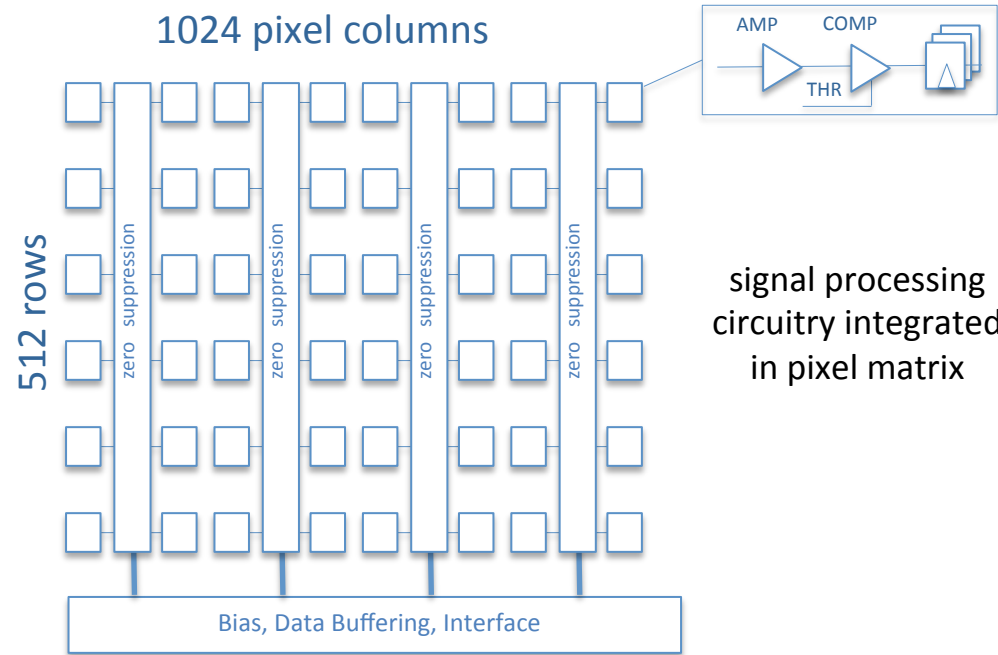
- ▶ High-resistivity ($> 1\text{k}\Omega \text{ cm}$) p-type epitaxial layer ($25\mu\text{m}$) on p-type substrate
- ▶ Small n-well diode ($2 \mu\text{m}$ diameter), ~ 100 times smaller than pixel => low capacitance ($\sim \text{fF}$)
- ▶ Reverse bias voltage ($-6\text{V} < V_{BB} < 0\text{V}$) to substrate (contact from the top) to increase depletion zone around NWELL collection diode
- ▶ Deep PWELL shields NWELL of PMOS transistors

→ full CMOS circuitry within active area

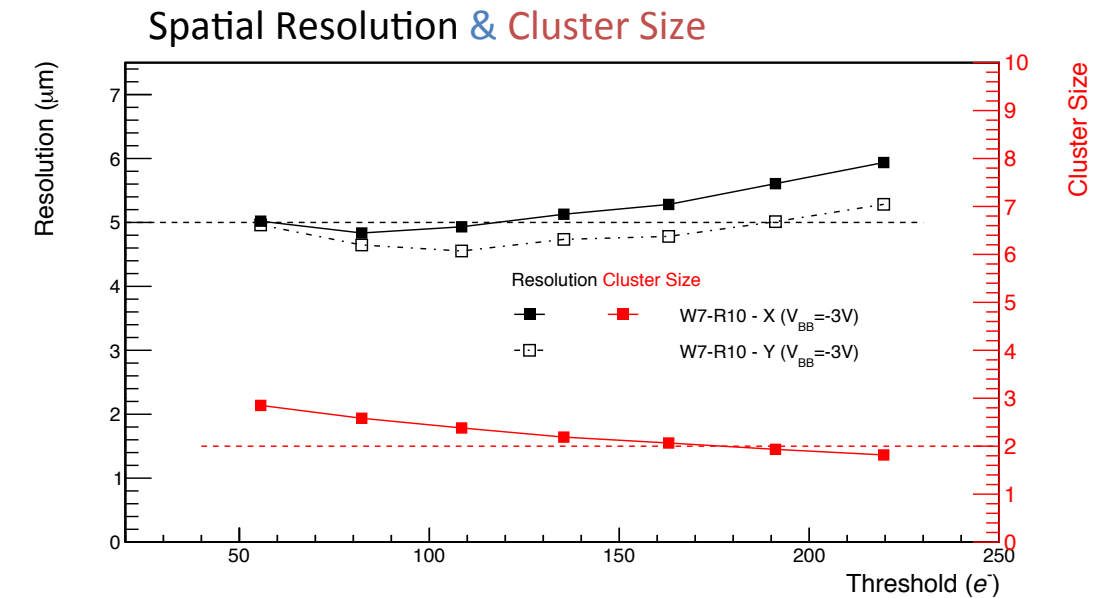


Artistic view of a SEM picture of ALPIDE cross section

ALICE CMOS Pixel Sensor



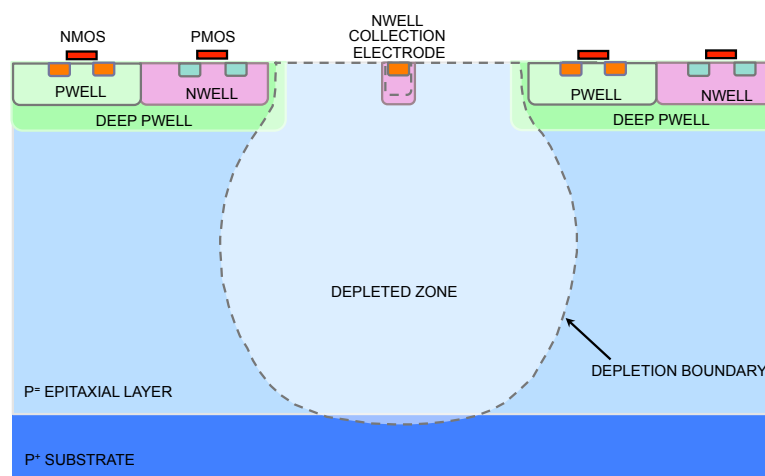
130,000 pixels / cm^2 $27 \times 29 \times 25 \mu\text{m}^3$
charge collection time $< 10\text{ns}$ ($V_{bb} = -3\text{V}$)
spatial resolution $\sim 5 \mu\text{m}$
max particle rate $\sim 100 \text{ MHz} / \text{cm}^2$
fake-hit rate: $< 10^{-9} \text{ pixel} / \text{event}$
power : $\approx 300 \text{ nW} / \text{pixel}$



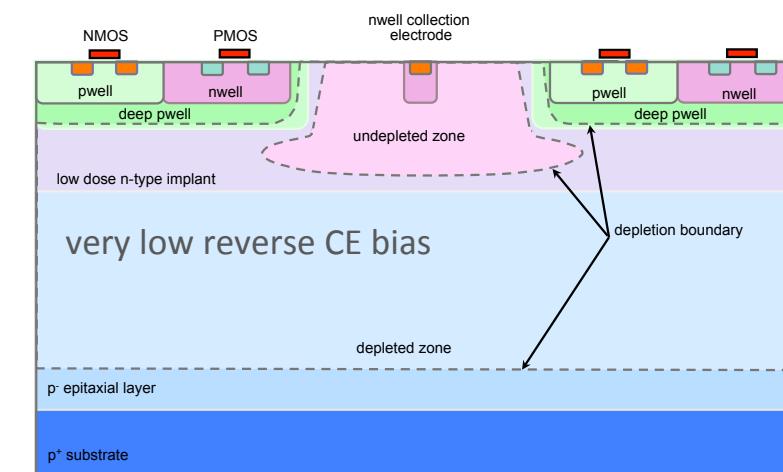
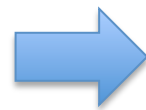
CMOS APS Fully Depleted

Improving timing performance and radiation tolerance

A **process modification** for **CMOS Active Pixel Sensors** for enhanced depletion, timing performance and radiation tolerance



Standard Process (+DEEP PWELL)



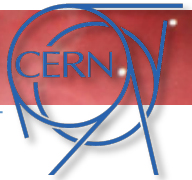
Modified Process with low-dose n-type implant (+DEEP PWELL)

The process modification requires a single additional process mask with no changes on the sensor and circuit layout

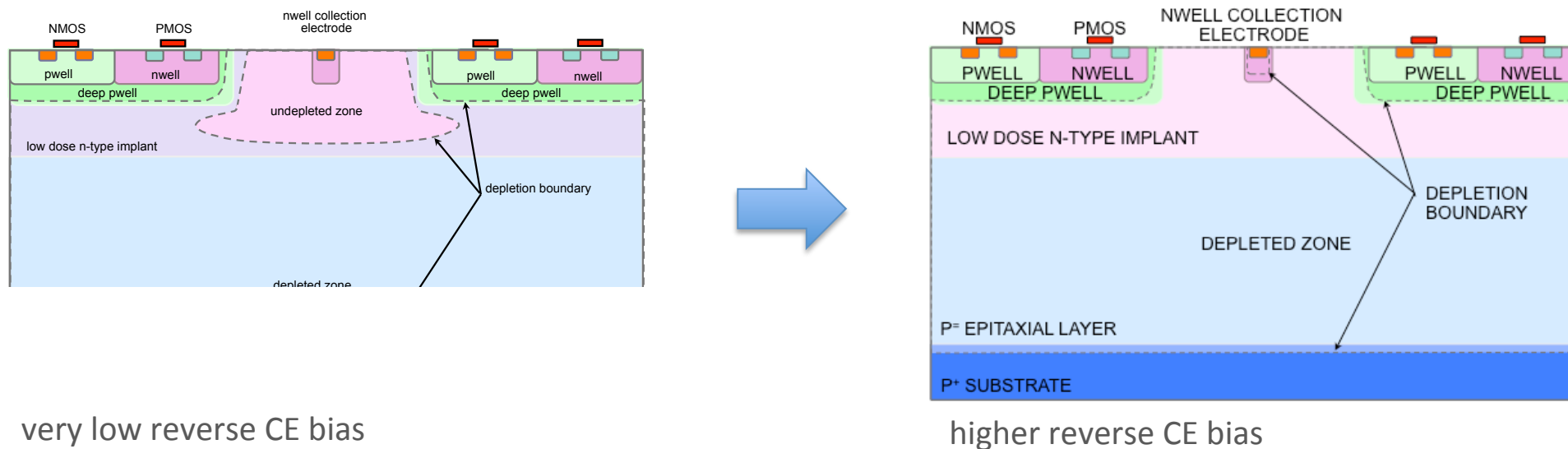
For details on process modification and experimental results see: NIM, A 871C (2017) pp. 90-96 (CERN/Tower)

The ALICE test vehicle chip (investigator) and prototype ALPIDE chips exist with both flavors

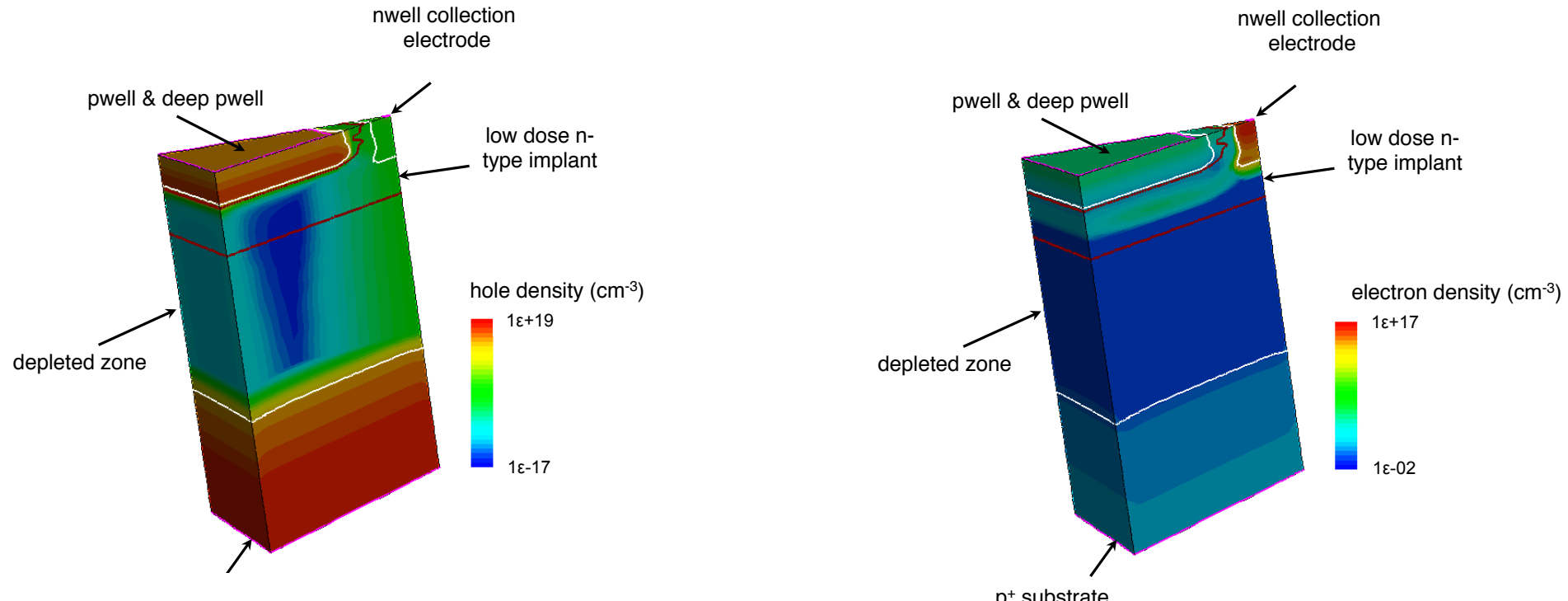
A process modification for CMOS APS for full depletion



Depletion of the low-dose implant up to the Charge Collection Electrode (NWELL) is obtained at moderate reverse bias voltage ($\approx -5V$)



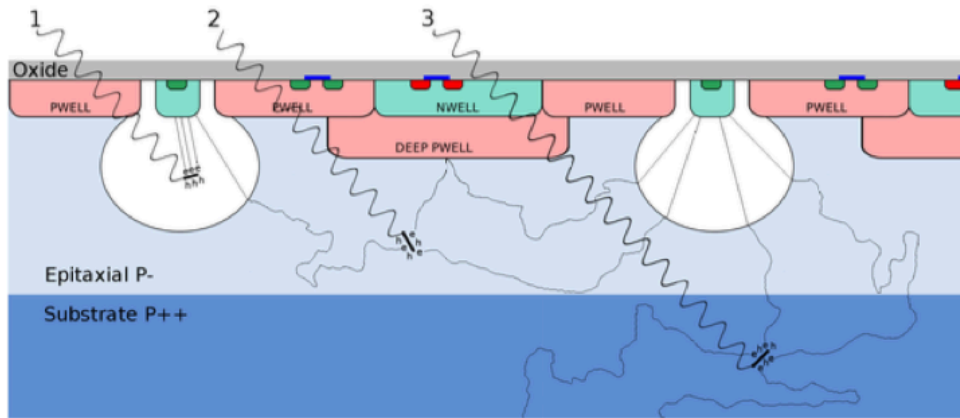
Depletion of the epitaxial layer and the low dose implant



$$\text{High-res} = 18\mu\text{m}, V_{CE} = 5\text{V}, V_{\text{substrate}} = -15\text{V}$$

Simulated hole (left) and electron (right) densities. The junctions are indicated with a red line and the edge of the depleted cone with white lines.

A process modification for CMOS APS for full depletion

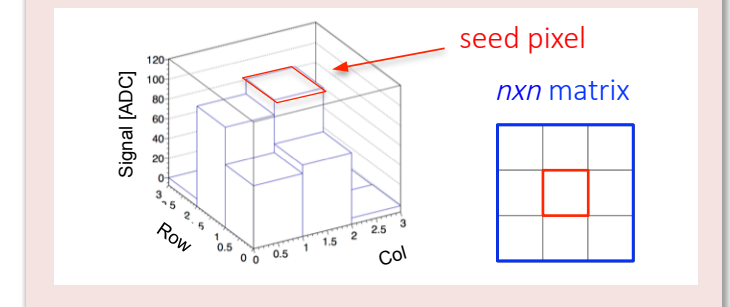
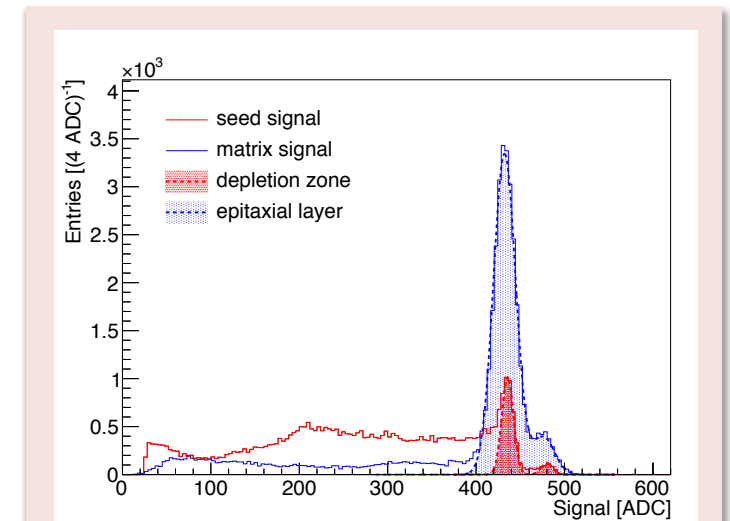


^{55}Fe : two X-Ray emission modes:

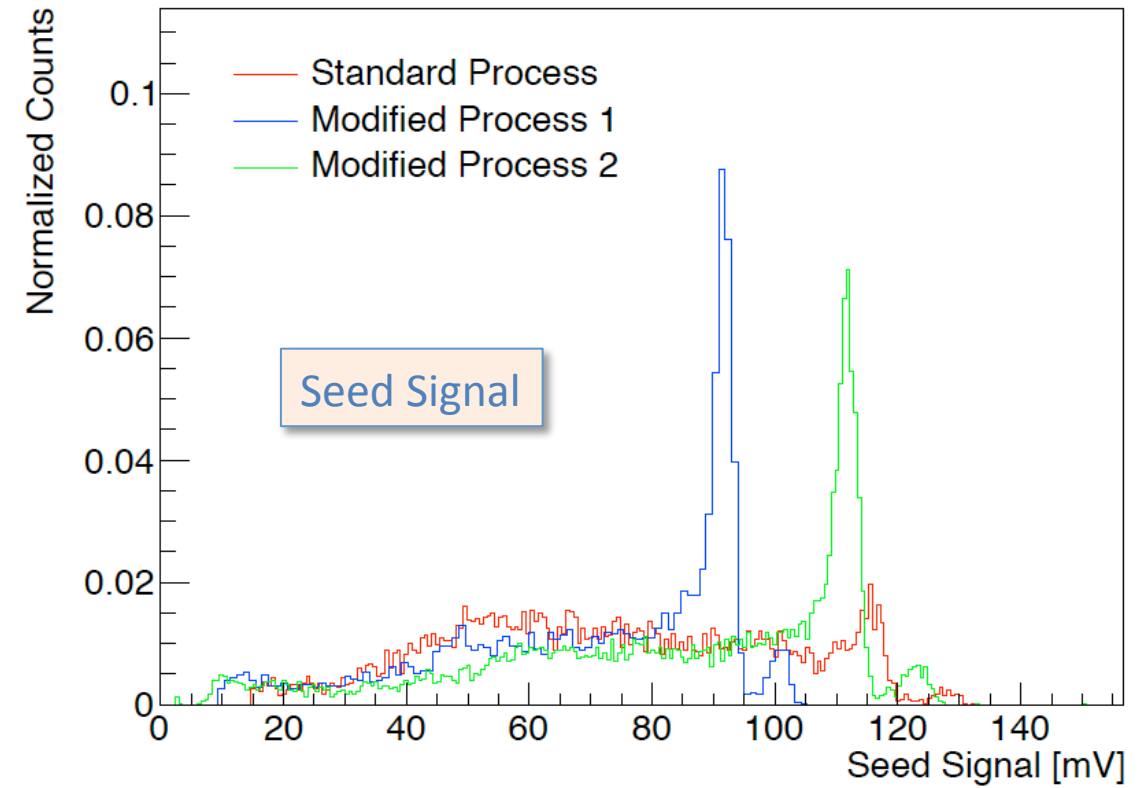
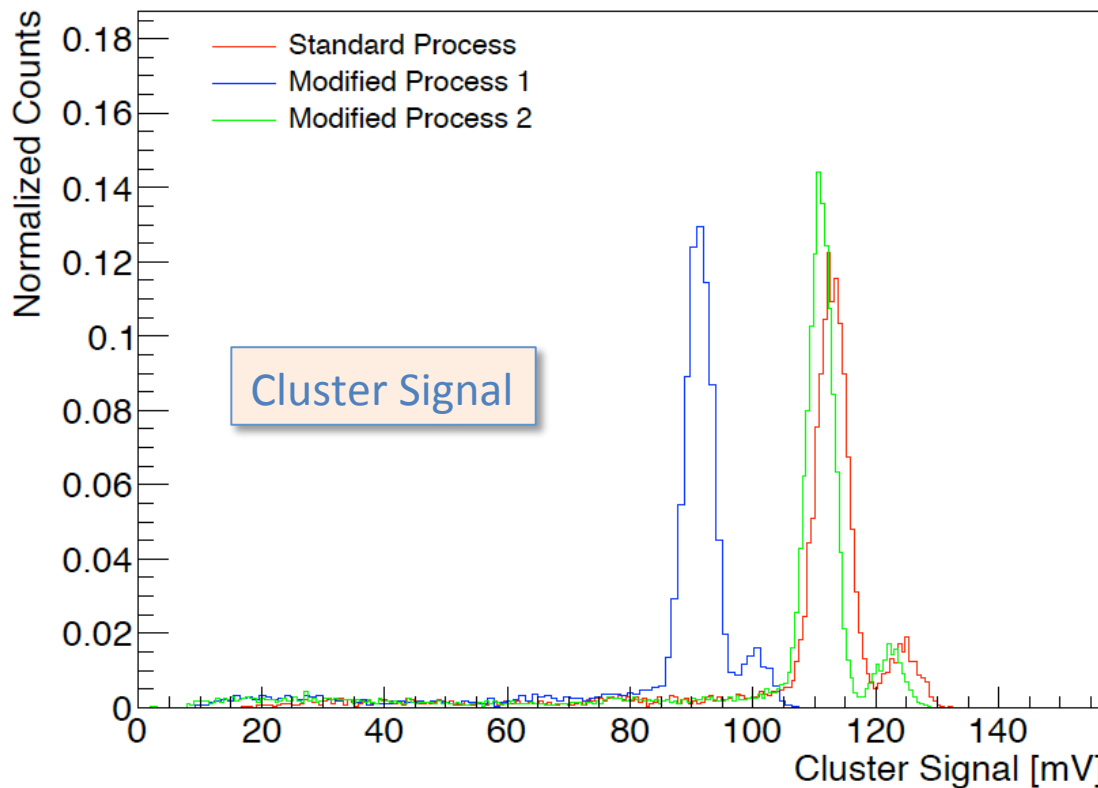
1. K- α : 5.9 keV (1640 e/h), rel. freq.: 89.5% atten. length in Si: 29 μm
2. K- β : 6.5 keV (1800 e/h), rel. freq.: 10.5% atten. length in Si: 37 μm

For X-Ray absorption in sensor with the std process three cases can be defined:

1. Absorption in depletion volume: charge collected by drift, no charge sharing, single pixel cluster:
 - Events populate the calibration peak in signal histograms
 - charge collection time expected to be $\approx 1\text{ns}$
2. Absorption in epitaxial layer: charge partially collected by diffusion and then drift, charge sharing between pixels depending on position of X-Ray absorption
 - Charge collection depends on distance of the X Ray absorption from depletion
3. Absorption in substrate
 - Contribution depending on depth of X-Ray absorption position in substrate and charge carrier lifetime within substrate

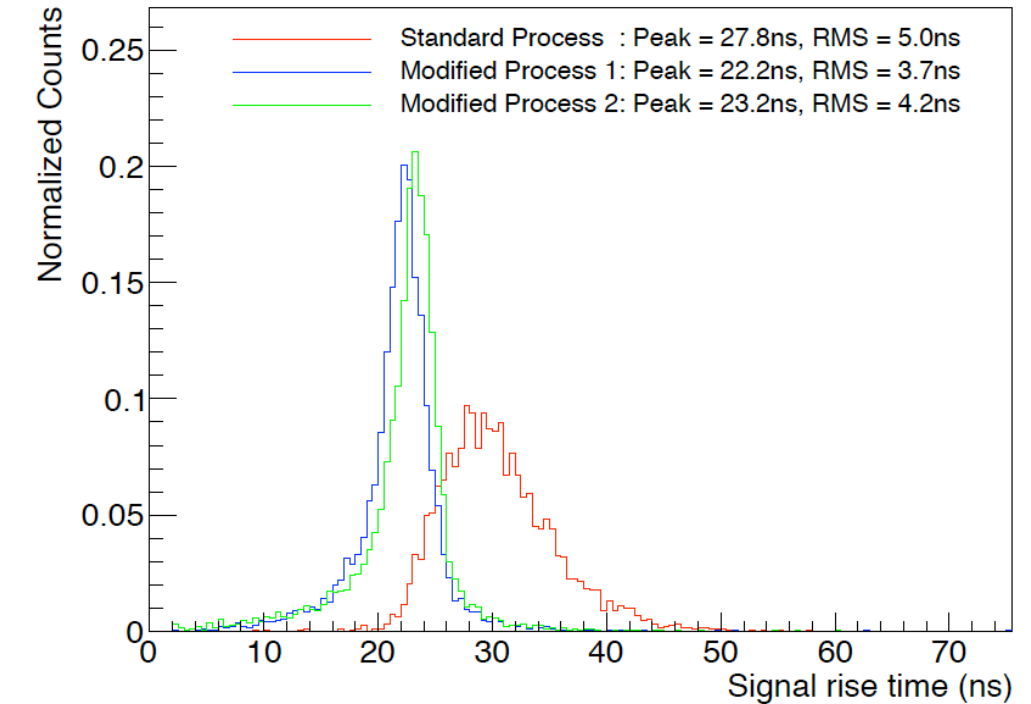
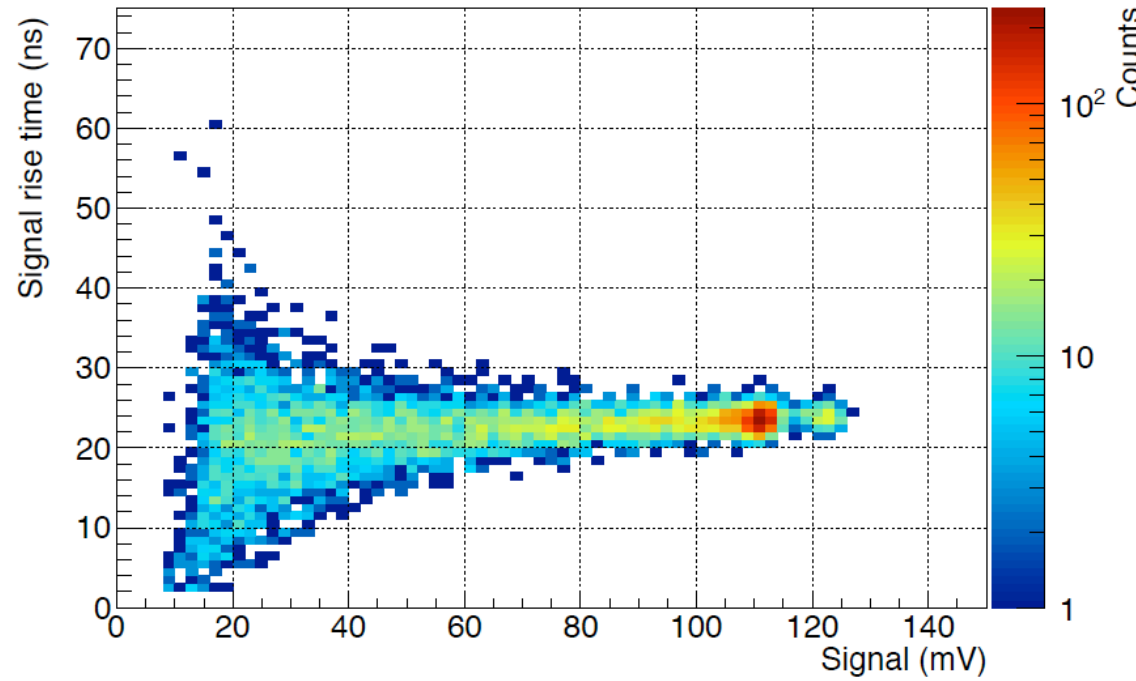


Experimental Results with the INVESTIGATOR CHIP (an ALICE test vehicle chip)



Signal and cluster distribution from a ^{55}Fe radioactive source measured at room temperature for standard and modified process with higher (modified process 1) and lower (modified process 2) dose for the low-dose implant

Experimental Results with the INVESTIGATOR CHIP (an ALICE test vehicle chip)



Charge collection time vs. signal (left) and signal rise time distribution (right) from a ^{55}Fe radioactive source for standard and modified process with higher (modified process 1) and lower (modified process 2) dose

Time resolution limited by chip output buffer speed ($\approx 20\text{ns}$) and noise

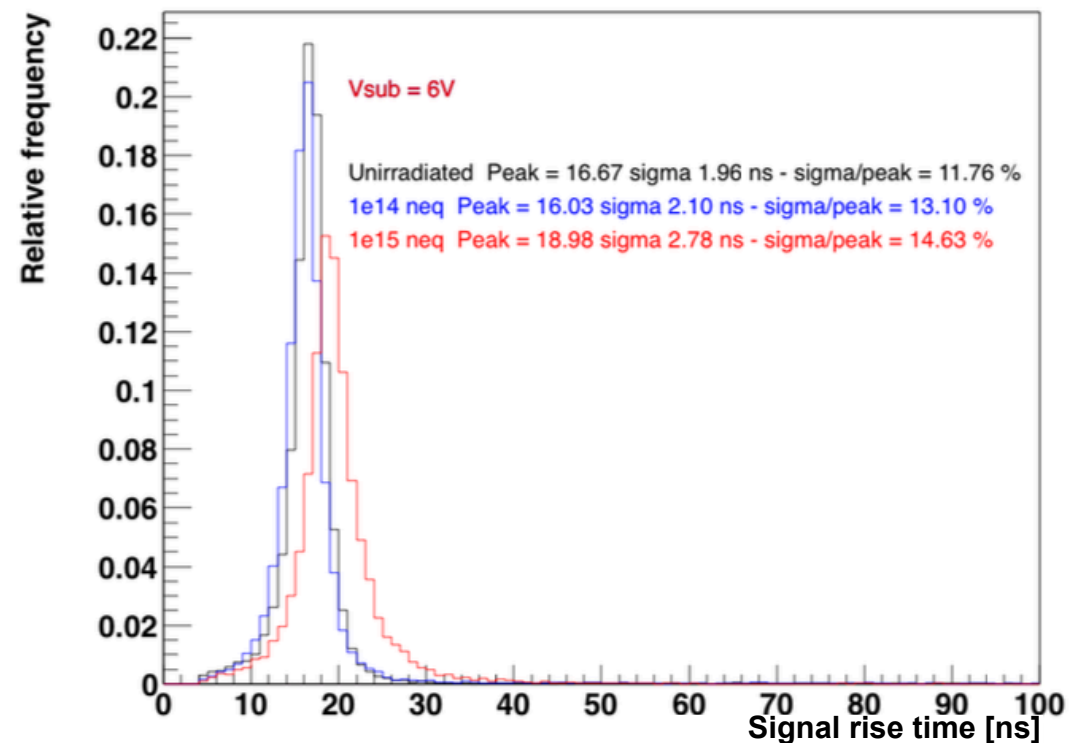
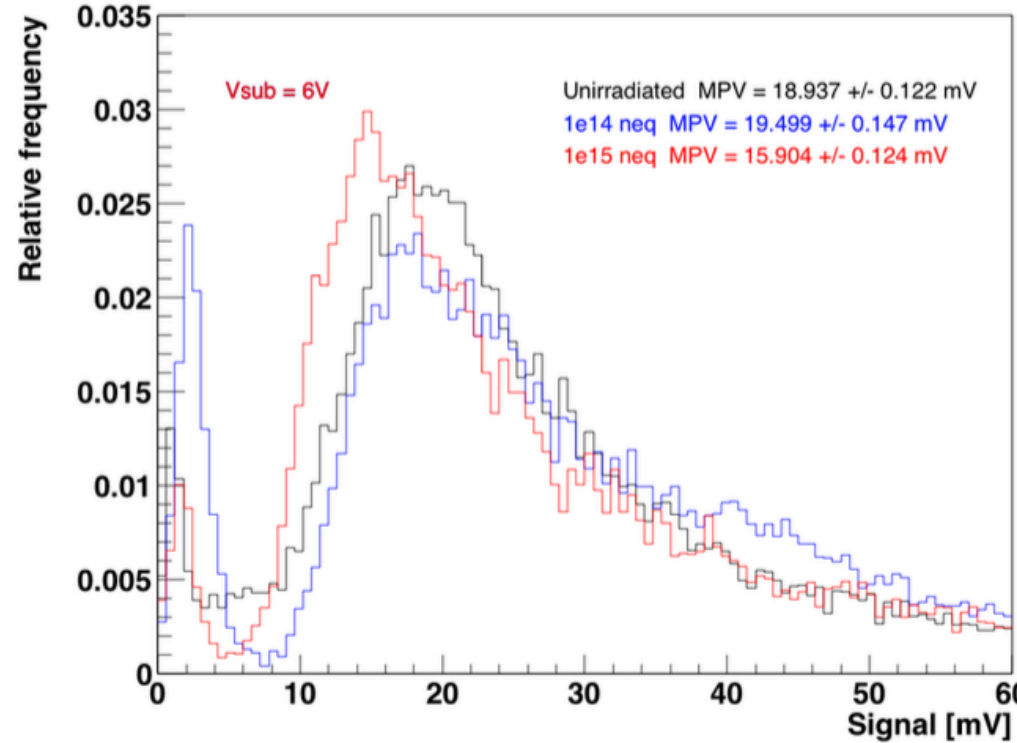
A new version of the investigator chip w/o buffer speed limitation is being tested now

A process modification for CMOS APS for full depletion



^{90}Sr measurements on modified-process (INVESTIGATOR chip)

Non-irradiated, $1\times 10^{14} \text{ 1MeV n}_{\text{eq}}/\text{cm}^2$ (NIEL) and 100 krad (TID), $1\times 10^{15} \text{ 1 MeV n}_{\text{eq}}/\text{cm}^2$ (NIEL) and 1Mrad (TID)

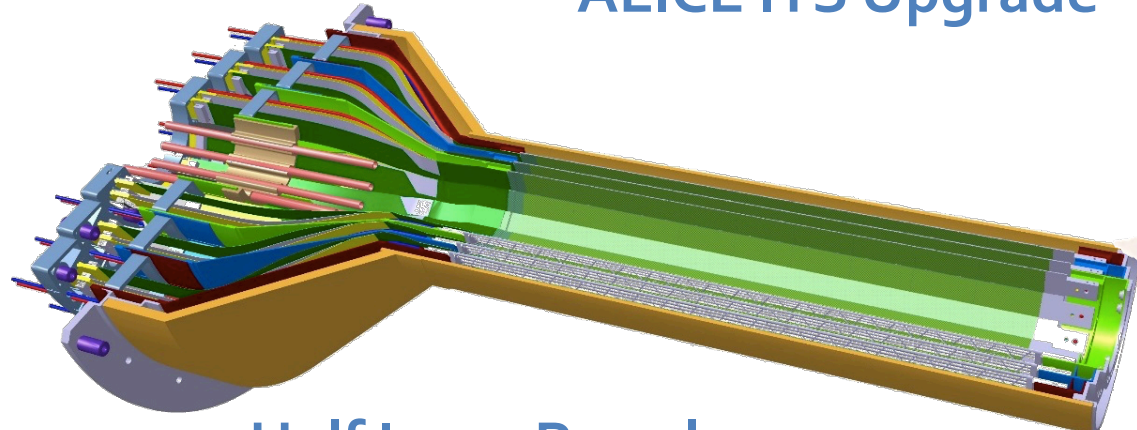


Little signal loss after irradiation, signal well separated from noise

Ultra-lightweight Vertex Detector

Approaching 0-mass detector

ALICE ITS Upgrade

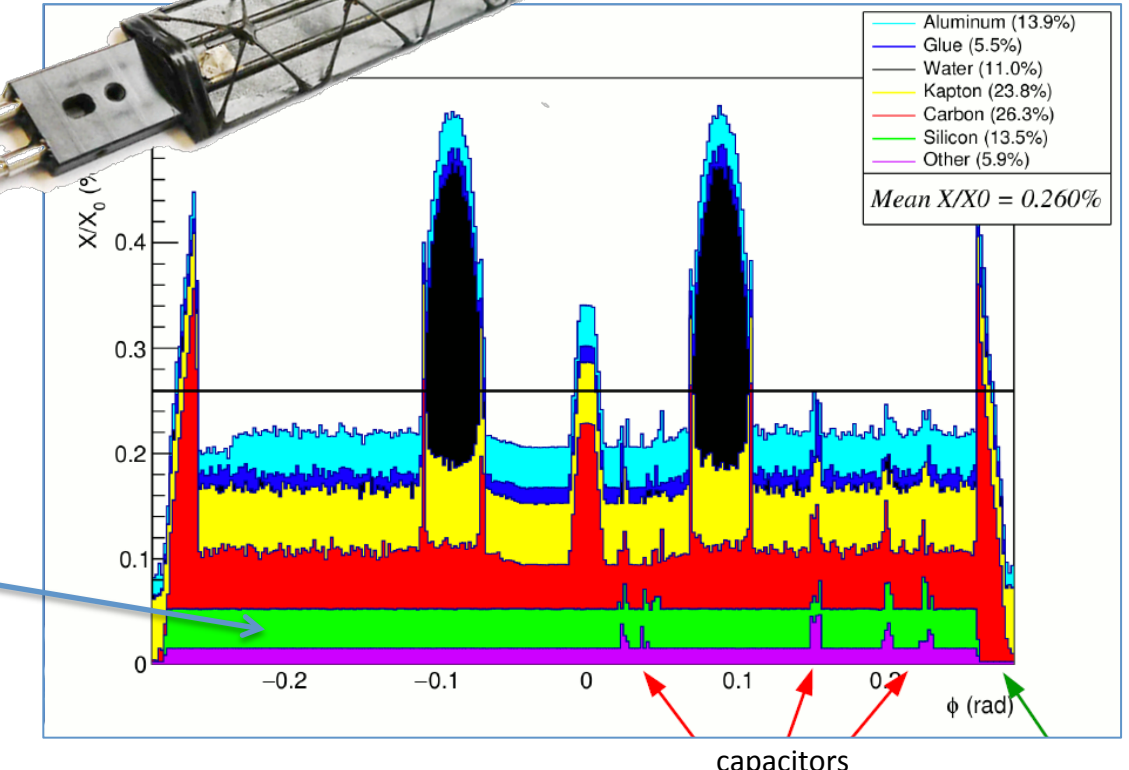


Half Inner Barrel

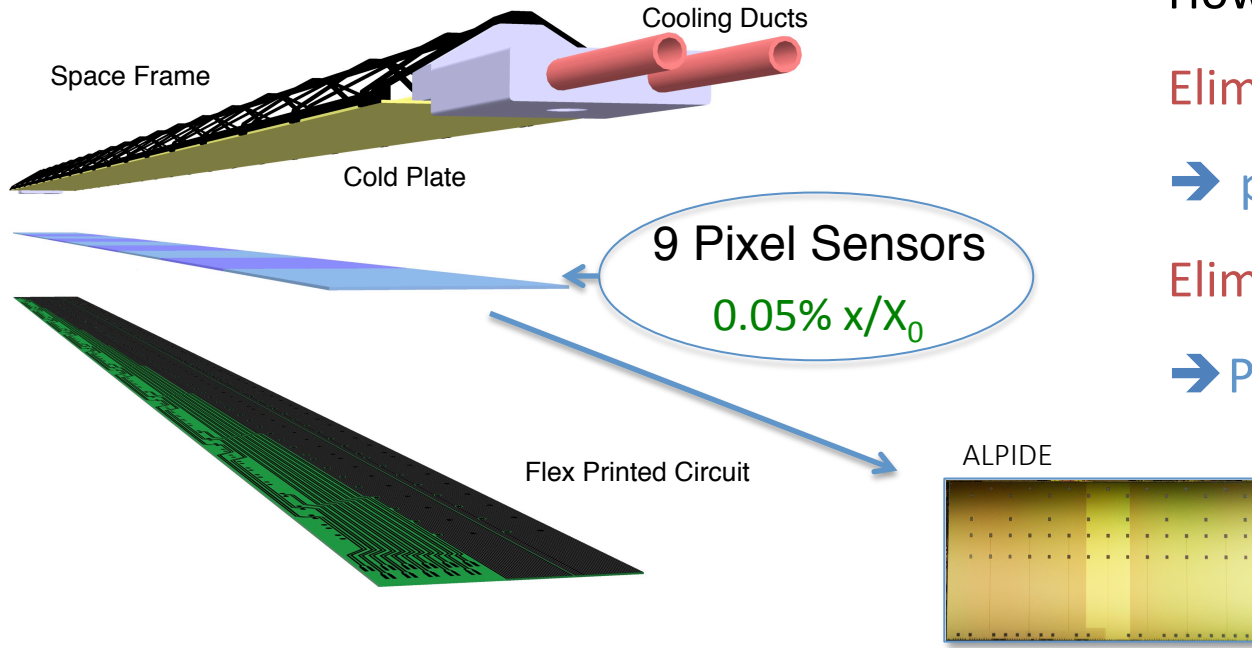
Inner Barrel Stave



Silicon sensor + readout circuitry
only 13% of the total material budget



Can we further reduce the mass of a vertex detector?



ALPIDE Chip: pixel matrix power $\sim 7\text{mW/cm}^2$...
... the rest ($\sim 30\text{mW/cm}^2$) is dissipated at the sensor periphery

Can we put the circuit periphery at the periphery of the detector?

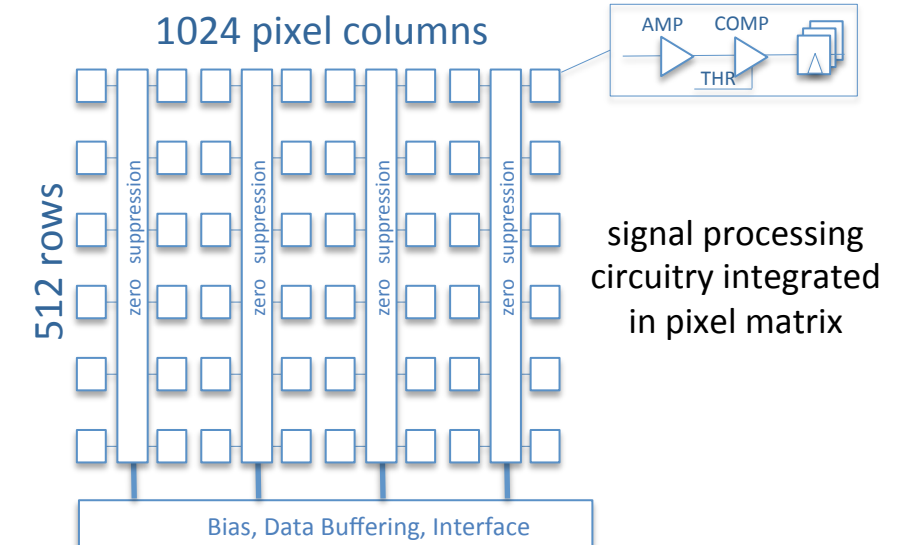
How to further reduce material budget?

Eliminate active cooling

→ possible for power densities below 20mW/cm^2

Eliminate electrical substrate

→ Possible if sensor covers the full stave length

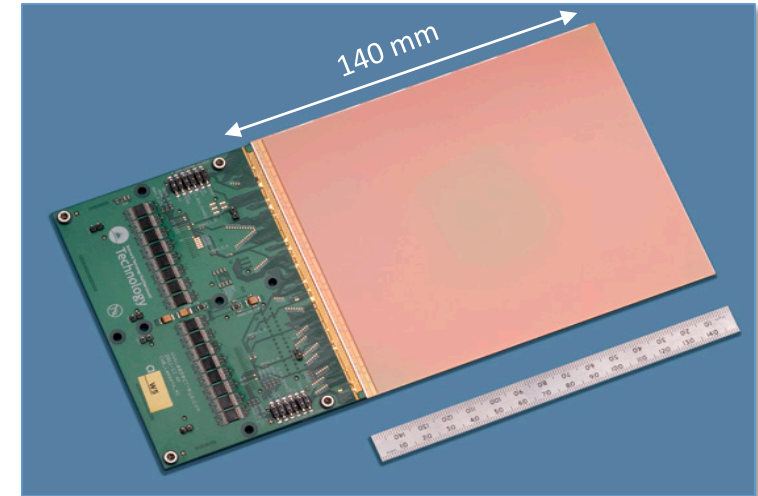
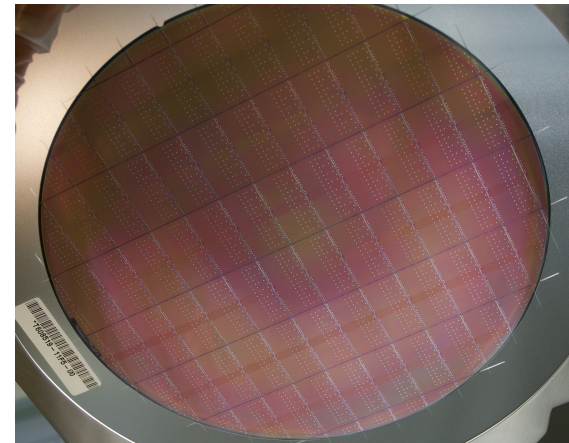


What's next? - Future R&D opportunities using CMOS technologies



Stitching allows building circuits as large as an entire wafer (standard process for several CIS technologies)

1-D or 2-D stitched version of a sensor chip



Stitching available also for 300mm technologies

The use of CMOS and stitching technologies open new opportunities

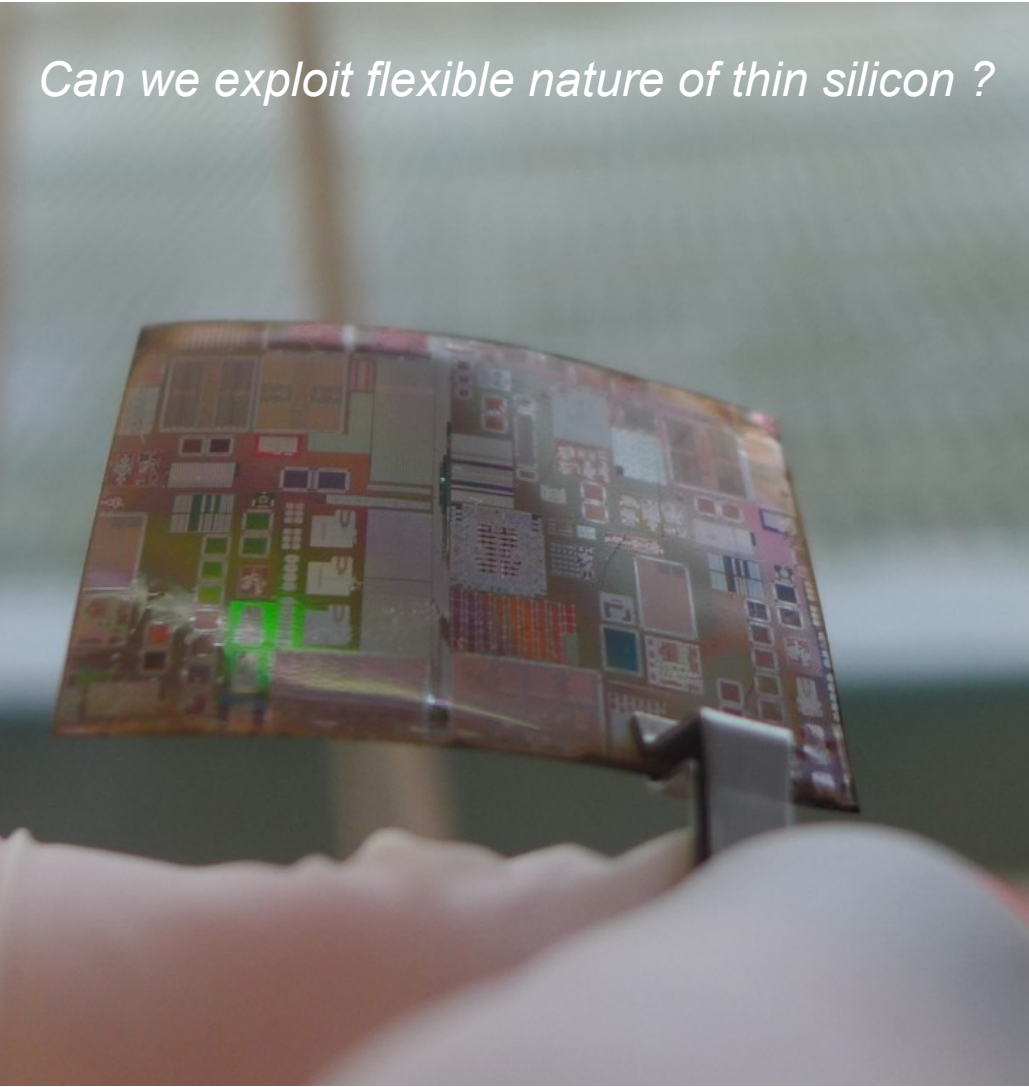
⇒ **Vertex detectors, large area tracking detectors, digital calorimeters**

- enhanced performance (spatial and time resolution)
- reduction of power consumption and material budget

large cost saving due to low production costs

Migration to smaller technology nodes (180nm ⇒ 65nm, 40nm) ⇒ large power reduction

What's next? - Future R&D opportunities using CMOS technologies



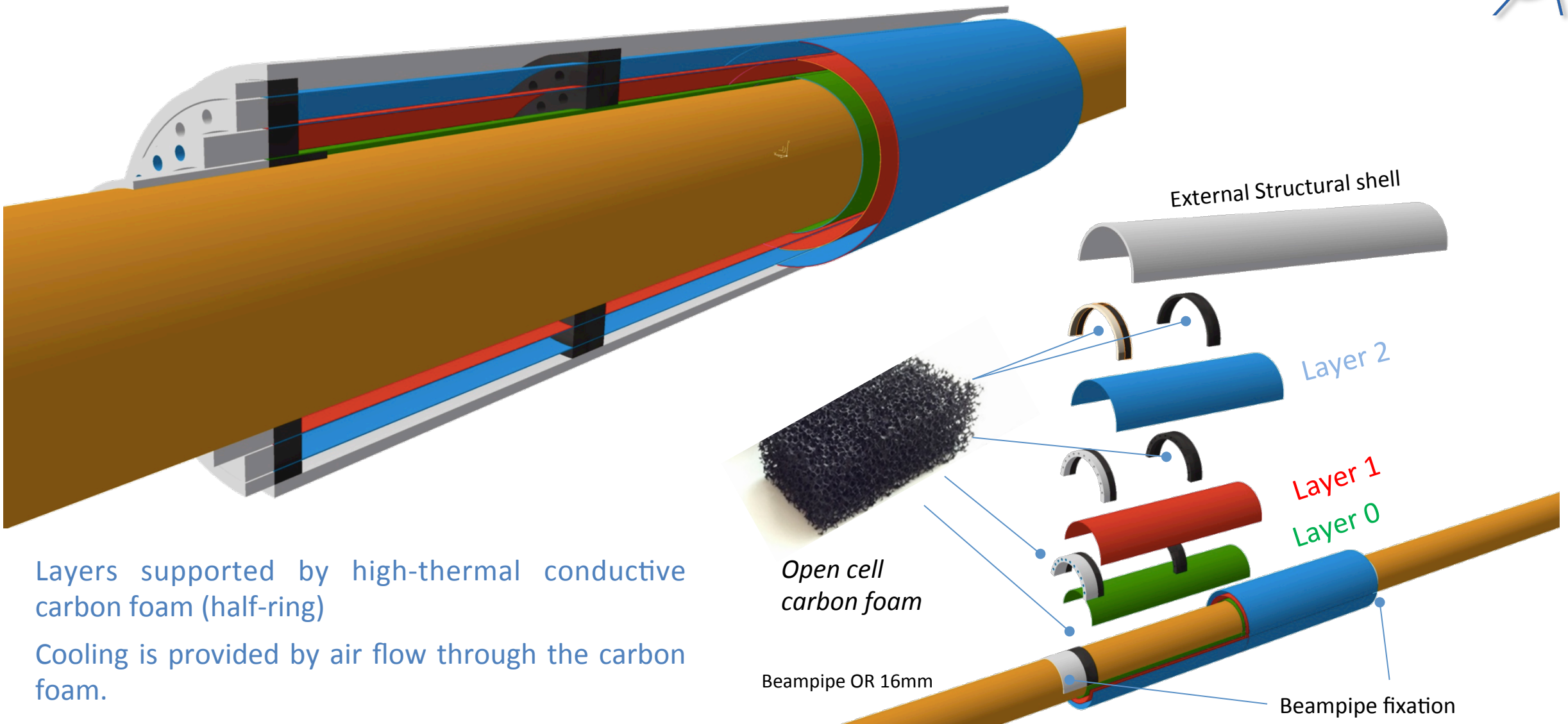
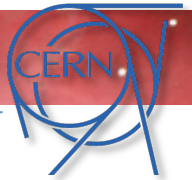
Can we exploit flexible nature of thin silicon ?



Ultra-thin chip (<50 um): flexible with good stability

Silicon Genesis: 20 micron thick Si wafer

“Silicon-only” Cylindrical Vertex Detector (Inner Barrel)



A 3D Pixel Chamber

Active target using CMOS APS

Studies on **3D Pixel Chamber Imager** for measuring **charm and beauty** at a fixed target experiment

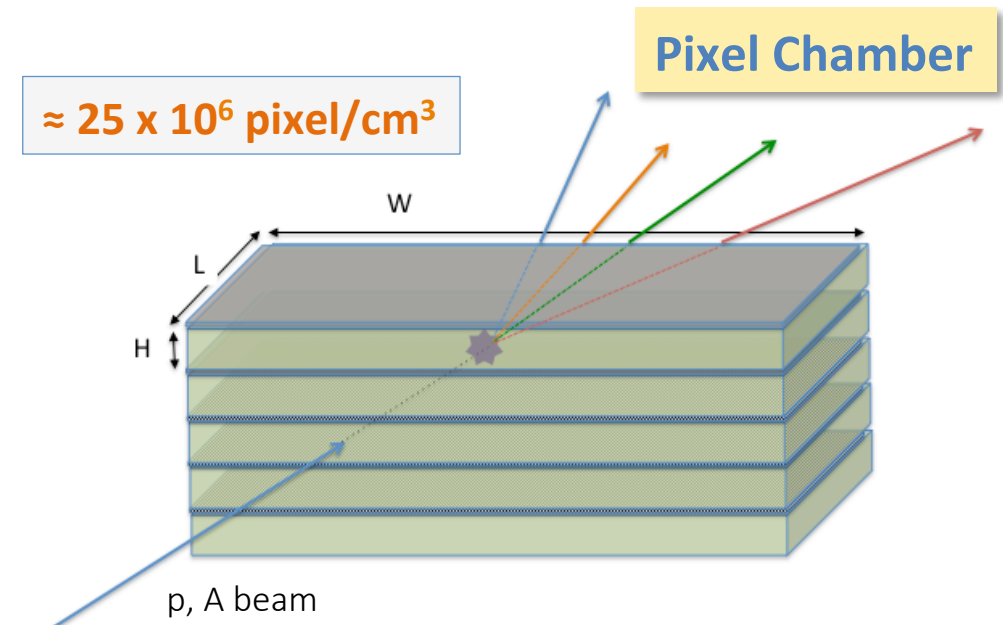
The heart is a **3D pixel chamber** used as active target

The idea is to have a detector able to provide the image of the proton-nucleus or nucleus-nucleus interaction and track the particles generated in the inelastic collision just starting at the interaction point

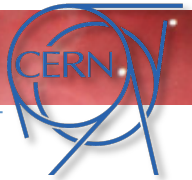
The pixel chamber is realized with a stack-up of **thin CMOS sensors** providing **truly 3D (almost) continuous tracking** with a **precision of few microns** for very high rate and multiplicity environment

Nuclear interaction inside a stack-up of N fine pitch pixel sensor

- $N \approx 100$, $H \sim 50\mu\text{m}$, $L \approx 0.1$ nuclear collision length ($\approx 30\text{mm}$)
- *cm boost: ≈ 14 at $400\text{ GeV}/c$ (SPS), ≈ 60 at 7TeV (LHC)*



A pixel chamber as heavy-flavour imager



Using ALPIDE, **Pixel Chamber Detector** with a volume of about $15(w) \times 30(L) \times 5(H)$ mm 3

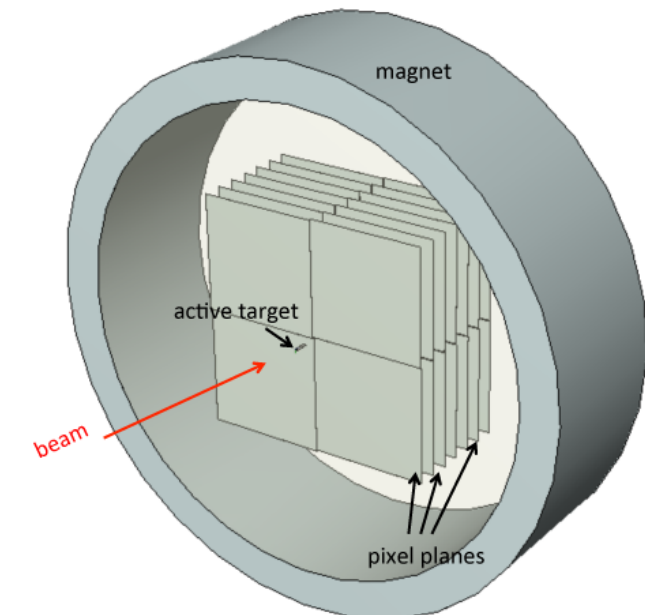
- segmented in pixels of about $27 \times 29 \times 50$ μm^3
- providing the measurement of 25×10^6 space points / cm 3
- with a spatial resolution of $\approx 5\mu\text{m}$ in the three dimensions

Besides the huge granularity which ensures a three-dimensional image-like reconstruction of the event, this detector is sufficiently radiation hard (10^{14} - 10^{15} 1MeV n_{eq}) and fast for measurements in fixed-target mode (integration time O(1μs)).

The Pixel Chamber is coupled to a compact silicon telescope immersed in a magnetic field of few tesla for precise measurement of particle momenta.

In this way a very compact instrument for imaging of heavy flavors with unprecedented precisions can be realized.

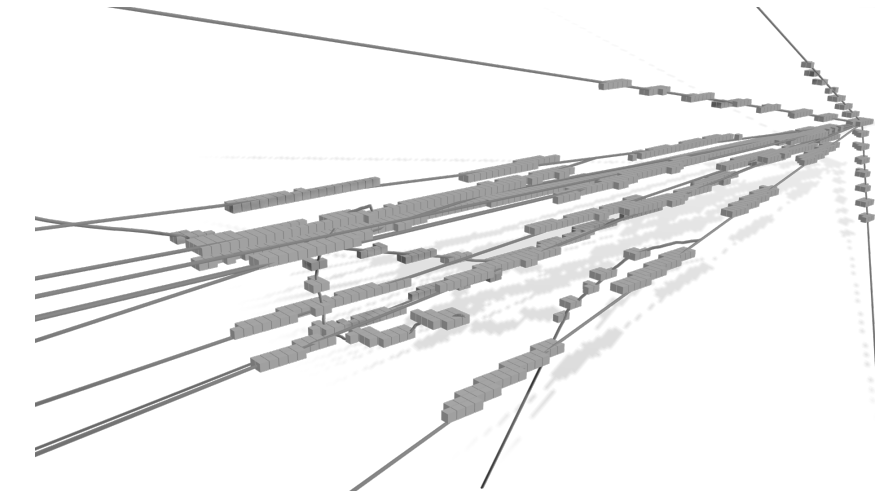
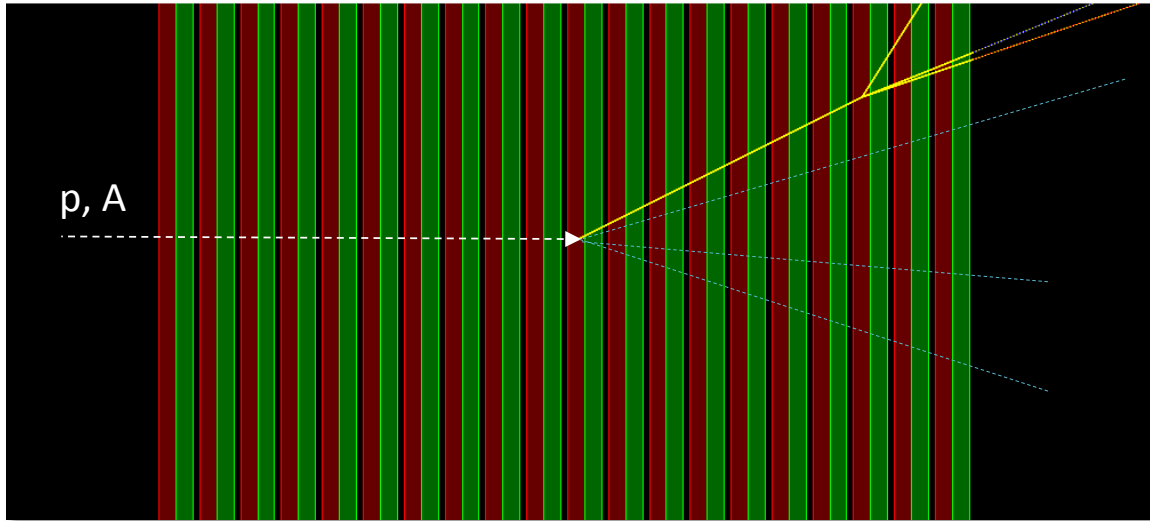
The detector could also be complemented with other detectors specialized for specific measurements (e.g. electrons, muons, photons)



Pixel Chamber - proof of principle demonstrator



A different configuration based on planes transverse to the beam direction

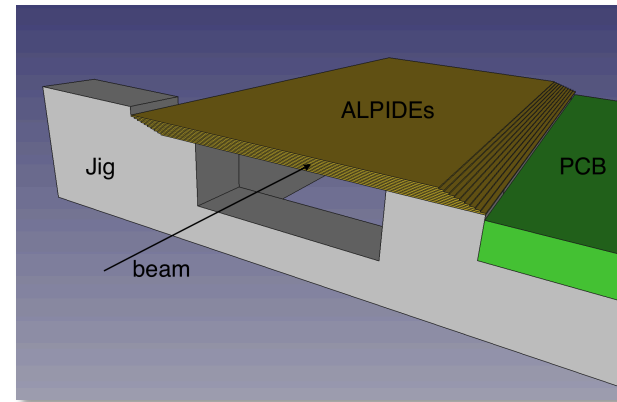


GEANT Simulation

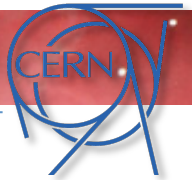
The target is a different material, which is used as support and cold plate for the sensors

Demonstrator will be
tested at SPS summer 2018

Pixel Chamber + telescope
to measure beam position
and emerging particles

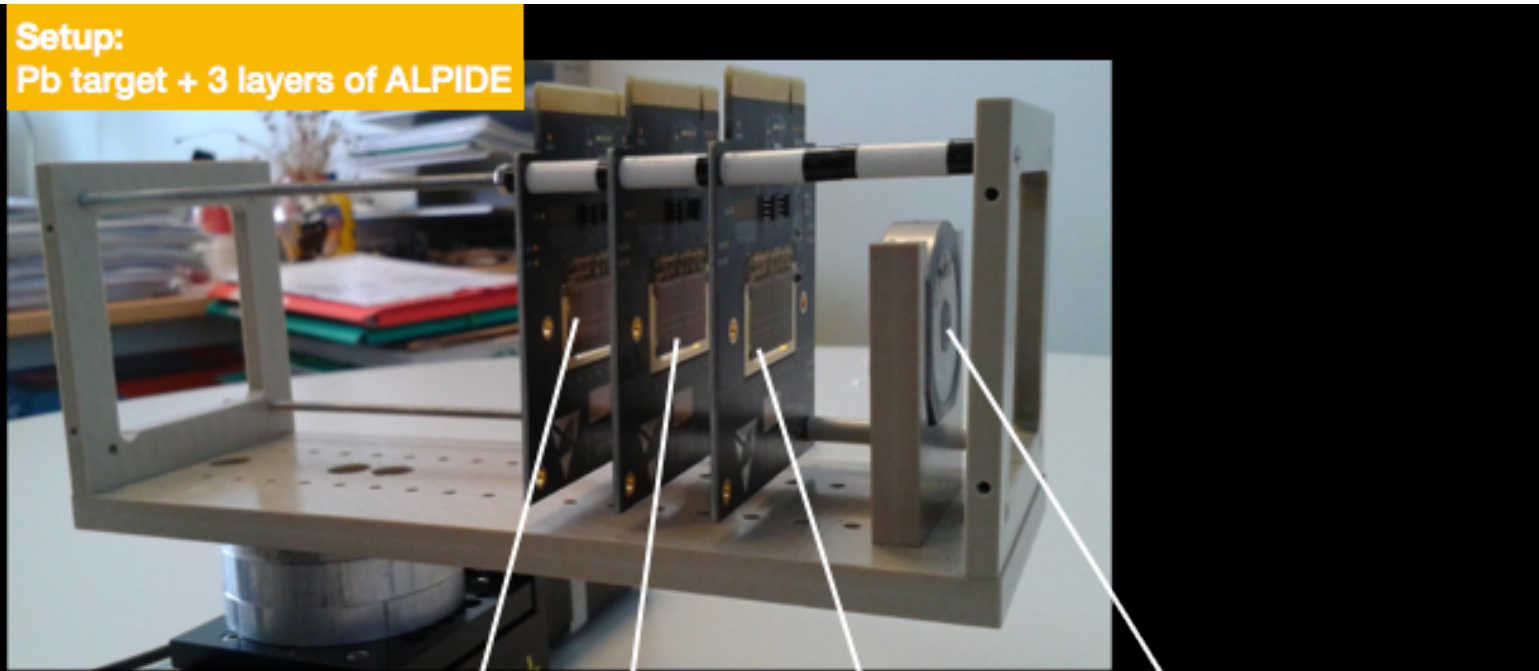


Xe-Pb measurements at SPS with ALPIDE

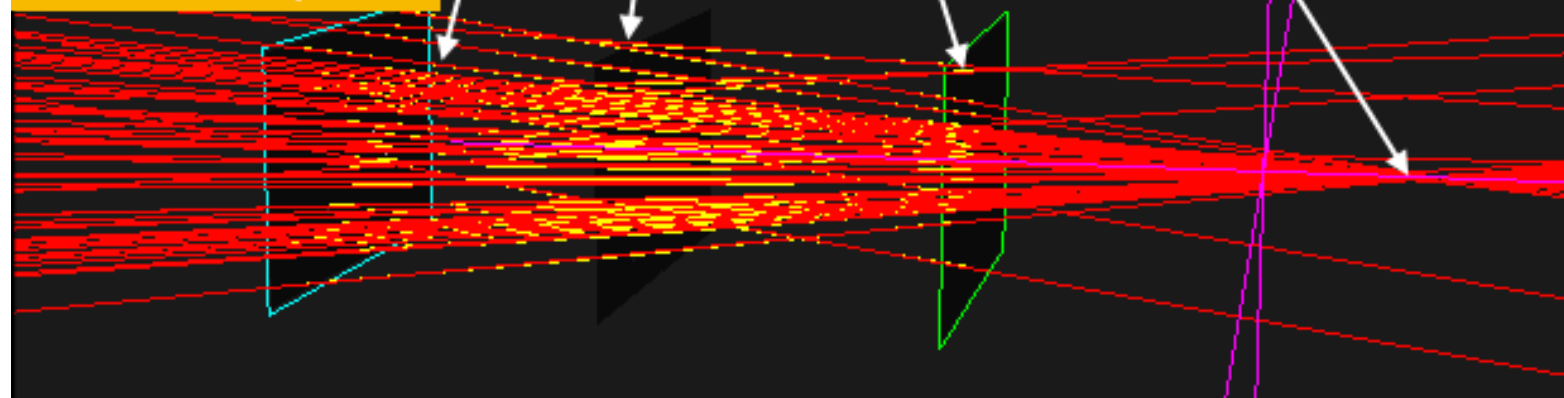


Setup:

Pb target + 3 layers of ALPIDE



Reconstructed event:
linear track extrapolation

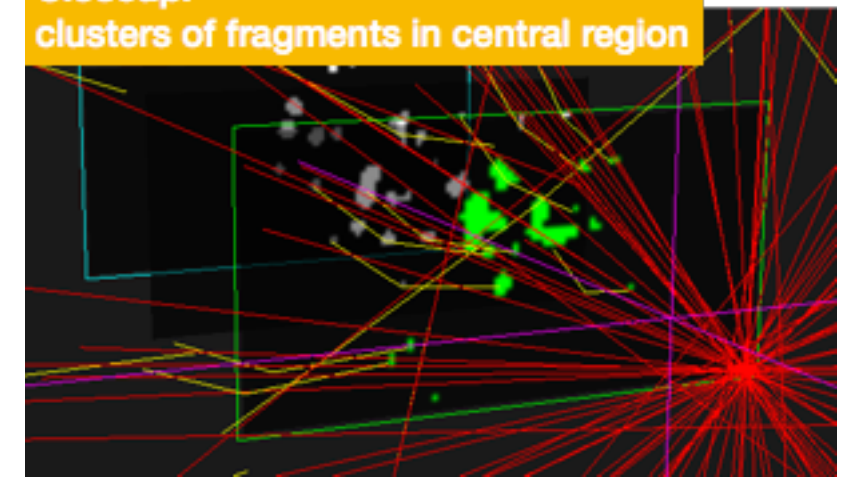


Xe – Pb @ SPS (2017)

- 15 AGeV/c Xe
- 10 mm Pb target, 3cm away
- 3 ALPIDE layers
- 2 cm plane spacing

First look at data: plenty of events
some with interaction in silicon

Closeup:
clusters of fragments in central region



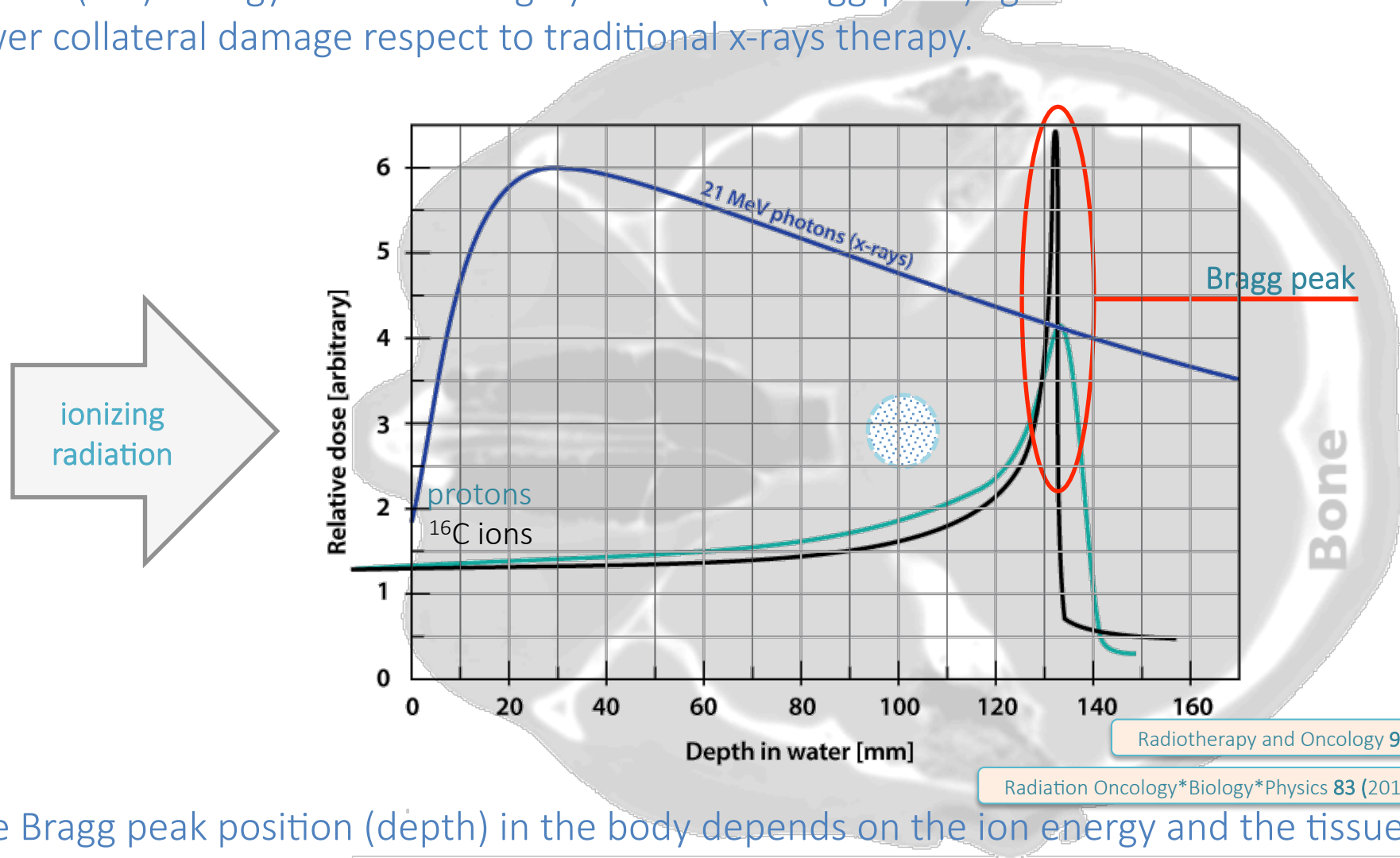
Hadron Therapy

Use of CMOS APS for pCT

Hadron therapy: physics rationale

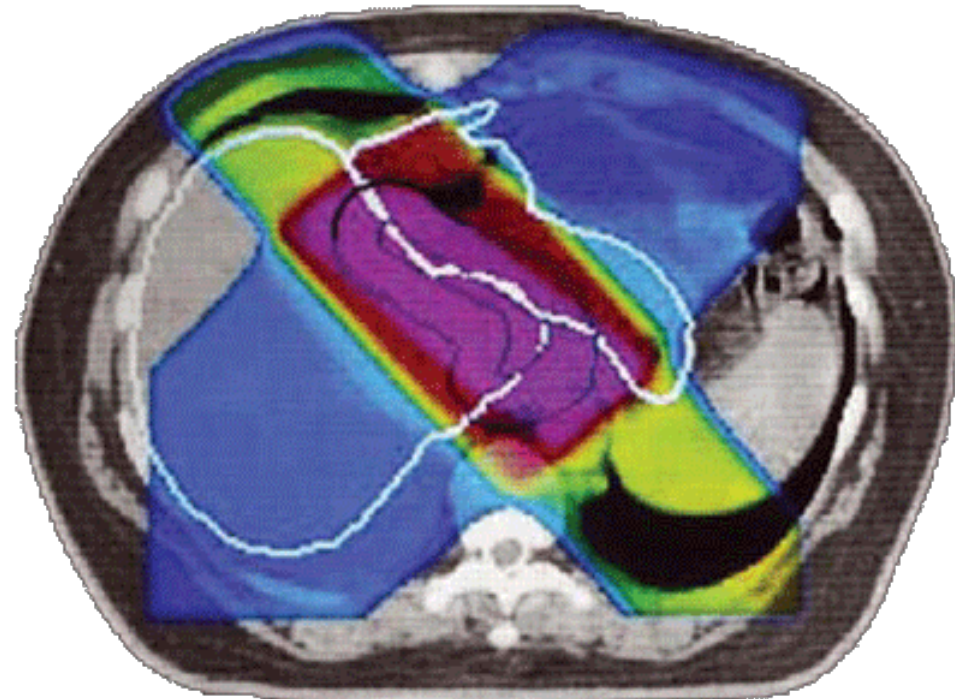
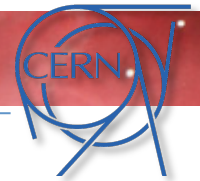


Proton (ion) energy transfer is highly localized (Bragg peak): greater effectiveness and much lower collateral damage respect to traditional x-rays therapy.

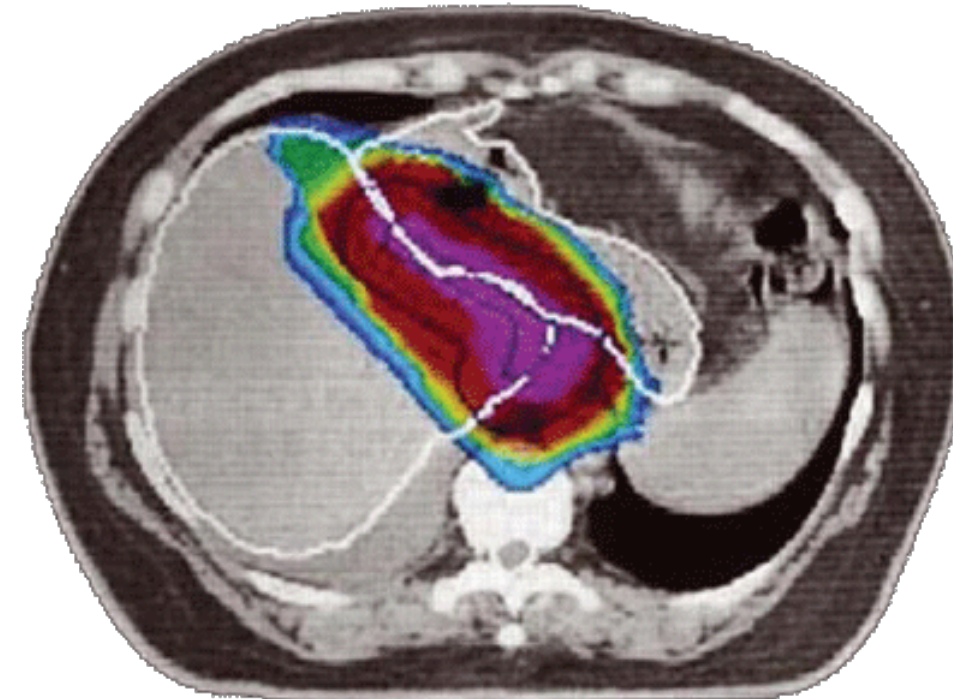


The Bragg peak position (depth) in the body depends on the ion energy and the tissue density it traverses. Changing energy determines the aiming depth.

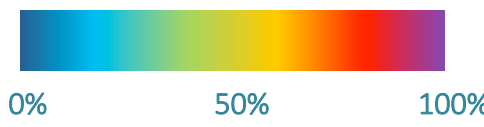
Hadron therapy: reduced collateral damage



X-Rays treatment



Protons treatment



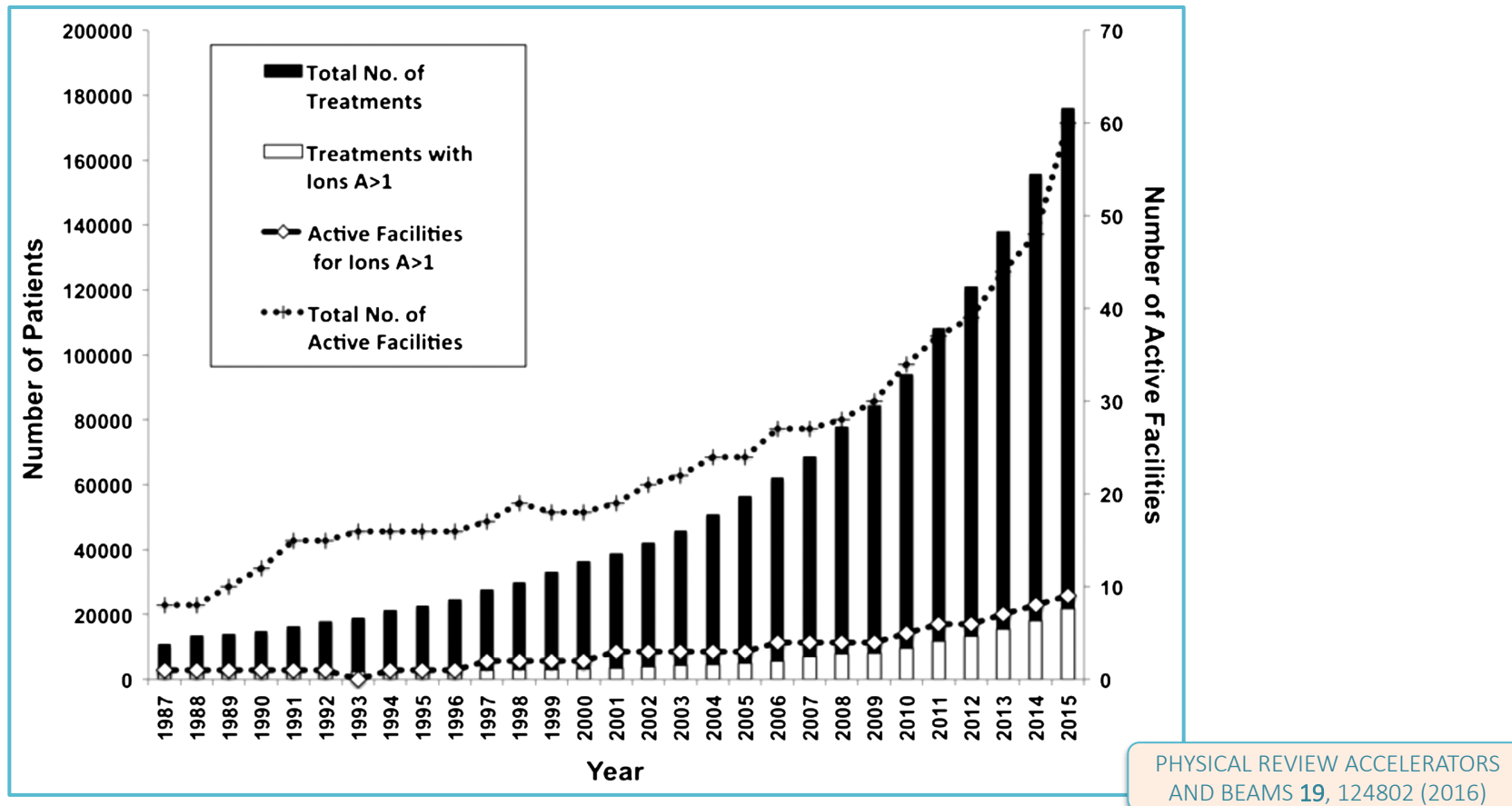
JAMA 307 (2012) 1611-20

Radiation Oncology*Biology*Physics 83 (2012) 1549–1557

Hadron therapy facilities around the world

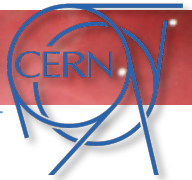


Only $\approx 1\%$ of the candidates for proton therapy can be treated in the active facilities worldwide

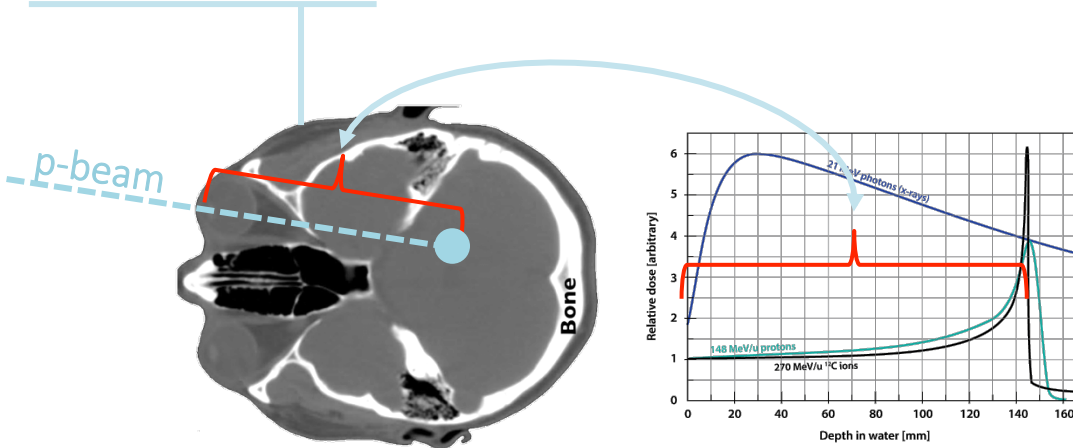


≈ 8000 more treatment rooms are needed around the globe

Hadron therapy: the aiming limit problem

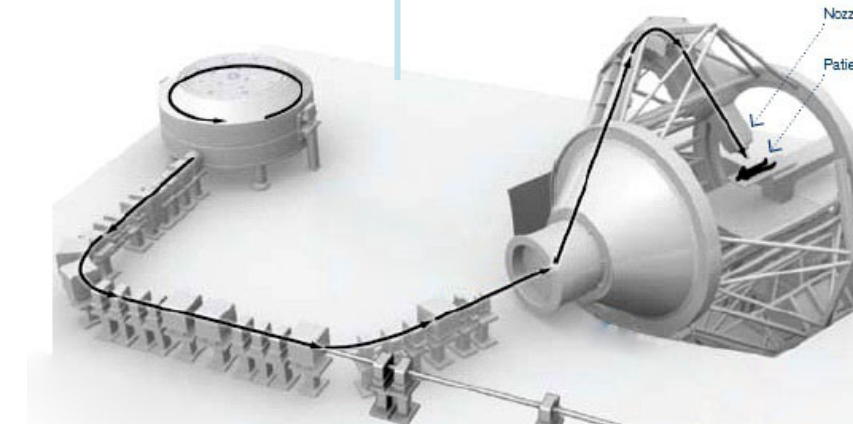


Aiming the Bragg peak requires fine tuning of the proton energy to account for the tissue densities they have to traverse to reach the tumor.



Poor tissue density resolution from X-Rays CT

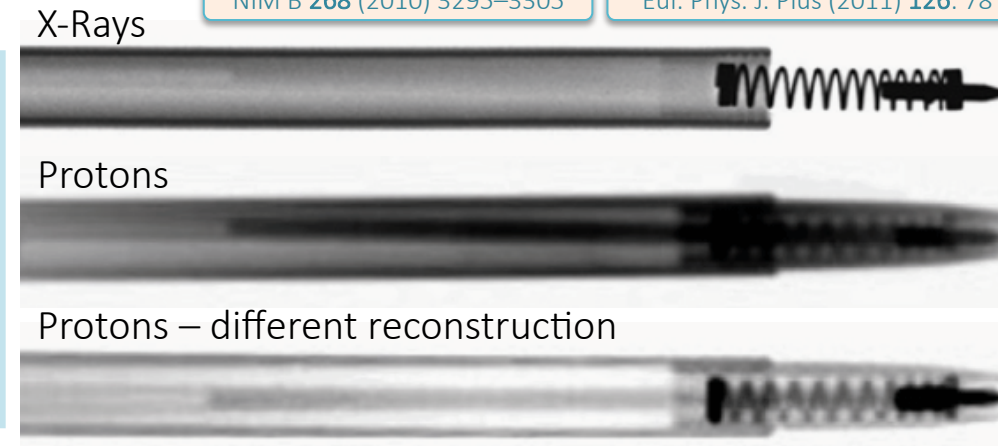
X-ray 3D CT cannot distinguish tissue densities with the required precision: proton therapy limit today (bigger systematic error, up to 5%). But protons actually can (and with much less dose, ≈ 1.5 mGy vs. 10-100 mGy).



Fine energy tuning better than 0.5%

NIM B 268 (2010) 3295–3305

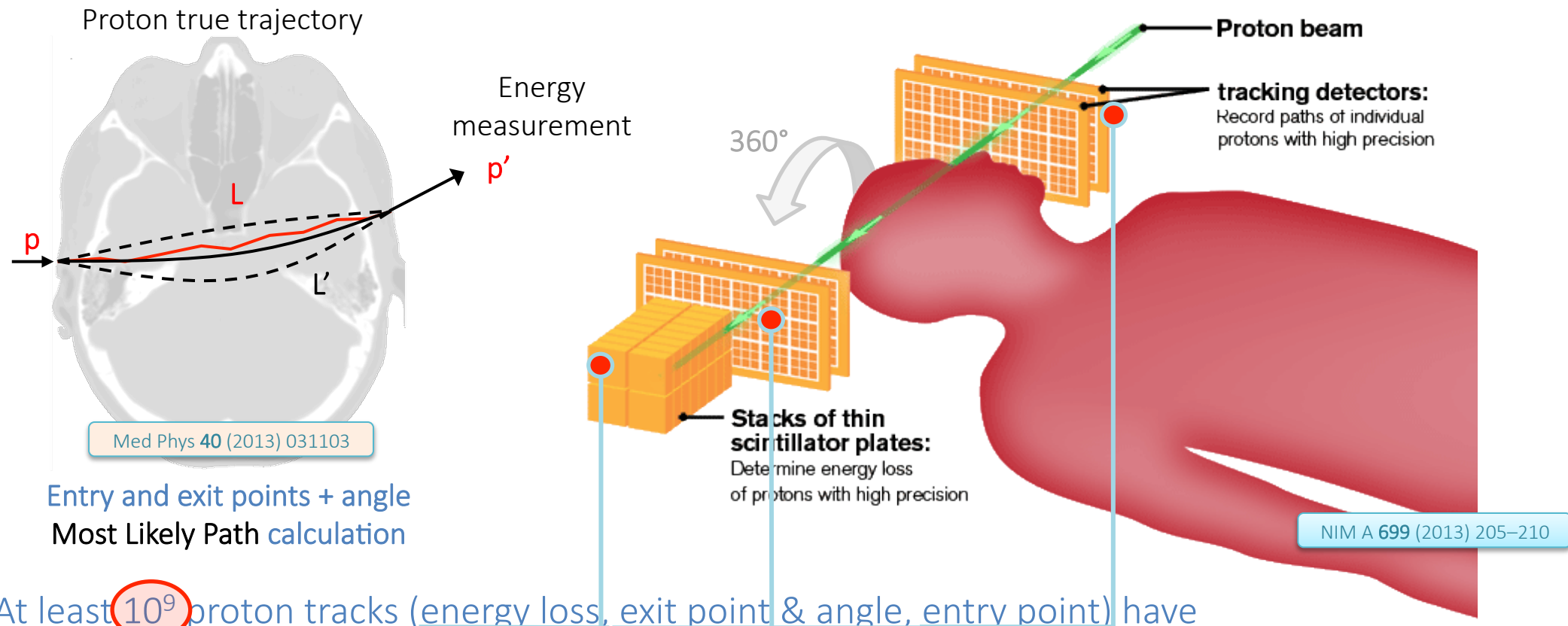
Eur. Phys. J. Plus (2011) 126: 78



The proton Computed Tomography (pCT) scanner



The pCT works on the same principle as a “standard” x-rays CT: recording particles passing through the target from different angles to reconstruct a 3D image. Main difference is that, while photons are simply absorbed, protons also scatter.

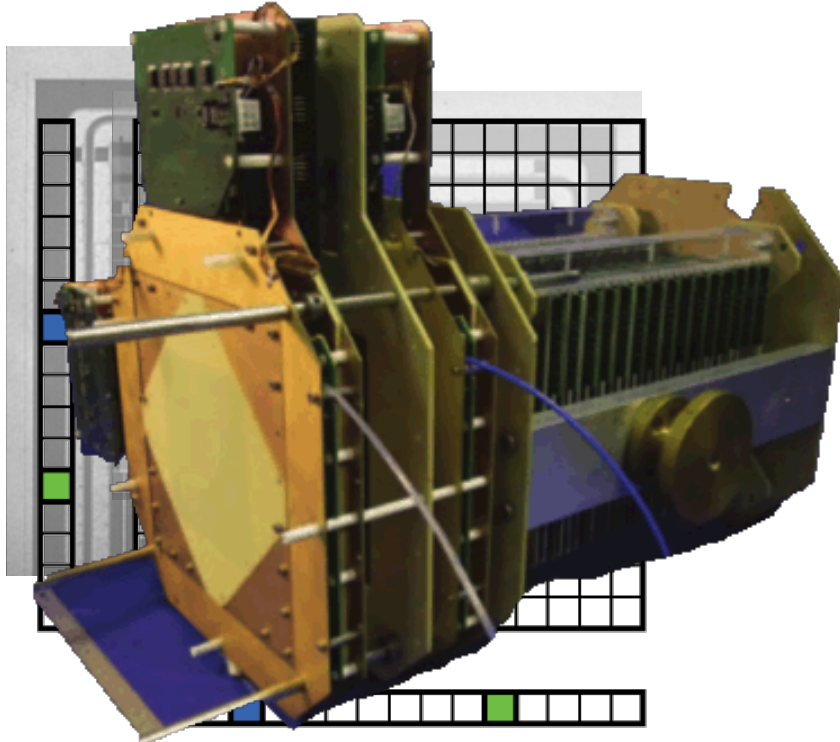


At least 10^9 proton tracks (energy loss, exit point & angle, entry point) have to be recorded to provide a detailed enough image. This leads to long exposure time (10s minutes) with current state of the art: limited to R&D only.

State-of-the-art: pCT scanner in R&D world



State of the art prototypes pCT trackers employ silicon micro-strips or scintillating fibers to get high speed readout over large area at reasonable bandwidth



Current state of the art, in-house built gaseous detector

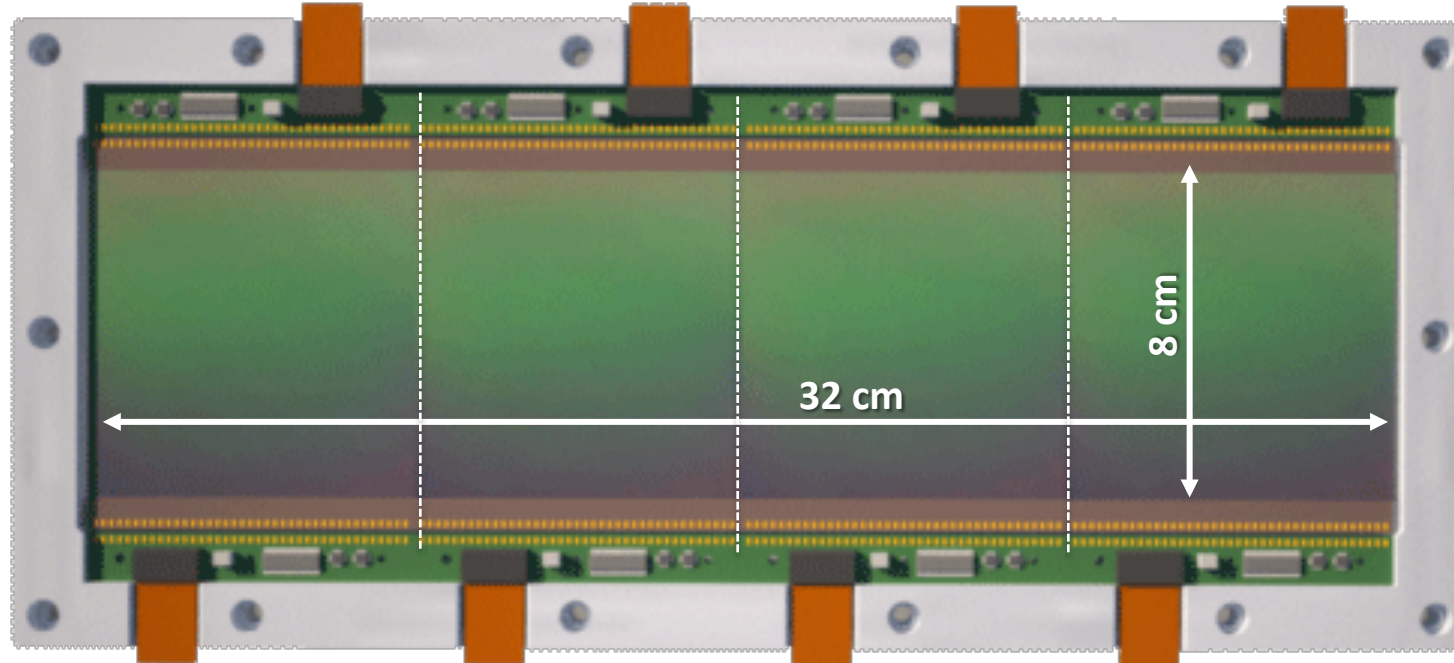
- 1 “Slow”, as readout speed of 10s MHz (and actual particles rate much less due to Poisson). **10 minutes for a full pCT!**
NIM A 699 (2013) 205–210
- 2 Requires two layers (x and y) for every station, **material budget** affects protons scattering + **high voltage** or **gas**.
- 3 **Non commercial** technology, built in house (scintillating fibers) or derived from HEP experiments (micro-strips).

Such approach covers the large area necessary to track particles over a head-sized target ($\approx 10 \times 30 \text{ cm}^2$) with “affordable” complexity and bandwidth. Effective for R&D, unlikely to meet the requirements of a commercially feasible pCT system

Large CMOS sensors – Tracking layer requirements for pCT



- Fast ($> 10 \text{ MHz cm}^{-2}$) proton tracking at low power in silicon (50 mW cm^{-2})
- Monolithic, thinned ($\leq 50 \mu\text{m}$) and large area ($> 16 \text{ cm}^2$) device to minimize proton scattering.
- No support structure behind the silicon.
- **Cost effective**, reliable, simplified commissioning & operations, commercial process (for large production)
- **Low voltage** for real clinical usage

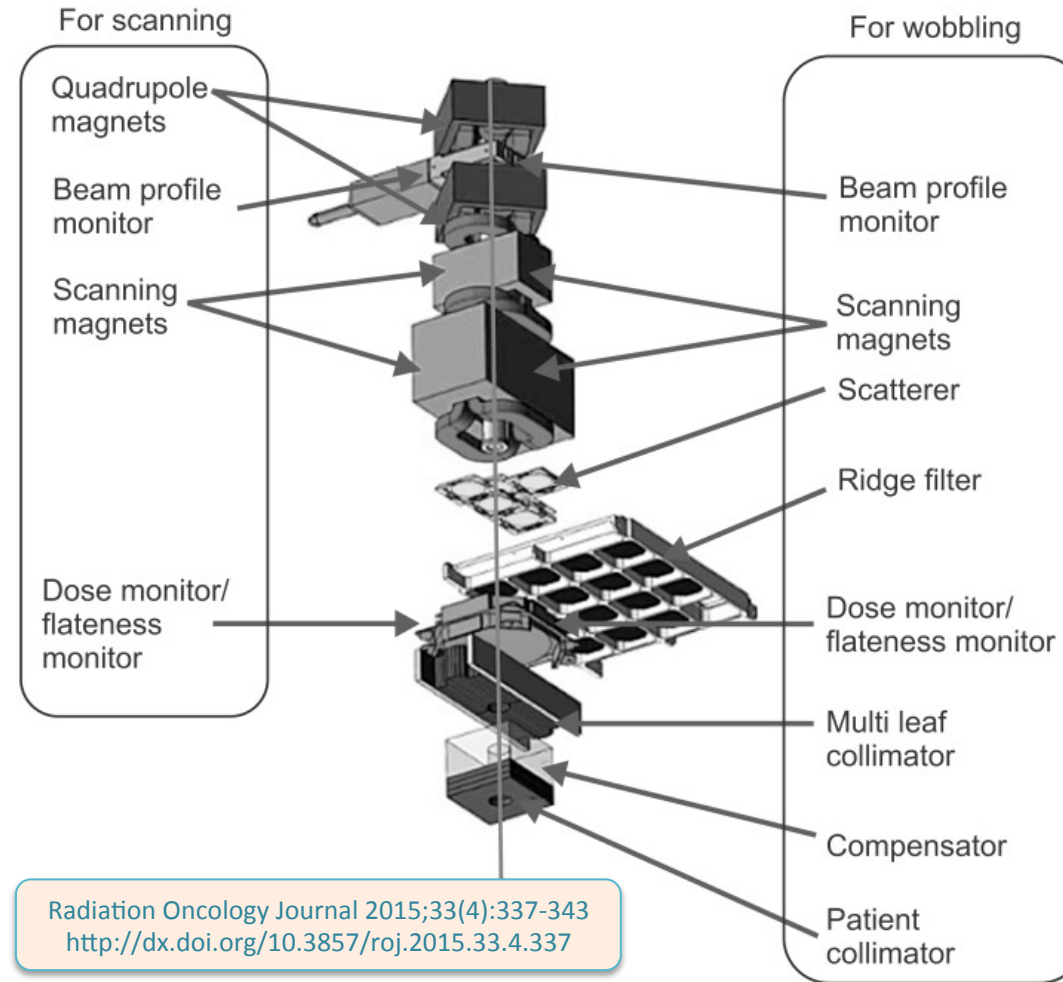


Large sensors – broad beam useful for imaging purposes



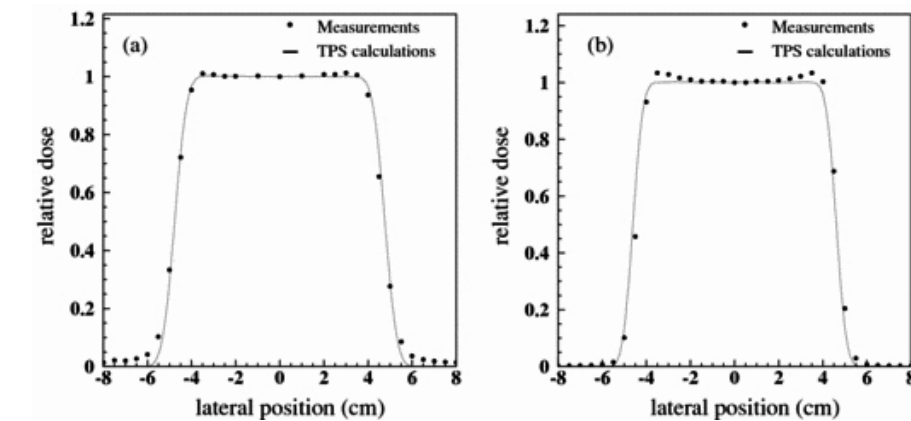
Broad beam over the entire target area put lesser requirements on the tracking and calorimeter system

Mix of fast (MHz) wobbling magnets and scatterer(s) generates an almost uniform illumination profile (typical example reported in plot)



- Mitsubishi multi-purpose nozzle system
- Broad beam area: $25 \times 25 \text{ cm}^2$
- Scanning beam area: $24 \times 24 \text{ cm}^2$
- For a $20 \times 20 \text{ cm}^2$ imaging area, 10^9 protons in 10 s exposure $\rightarrow 250 \text{ kHz cm}^2$
- Considering non uniformity, time fluctuations, etc...

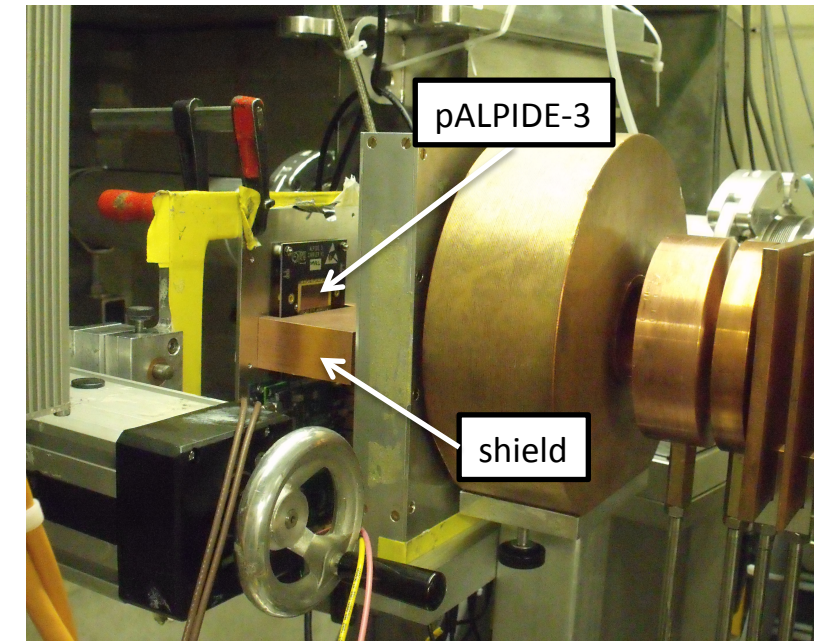
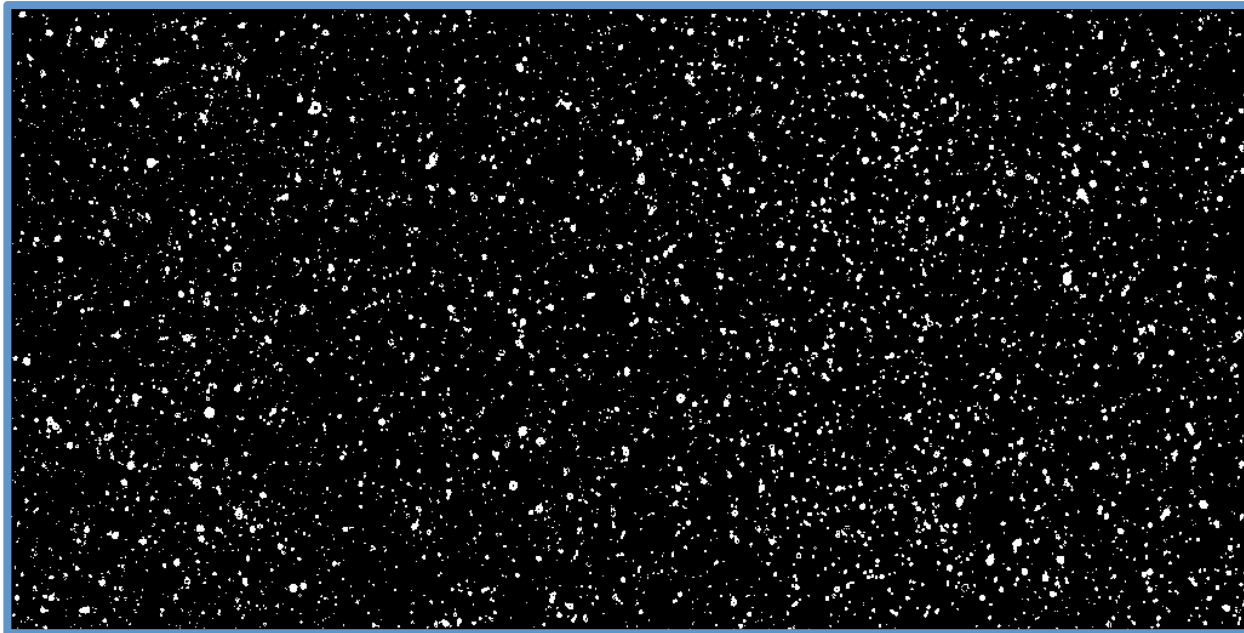
$$\approx 1 \text{ MHz cm}^{-2}$$



Radiation Oncology Journal 2015;33(4):337-343
<http://dx.doi.org/10.3857/roj.2015.33.4.337>

ALPIDE pixel matrix can cope with particle rates of $\approx 100 \text{MHz cm}^{-2}$ (power density 40mW/cm^2)

pALPIDE-3 Sensor ($0\text{V } V_{\text{sub}}$)



PIF @PSI - Nov 2015, 200 MeV protons, $1.6 \times 10^8 \text{cm}^{-2}\text{s}^{-1}$

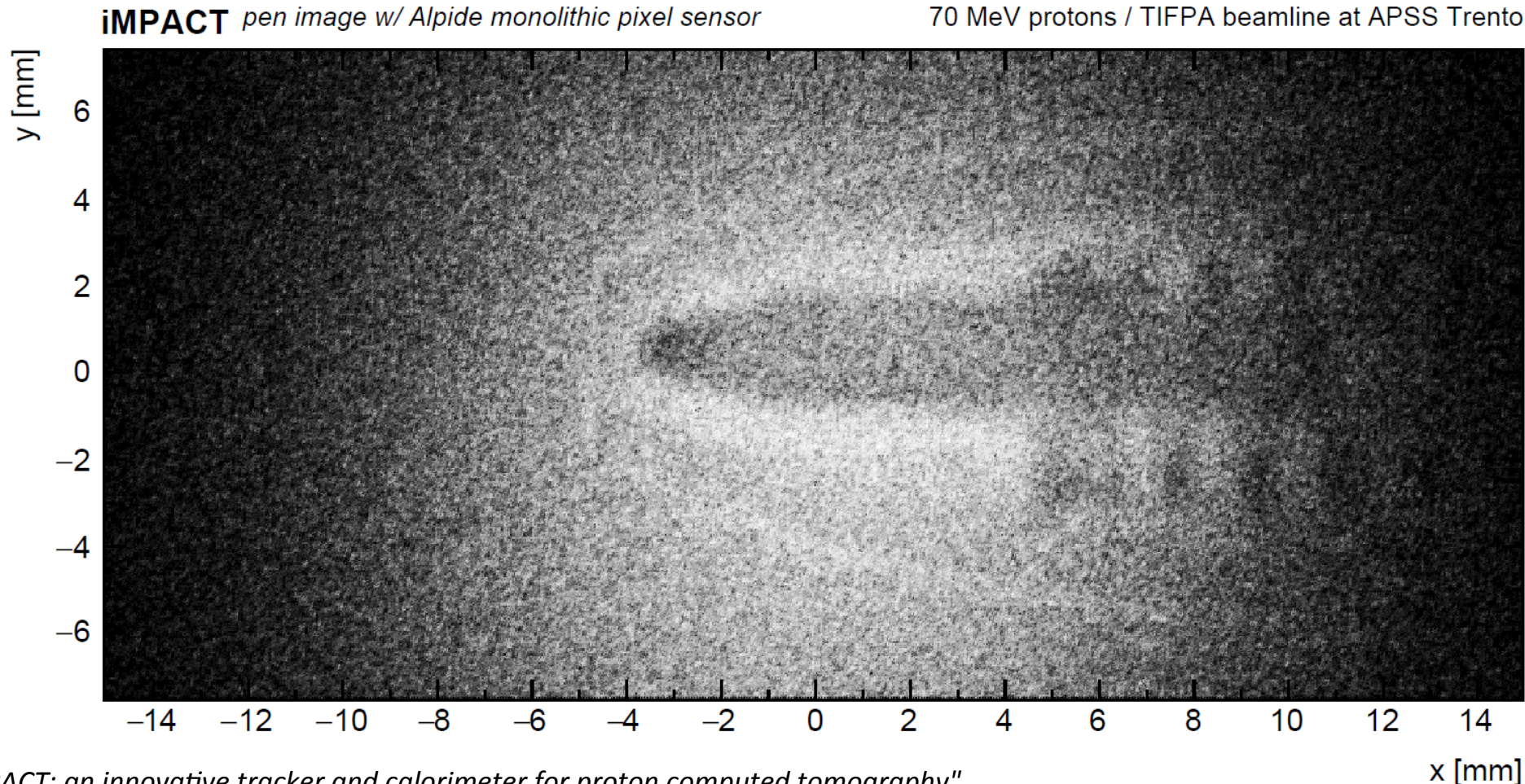
Output bandwidth of ALPIDE (1 Gbit/s) limits maximum rate to 14MHz cm^{-2}

Large sensors – ALPIDE first “proton” light

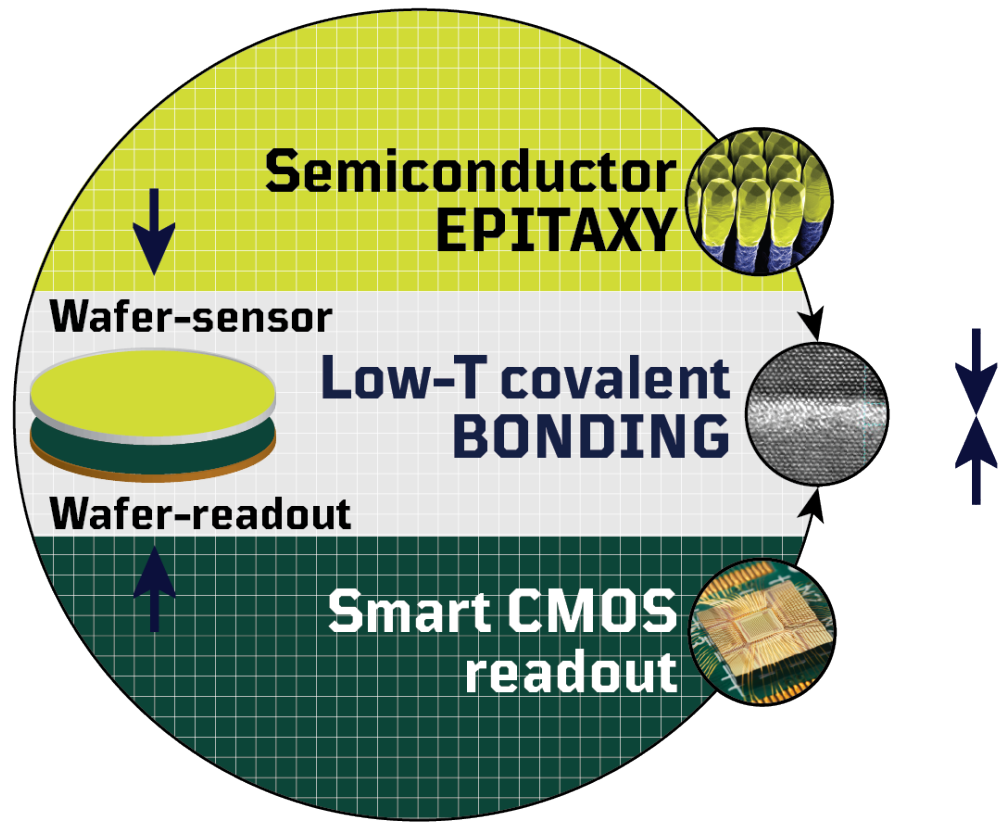


ALPIDE used to take a demonstrative proton radiography of a pen:
metal, different plastic densities, air distinguishable

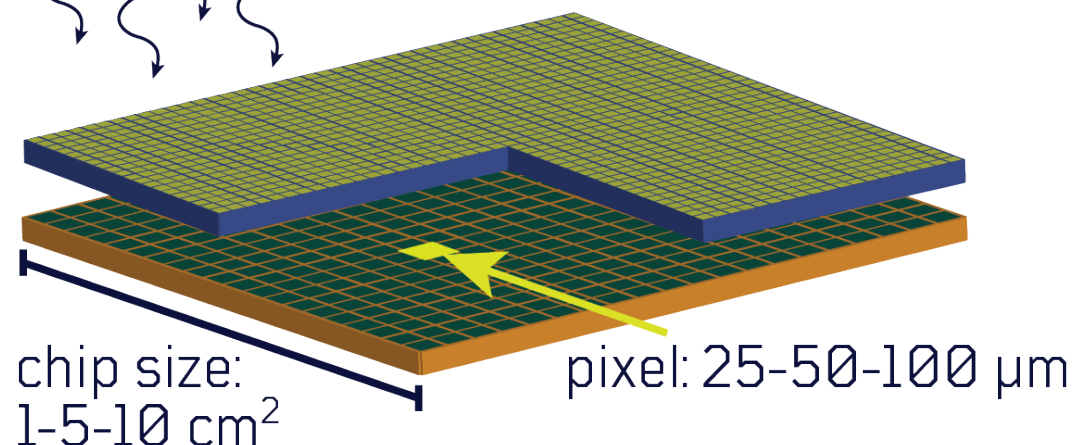
Raw data of a single projection (4.5×10^5 hits)



"iMPACT: an innovative tracker and calorimeter for proton computed tomography"
TRPMS-2018-0013.R1 Transactions on Radiation and Plasma Medical Sciences



Absorber: SiGe (IR and low-energy X-rays)
GaAs (medium-energy X-rays)
CZT (high-energy X-rays)



CMOS-ASIC readout (X-rays)
SPAD (infrared)

Courtesy of G-Ray

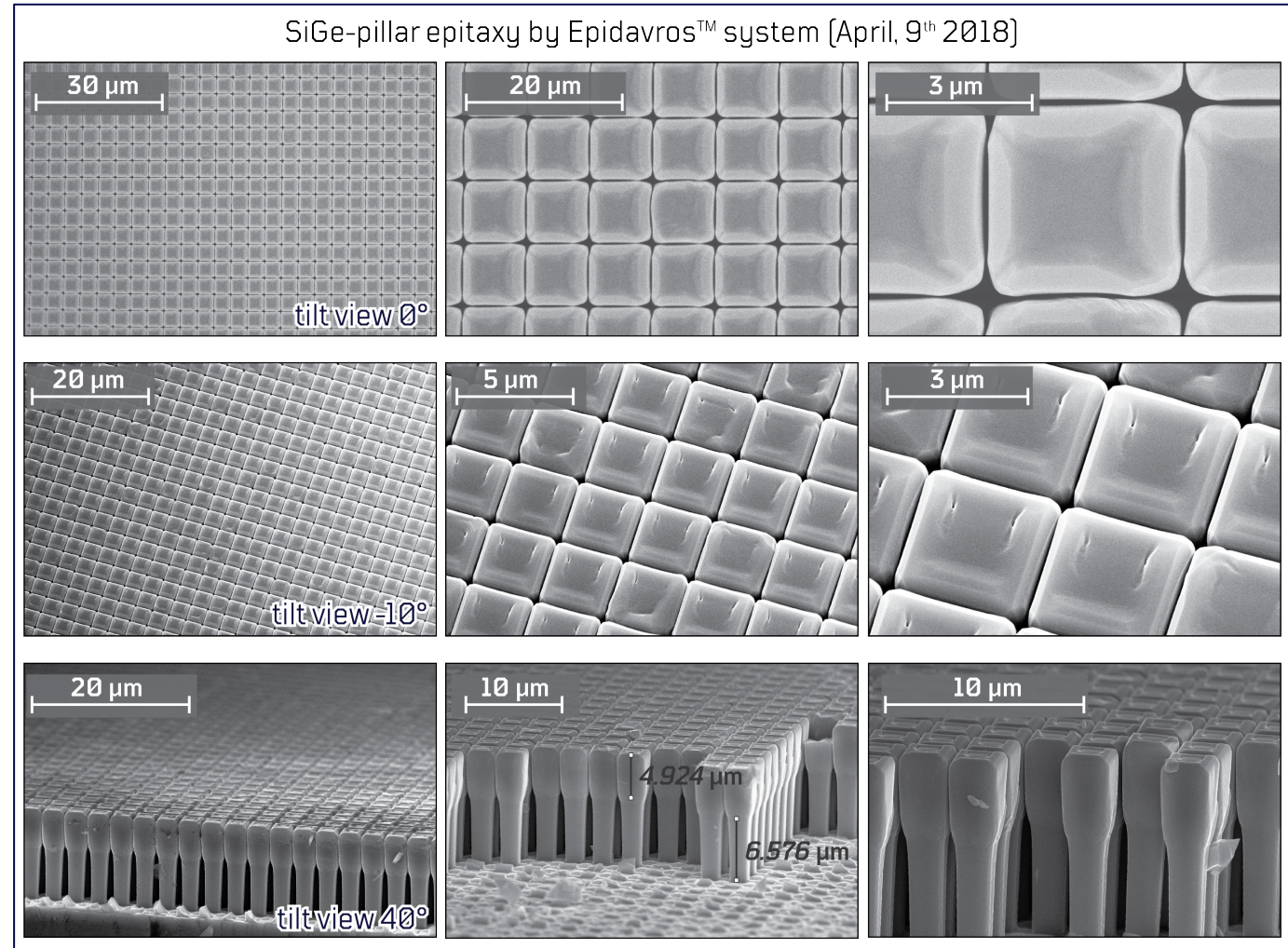
Covalent bonding of optimized absorbers to CMOS chip



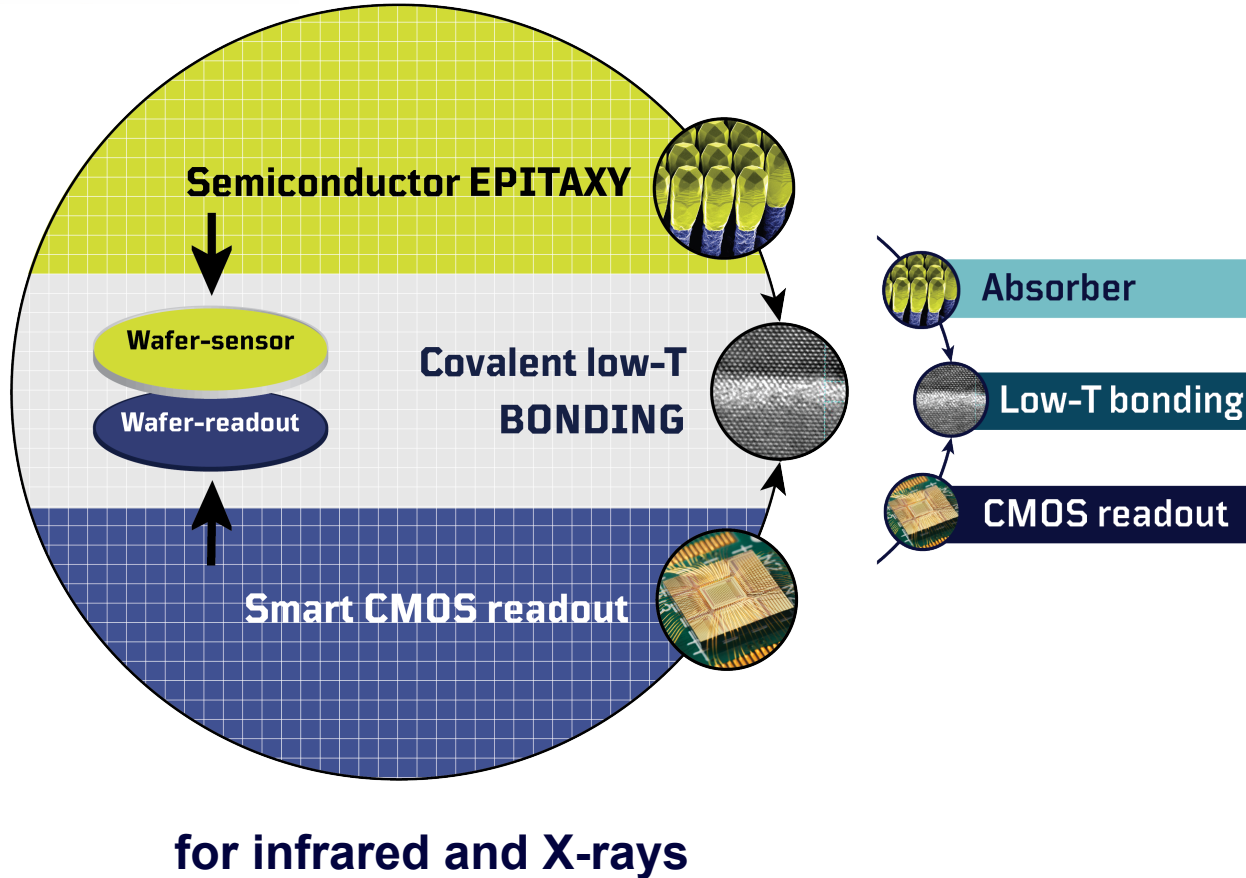
G-ray's unique and proprietary
Epidavros™ system



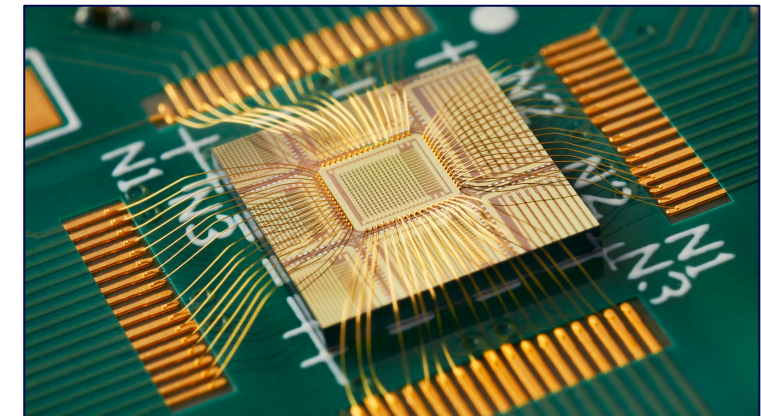
Courtesy of G-Ray



Covalent bonding of optimized absorbers to CMOS chip

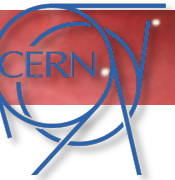


INVESTIGATOR CHIP @ CERN



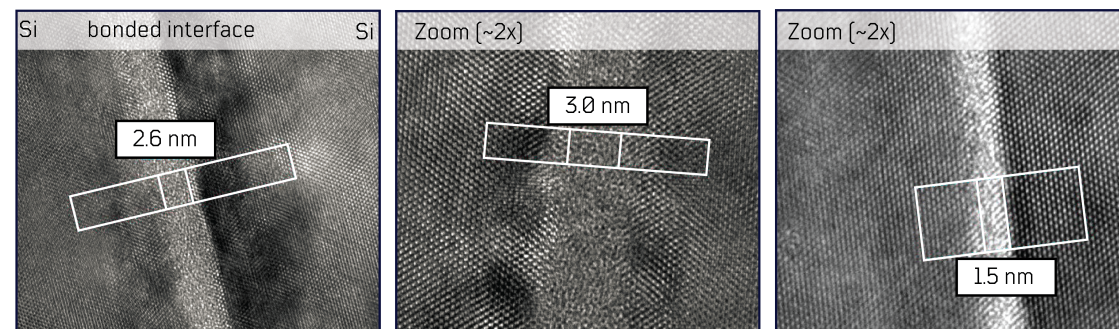
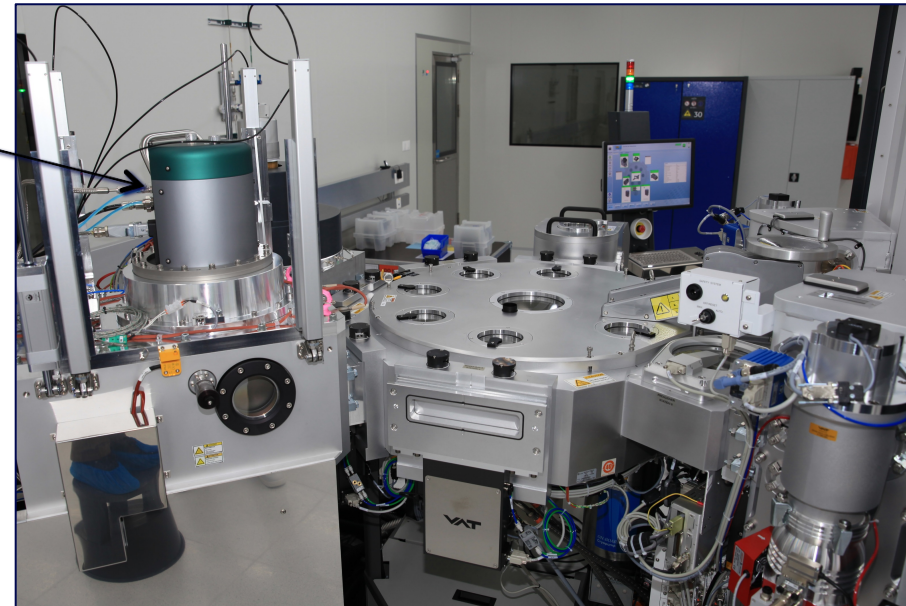
NOVIPIX CHIP @ CSEM & Empa

Low-temperature bonding: technology development



Modified EVG ComBond® System at G-ray

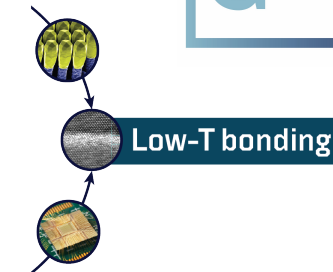
G-ray's Argon
Plasma Module
for atomic-scale
wafer's surface
cleaning



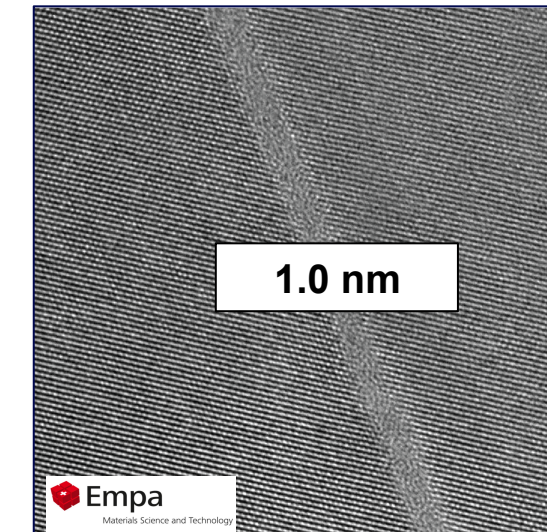
Experiments
2016

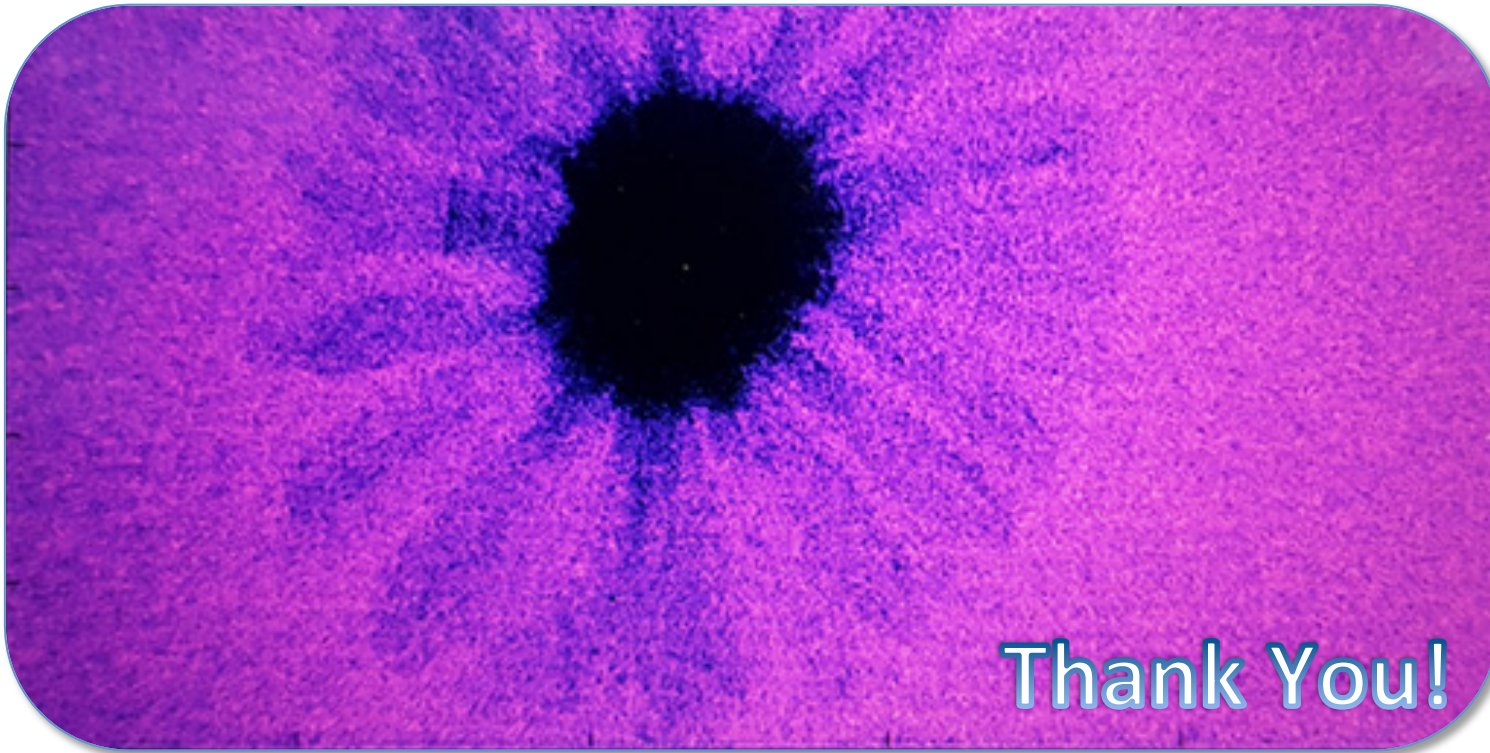
Experiments
2017

Experiments
2018



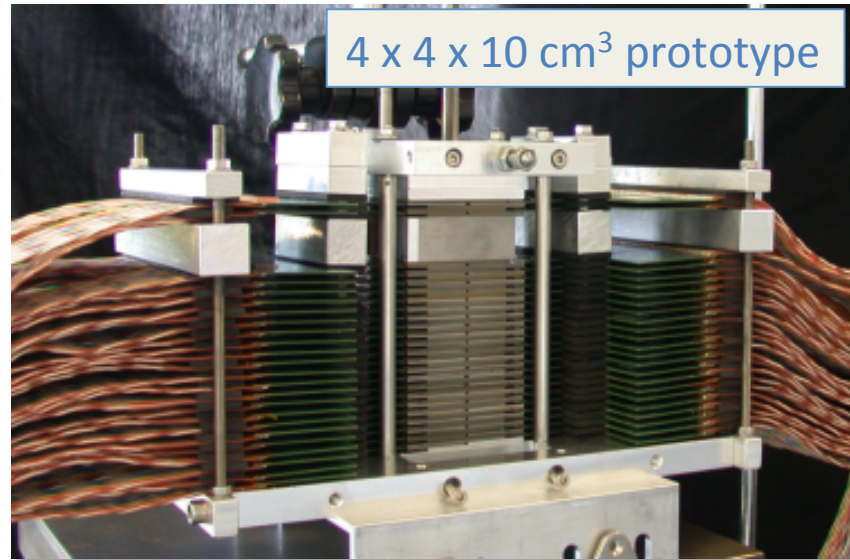
bonded interface reduced to a
seamless 1 nm (Q1-2018)!





Picture (^{55}Fe) of a flower 30 x 1s
“photographed” with ALPIDE

High-Granularity Digital Calorimeter Prototype



Prototype based on MIMOSA pixel chip

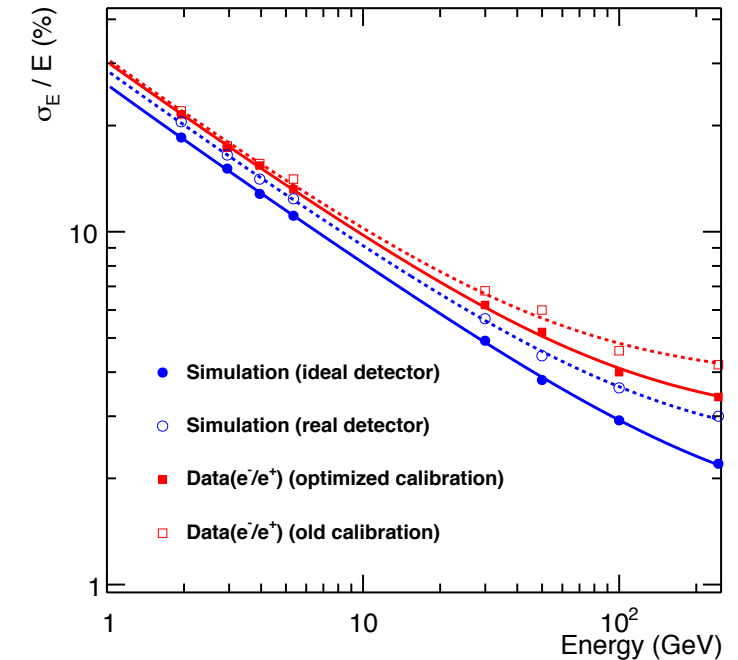
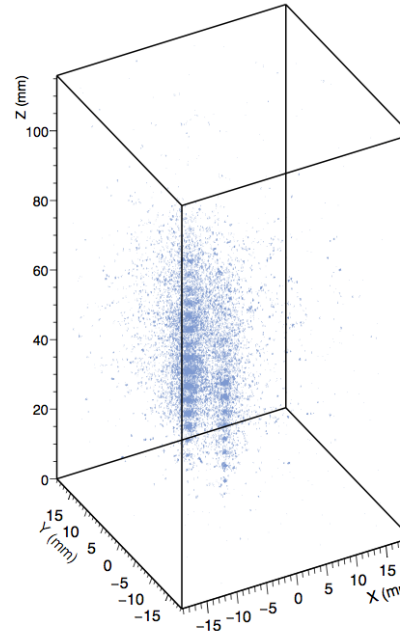
- 24 layers (1 X_0 W + MIMOSA23)
- 39M pixels, 30 μm pitch
- Beam tests from 2 to 250 GeV/c (DESY, CERN PS & SPS,
- Cosmic muons

Preparing next generation prototype with ALPIDE

R&D in the context of FoCal in ALICE

Extremely compact design

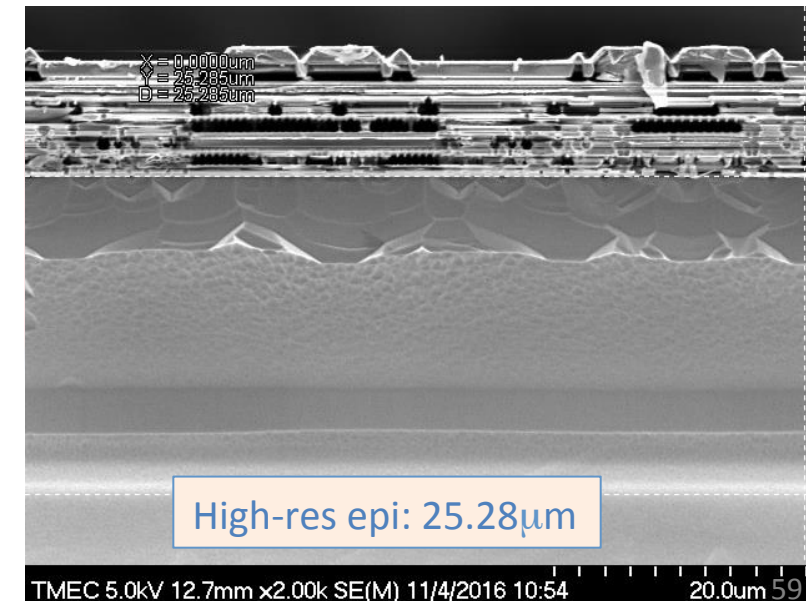
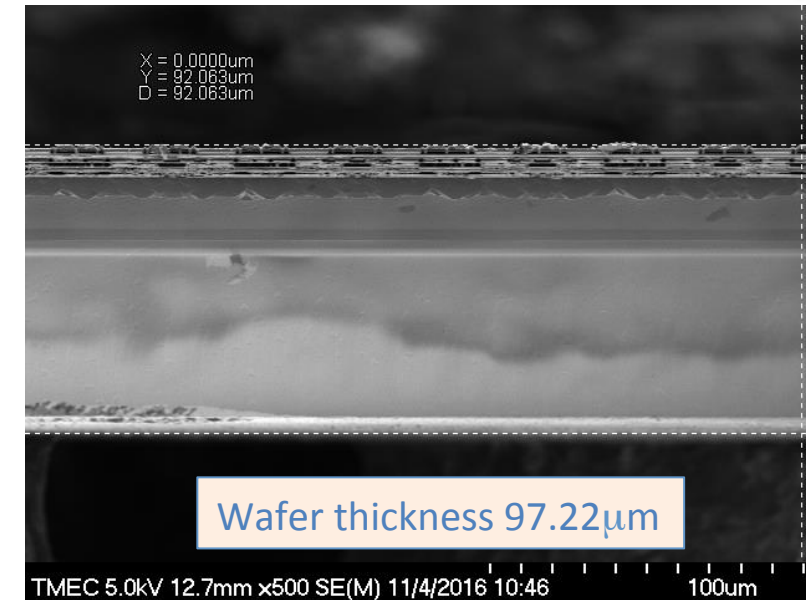
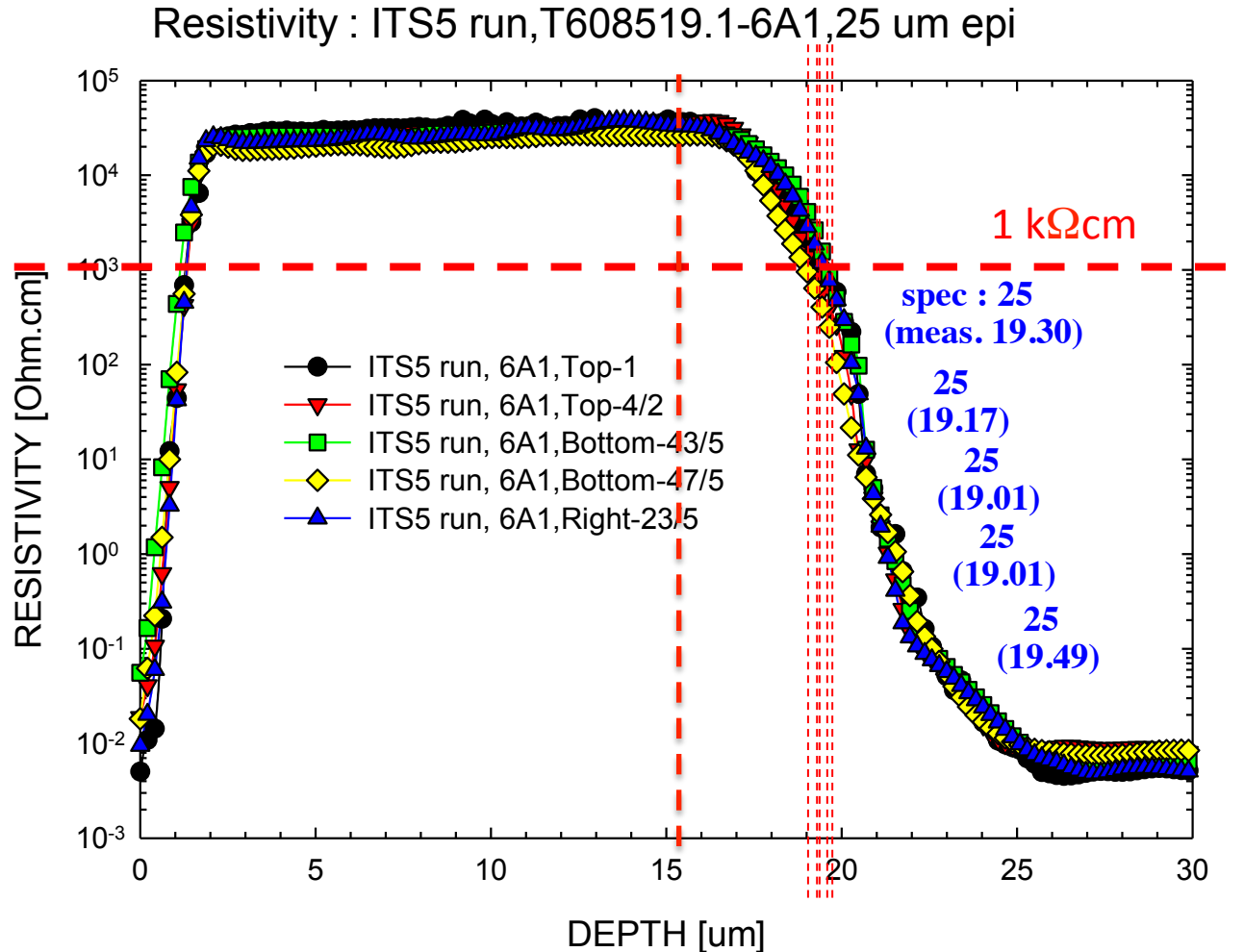
Small Moliere radius ($RM = 10.5 \pm 0.5\text{mm}$)



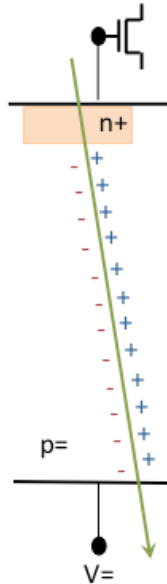
Very good energy linearity and resolution

Extremely good position resolution

Blank Wafers QA at TMEC (SRP and XSEM measurements)



Low capacitance → large S/N at low power



NWELL DIODE output signal = Q / C

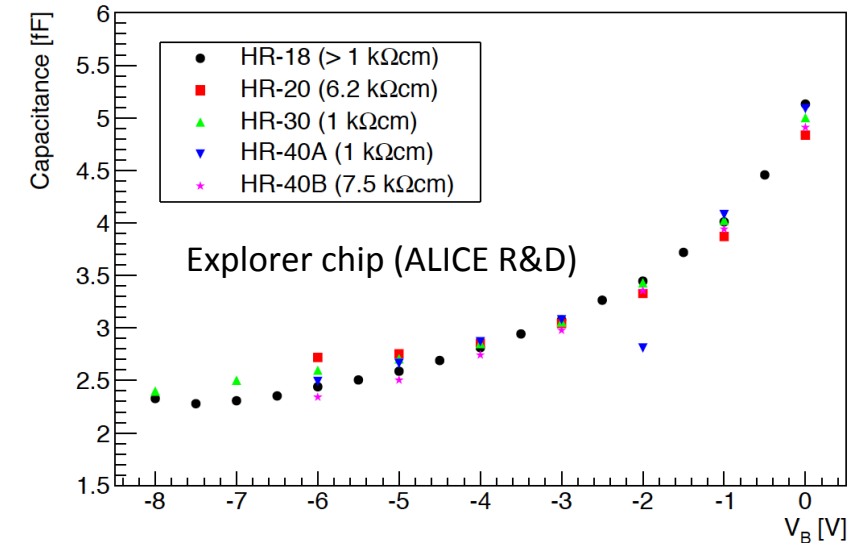
- Minimize spread of charge over many pixels
- minimize capacitance:
 - small diode surface
 - large depletion volume

☞ Silicon strip capacitance: $> 10 \text{ pF} (\sim 1.5 \text{ pF} / \text{cm})$

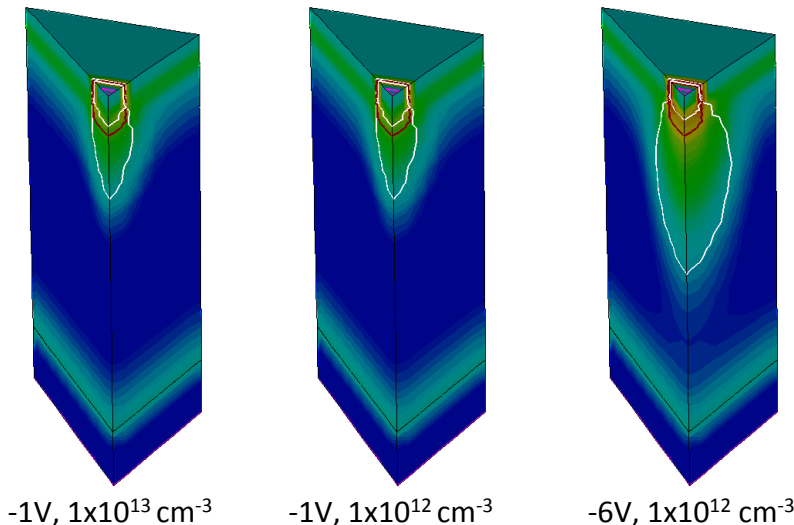
☞ Hybrid pixel capacitance: $\sim 300 \text{ fF}$

☞ Monolithic pixel capacitance: $< 5 \text{ fF}$

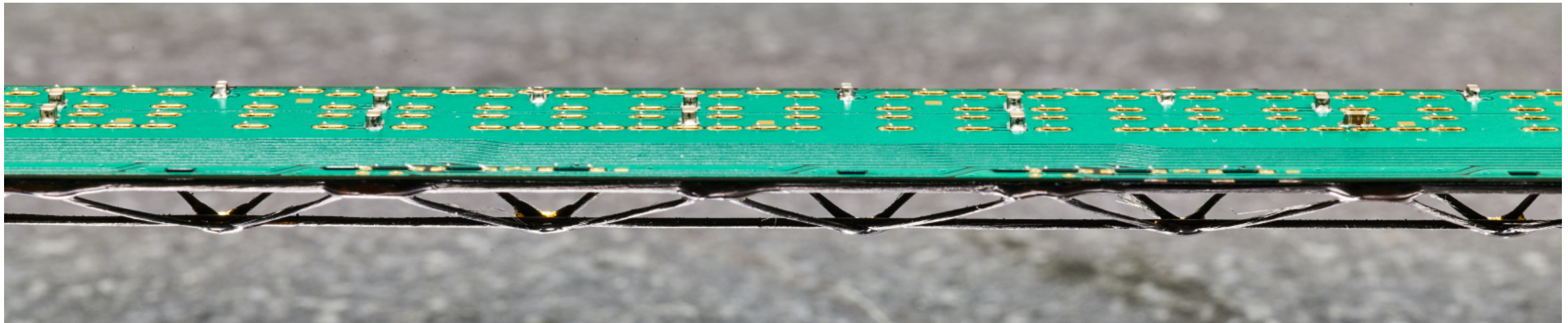
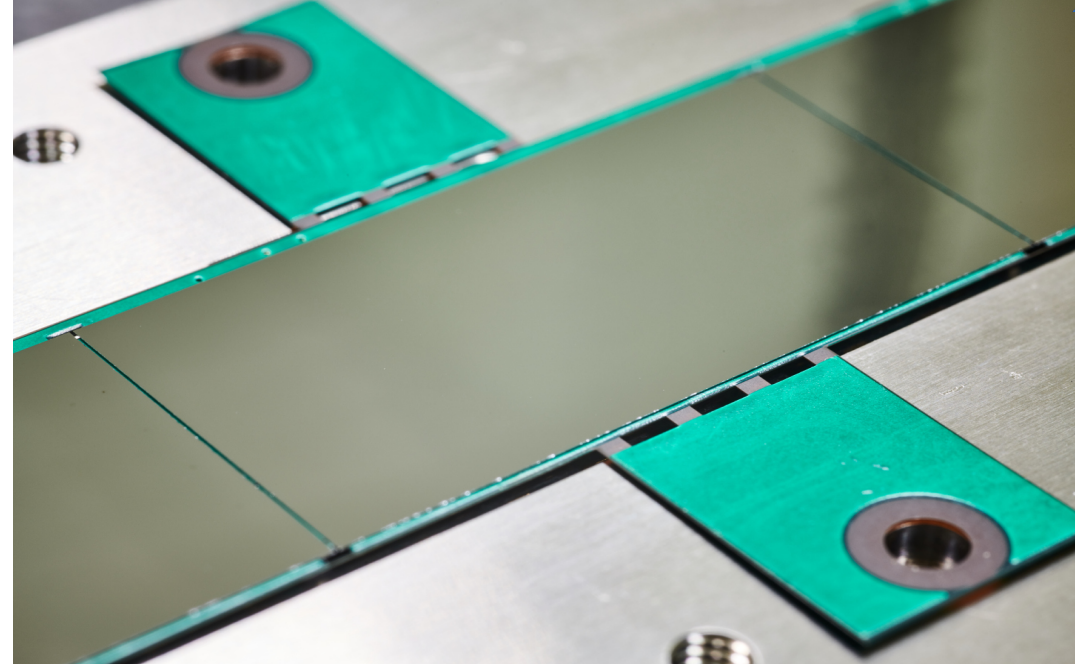
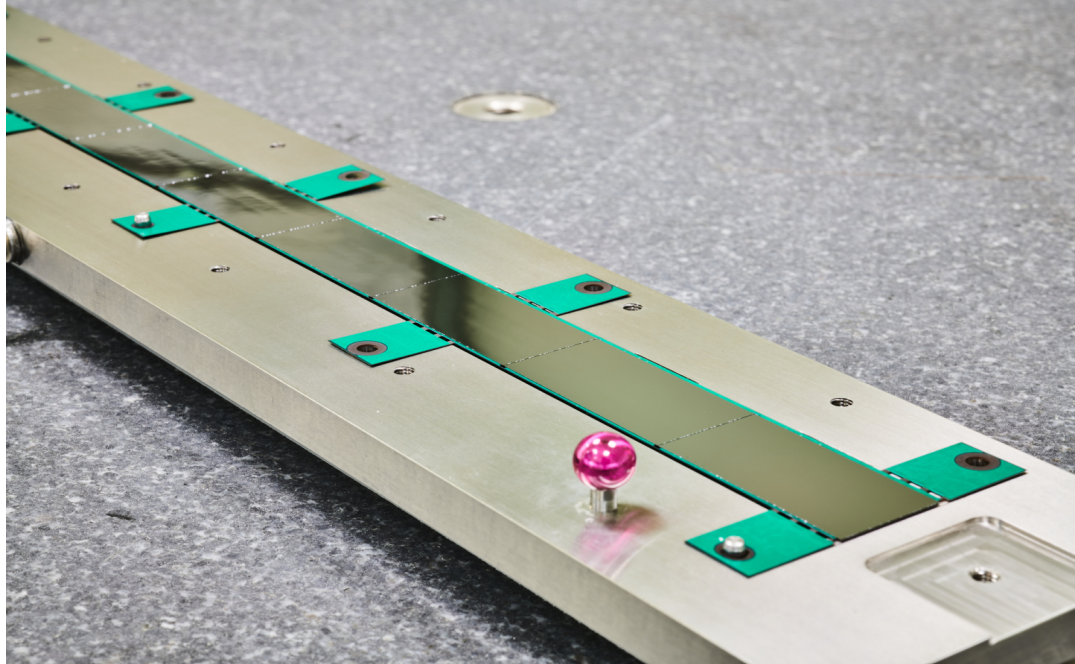
$$C_d = 1\text{fF}: 1300 \text{ e}^- \rightarrow 200\text{mV} \text{ (almost a digital signal)}$$



Diode $3\mu\text{m} \times 3\mu\text{m}$ square n-well , White line: boundaries of depletion region



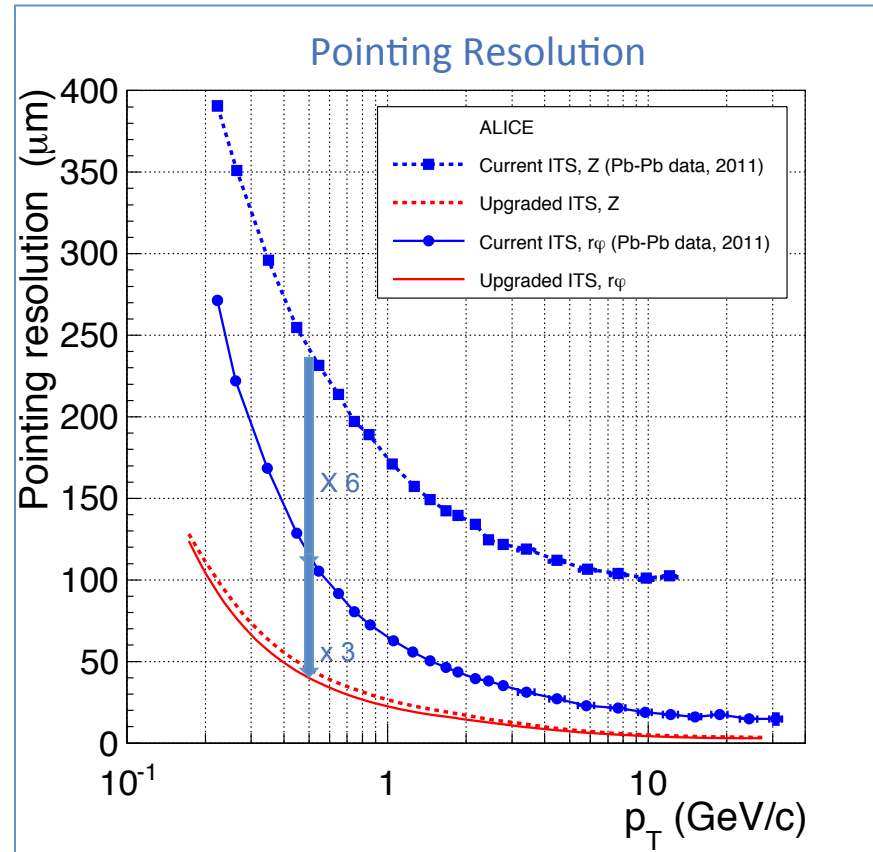
Detector stave based on ALPIDE



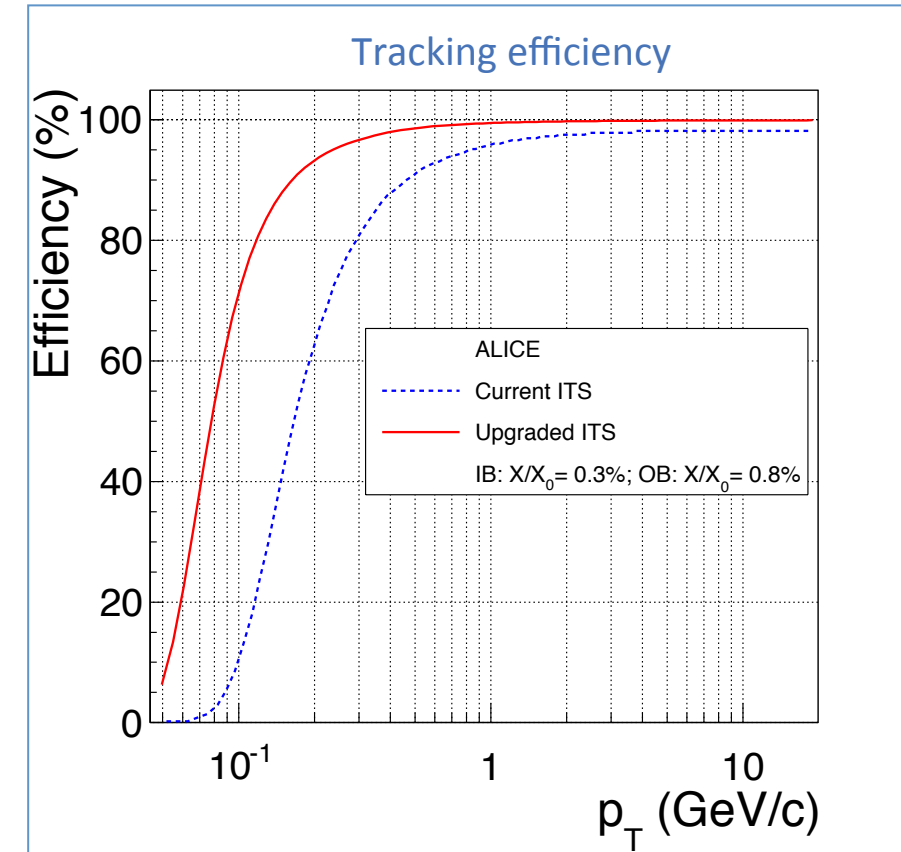
Projected performance of the ALICE ITS Upgrade



Impact parameter resolution



Tracking efficiency (ITS standalone)



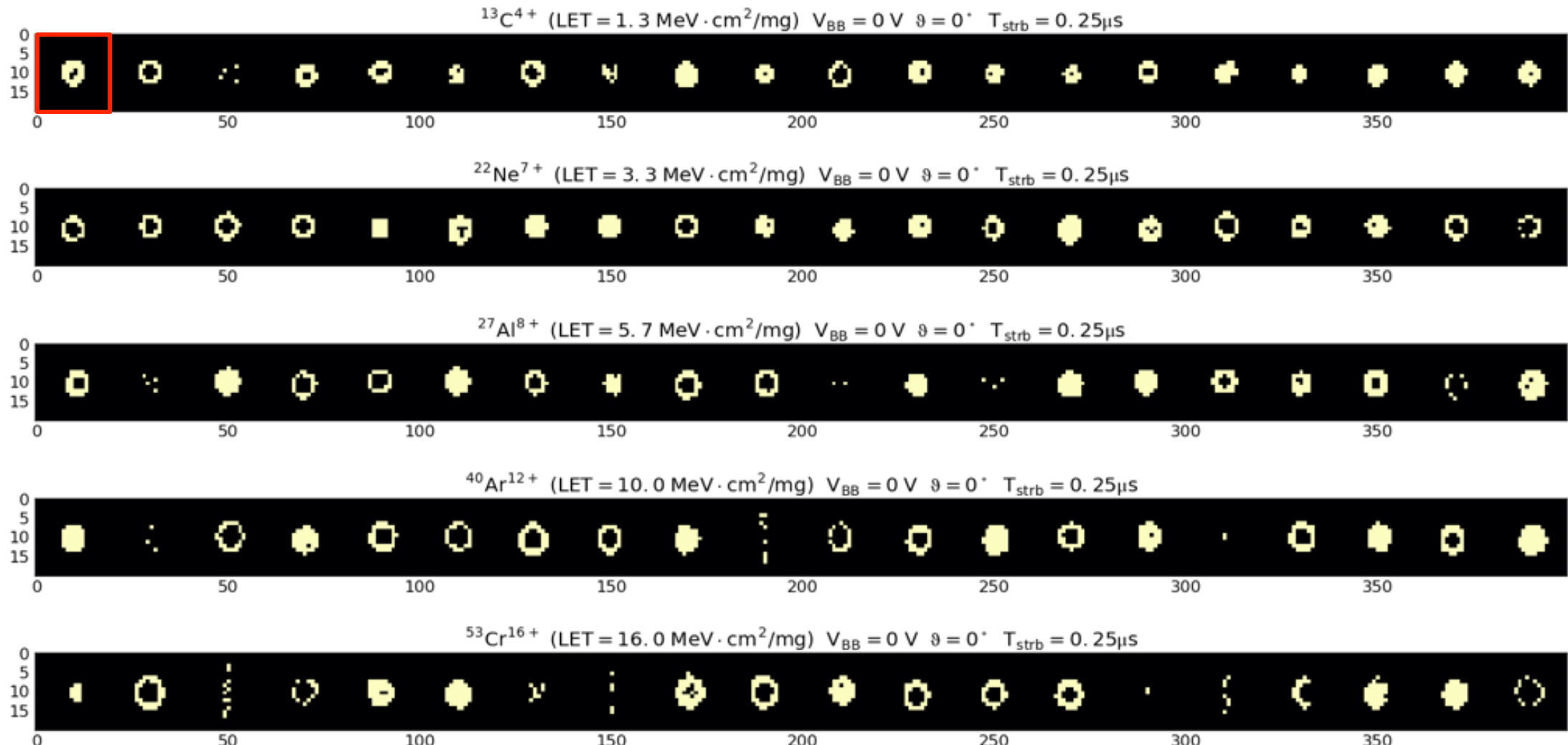
~40 μm at $p_T = 500 \text{ MeV}/c$

LET Response studies – Lovain-la-Neuve



Sequence of images of single clusters. Each image corresponds to 20 x 20 pixels

VS. LET @ $V_{BB} = 0$

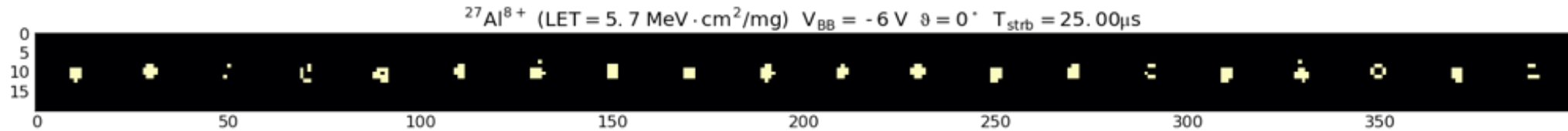
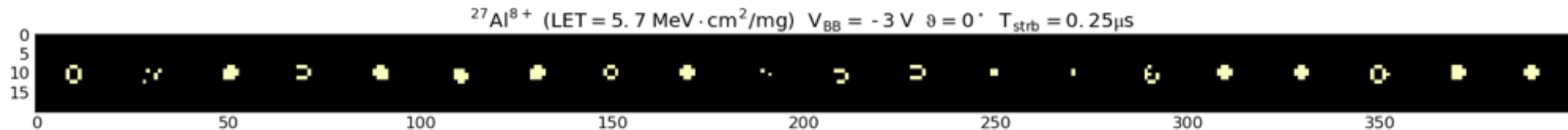
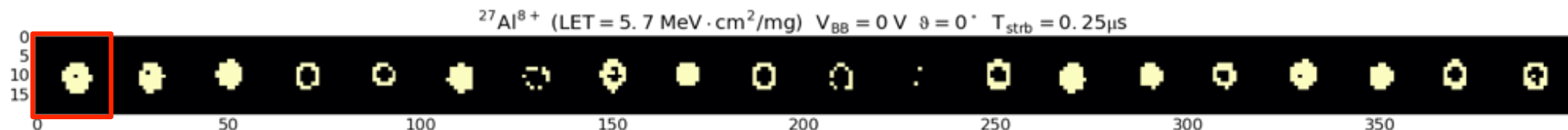


LET Response studies – Lovain-la-Neuve



Sequence of images of single clusters. Each image corresponds to 20 x 20 pixels

VS. V_{BB} @ LET = 5.7

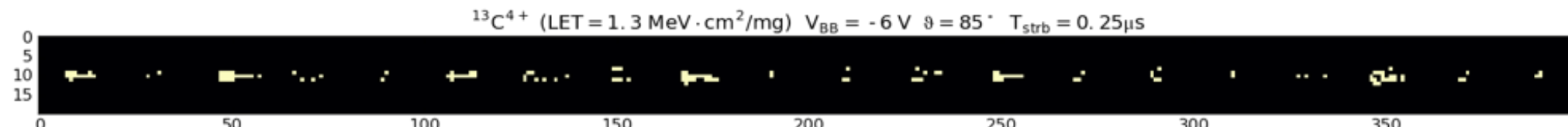
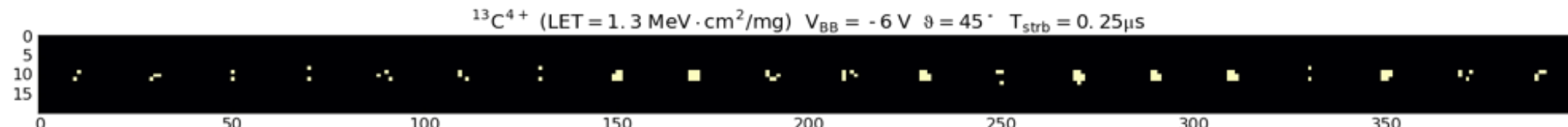
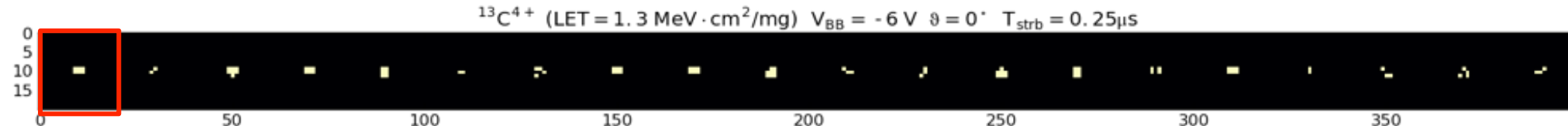


LET Response studies – Lovain-la-Neuve



Sequence of images of single clusters. Each image corresponds to 20 x 20 pixels

vs. angle @ $V_{BB} = -6$



^{13}C : DUT energy [MeV] = 131, Range in Si [μm] = 269.3 (≈ 10 pixels)